INTEGRATED DRAFT FEASIBILITY REPORT

APPENDIX C
HYDRAULICS, HYDROLOGY & CLIMATE PREPAREDNESS AND RESILIENCE

U.S. Army Corps of Engineers
Mississippi Valley Division
New Orleans District
7400 Leake Avenue
New Orleans, Louisiana 70118

November 2019

REVISED DRAFT FEASIBILITY REPORT
DRAFT ENGINEERING REPORT

TABLE OF CONTENTS

TABLES

FIGURES

1. General

This appendix summarizes the preliminary hydrology, hydraulic, and climate change preparedness and resilience technical work completed to support the components of the South Central Coast Louisiana Integrated Feasibility Study. This report includes description of modeling tools, technical criteria, assumptions and results supporting evaluation, comparison and selection of a recommended alternative.

1.1 Introduction and hydraulic description of project area

The project area illustrated in Figure 1 intersects five hydrologic basins: Bayou Teche, Vermilion, Atchafalaya, Terrebonne, and Lower Grand. Bayou Teche and Vermilion can be considered two sub-basins in the combined Teche-Vermilion system. The Atchafalaya and Teche-Vermilion basins contain the dominant hydrologic features while the western portions of the Lower Grand and Terrebonne basins are peripherally relevant.

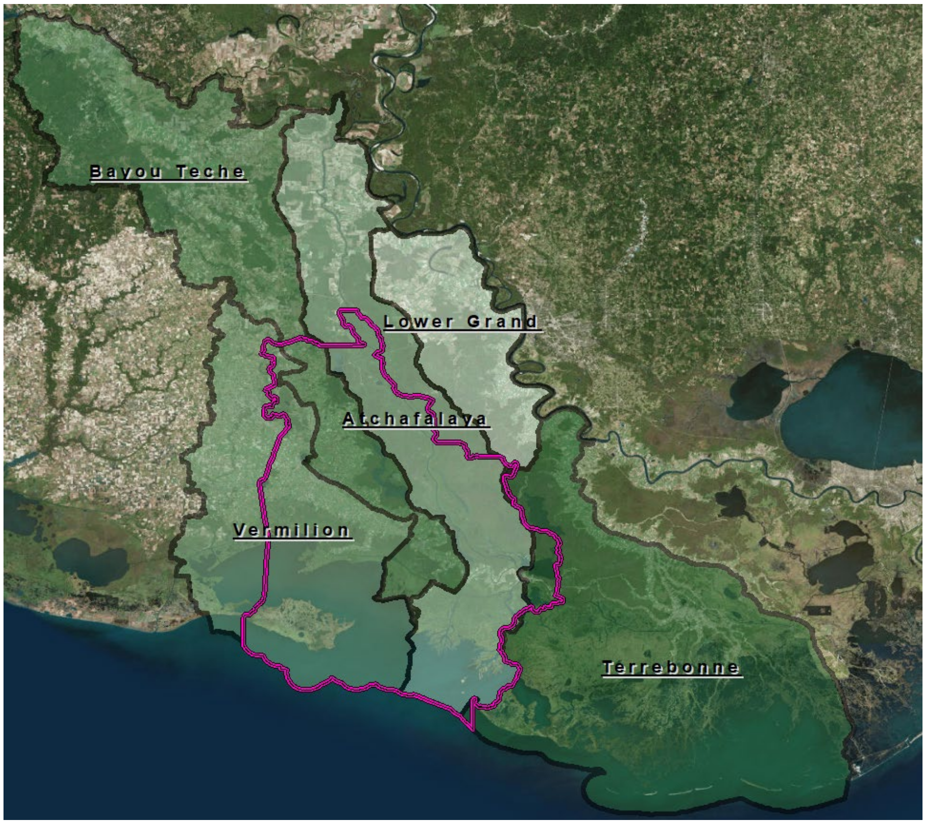

Figure 1. Schematic Delineating The Individual Basin Boundaries Overlaid With The Project Area.

Teche-Vermilon Basin – The Teche-Vermilion Basin occupies over 50% of the project area. The Teche sub-basin has a drainage area of 2,200 square miles spanning from the west bank of the Red River to Cote Blanche Bay. Bayou Teche (125 miles long) begins in Port Barre and drains into the lower Atchafalaya. Bayou Teche is an ancient Mississippi River channel, the banks create a natural ridge. Residential and commercial structures largely occur on the natural ridges (Breaux Bridge, New Iberia, Franklin). The density of structures located on the natural ridges were utilized to identify economic damage hot spots for identification of measures. Further details on economic damage hot spots is described in Appendix D Economics Evaluation.

Inland hydraulic features include Dauterive Lake and Lake Fausse Pointe which are hydraulically connected to Bayou Teche via the Loreauville Canal. The coastal boundary of this sub-basin includes the Golf Intercoastal Water Ways (GIWW) until the mouth Charenton Drainage and Navigation Canal. The Vermilion sub-basin has a total area of 2,100 square miles that includes the West Cote Blanche and Vermilion Bays, the Vermilion River, and Marsh Island. Much of the coastal area is tidal wetland habitat, transected by the GIWW. Unique to this sub-basin are exposed salt-dome deposits: Cote Blanche Island, Weeks Island, Avery Island, and partially Lake Peigneur.

Atchafalaya Basin – The Atchafalaya Basin contains the Atchafalaya River (137 miles long), a large freshwater body that spans the entire project area (north to south). The basin begins at the Old River Control Structure located upstream of Simmesport and ultimately drains into the Gulf of Mexico. The Atchafalaya receives 30% of the longitudinal flow from the Mississippi river, as well as the entire Red River, averaging 225,000 cfs. The floodway, bordered by large federal river levees, directs flow south towards the Atchafalaya Bay near Morgan City or via the Wax Lake outlet between Centerville and Calumet.

Terrebonne and Lower Grand – While the Terrebonne is a large basin, only the far western portion is considered in the authorization zone. The total area is 3200 square miles and is made up of mainly tidal wetlands. These range from fresh near Bayou Lafourche to oligohaline towards the GOM. The Lower Grand basin is contained between the east Atchafalaya levees and the west bank Mississippi levees. The main channels in this basin are the Gulf Intracoastal Water Way, Port Allen to Morgan City Alternative Route, and the Avoca Island cutoff. Much of the upper basin is alluvial and heavily used for agriculture. The main hydrologic contribution of this area is as a catchment area for rainfall.

1.2 Overview of analysis goals

The goal of this analysis to hydraulically analyze major sources of flooding from riverine and storm surge events to evaluate and compare measures carried forward into third and fourth planning iteration descriptions of measures are presented in Appendix D Plan Formulation and Chapter 3 of the Main Feasibility Report. The alternatives are examined for a range of flooding frequencies for both riverine and surge events combined with the effects of relative sea level rise in the future.

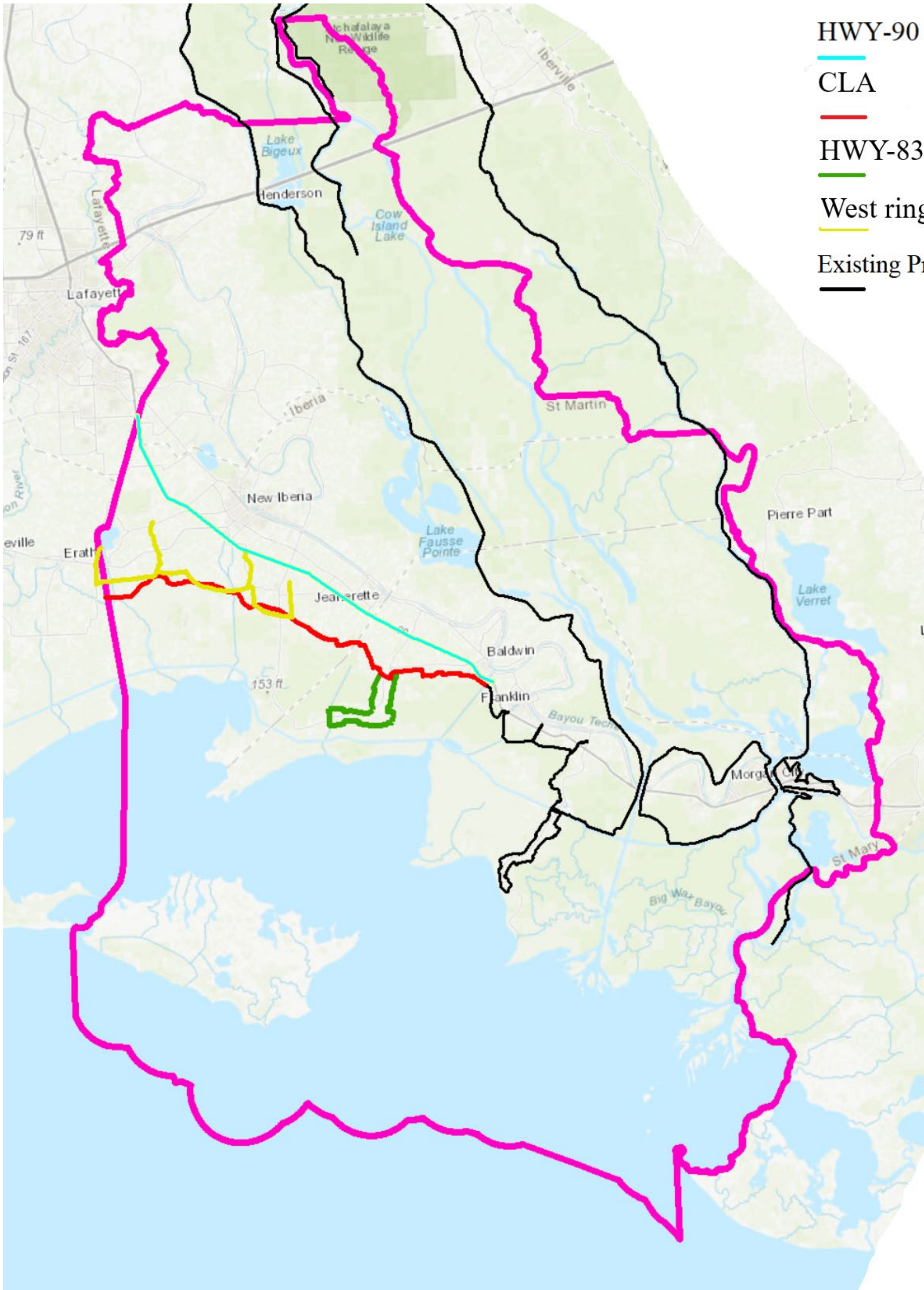

Figure 2. Project Area With Existing And Proposed Levees.

2. Surge

2.1 Background

While the study area has periodically experienced localized flooding from excessive rainfall events, the primary cause of the flooding events has been the storm surges from hurricanes and tropical storms. The past eight years, storm surges associated with four Category 2 or higher hurricanes (Lili, Rita, Gustav, and Ike),have greatly impacted the area. Structures have been frequently inundated resulting in billions of dollars in damages to southwest coastal Louisiana. Additional details on damages from flooding is described in Main Report Chapter 2 Inventory and Forecast. Hurricane storm surge also causes significant permanent damage to wetlands. Hurricane surge has formed ponds in stable, contiguous marsh areas and expanded existing, small ponds, as well as removed material in degrading marshes (Barras, 2009). Fresh and intermediate marshes appear to be more susceptible to surge impacts, as observed in Barras (2006).

Storms of Record. Hurricane Audrey (June 25 - 29, 1957) ranks as the 7th deadliest hurricane to strike the United States and was the deadliest natural disaster in the history of southwest Louisiana in modern record-keeping with at least 500 deaths

(source: http://www.srh.noaa.gov/lch/?n=audrey; accessed January 7, 2016).

Hurricane Lili (September 23 - October 3, 2002) was originally a Category 4 hurricane and first made landfall near Marsh Island in Iberia Parish with maximum sustained winds of 92 mph. Highest recorded rainfall amount was about 9 inches in some parts of Louisiana. The highest storm surge was over 11 feet in St. Mary Parish

(source: https://coast.noaa.gov/hes/docs/postStorm/Lili_%20final.pdf; accessed December 15, 2015).

Hurricane Rita (September 24 - 26, 2005) Hurricane Rita, reaching its peak intensity southeast of the mouth of the Mississippi River as a Category 5, first made landfall just west of Johnson's Bayou and east of Sabine Pass at the Texas-Louisiana border as a Category 3 hurricane. Sensors recorded storm-surge water levels over 14 ft above NAVD 88 at Constance Beach (LC11), Creole (LA12), and Grand Chenier (LA11), La., about 20 miles, 48 miles, and 54 miles, respectively, east of Sabine Pass, Texas. In general, storm-surge water levels increased eastward from the Sabine River into southwest Louisiana. The magnitude of the storm surge was greatest near the coast and decreased inland through the approximate latitude of I-10, about 35 miles inland from the coast (source: http://pubs.usgs.gov/circ/1306/pdf/c1306_ch7_j.pdf; accessed December 15, 2015).

Hurricane Gustav (August 25 - September 4, 2008) Gustav made landfall near Cocodrie, Louisiana on September 1, 2008 as a strong category 2 (based on 110 mph sustained winds) and continued to move northwest, spreading hurricane force wind gusts across portions of Southeast and South Central Louisiana (http://www.srh.noaa.gov/lix/?n=gustavsummary; accessed January 26, 2016). Due to the storm making landfall east of the study area, storm surge values were only 4-5 feet across St. Mary, Iberia, and Vermilion parishes

(http://www.srh.noaa.gov/images/lch/tropical/HPW1-SUN.pdf; accessed January 26, 2016).

Hurricane Ike (September 1-14, 2008) first made landfall near Galveston, Texas on September 13, 2008 as a Category 2 hurricane with maximum sustained winds of 110 mph

(http://www.srh.noaa.gov/hgx/?n=projects_ike08; accessed December 15, 2015).

Ike was a large hurricane with tropical-storm-force and hurricane-force winds associated at the time of its landfall extending approximately 275 miles and 120 miles from the storm center, respectively. In Louisiana, estimated wind speeds ranged from 80 mph near the Texas-Louisiana border to 50 mph in Vermilion Parish. Storm surge caused flooding in Cameron, Vermilion, and many parishes to the east, with over 9 foot stillwater levels estimated for Lake Charles

(http://www.fema.gov/media-library-data/20130726-1648-20490-1790/757_ch1_final.pdf; accessed December 15, 2015).

2.2 Adcirc Modeling

A version of the Southern Louisiana ADCIRC (Advanced Circuulation) model, coupled with the STWAVE (Steady State spectral WAVE) model was developed for evaluation and comparision of the Southwest Coastal Louisiana alternatives. The ADCIRC model is a two-dimensional, depth-integrated, barotropic time-dependent long wave, hydrodynamic circulation model that can be used to simulate storm surge response to hurricanes and tropical storms. STWAVE is a steady-state, finite difference, spectral model base on the wave action balance equation. STWAVE is used to model nearshore wind-wave growth and propagation. The modeling system used for this study was established by updating existing models used previously for the Joint Storm Surge (JSS) Analysis in Southern Louisiana for the Louisiana Coastal Protection and Restoration (LACPR) Project, as well as the recent flood insurance rate map modernization study conducted by the FEMA (USACE, 2008a and USACE, 2007). Details of the model development and results can be found in Annex 1 of the Engineering Report.

2.3 Statistical data processing

The statistics from the LACPR data set included results from 2, 1, 0.25, and 0.2% AEP return storms. In order to produce the requested stages for the 50, 20, 10, 5, and 0.5% AEP frequencies, linear interpolations were applied using the existing data. For the 0.5% AEP stages, the 1% and 0.25% AEP results were linearly interpolated at each data point. For the higher frequencies of 50, 20, 10, and 5% AEP, existing ground elevations were extracted to represent the 100% AEP stages. Applying this assumption, the high frequencies are linearly interpolated values between the 2% AEP data and the existing ground elevations for each point.

For future conditions, only simulations with a starting Gulf of Mexico (GOM) of +1.15ft and +5.0 ft NAVD88 (above 1.2 ft NAVD 88) were available. To estimate the future surge values, a linear interpolation between existing conditions and future conditions of +5.0 was applied to produce a +1.8 ft NAVD88 data set. The same process to acquire the 50, 20, 10, 5, and 0.5% AEP returns for existing conditions was applied to the future condition data set.

2.4 Existing Conditions Results

The existing condition results include direct output for the 2, 1, and 0.2% AEP statistics and the interpolated 0.5% AEP results along with the estimated high frequency returns of 50, 20, 10 and 5% AEP. Storm sets were run with a starting Gulf of Mexico water surface elevation of 1.2 ft NAVD 88. The data is presented in figures 3 – 10 for all points contained within the project authorization zone.

2.5 Future Conditions

The future condition results include direct output for the 2, 1, and 0.2% AEP statistics and the interpolated 0.5% AEP results along with the estimated high frequency returns of 50, 20, 10 and 5% AEP. The set was interpolated from the existing conditions and the +5.0 NAVD88 output for the intermediate RSLR of +1.8 ft NAVD88. The data is presented in Figures 11 – 18 for all points contained within the project authorization zone.

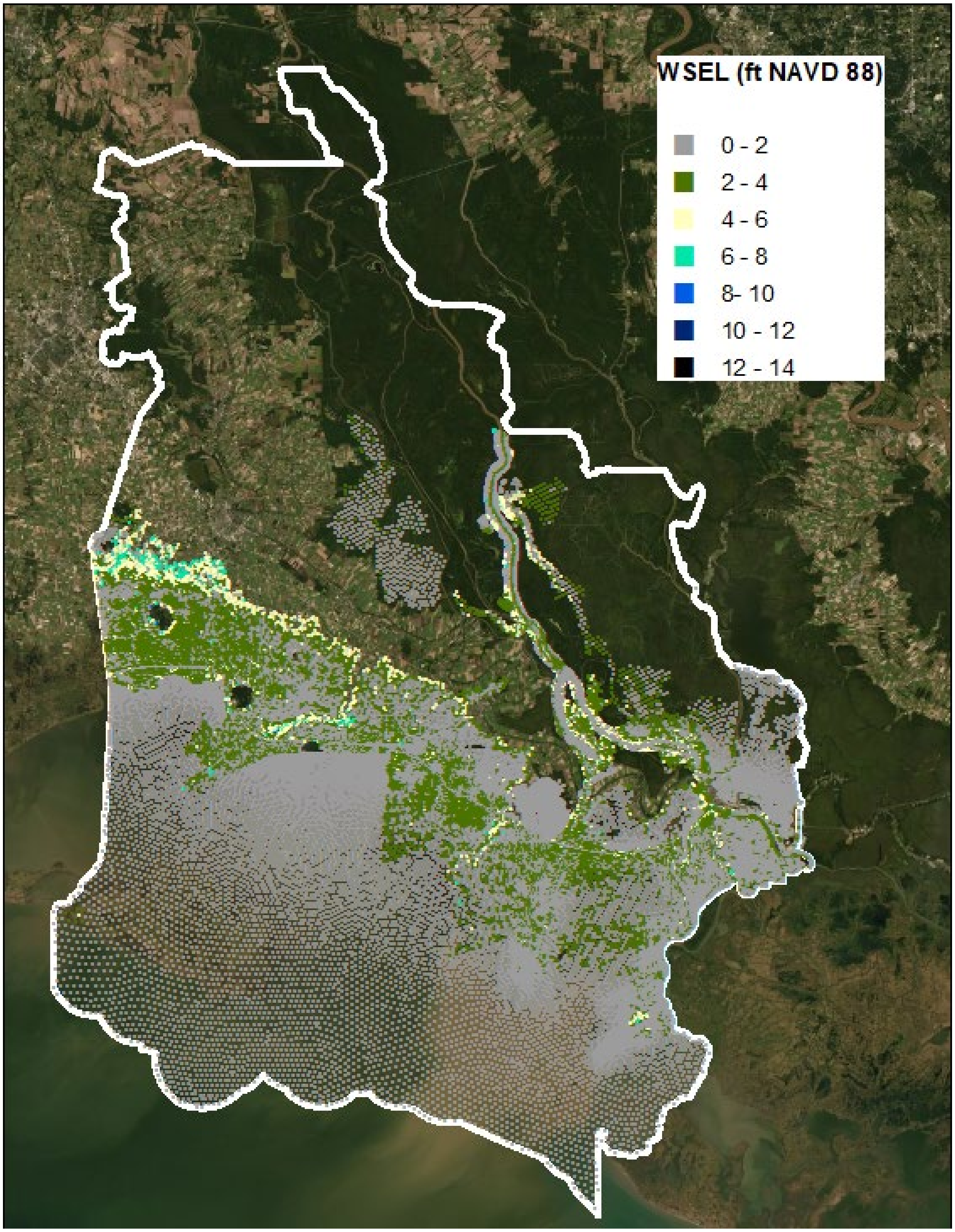

Figure 3. 50% AEP Storm Existing Conditions Water Surface Elevations (Ft. Navd88).

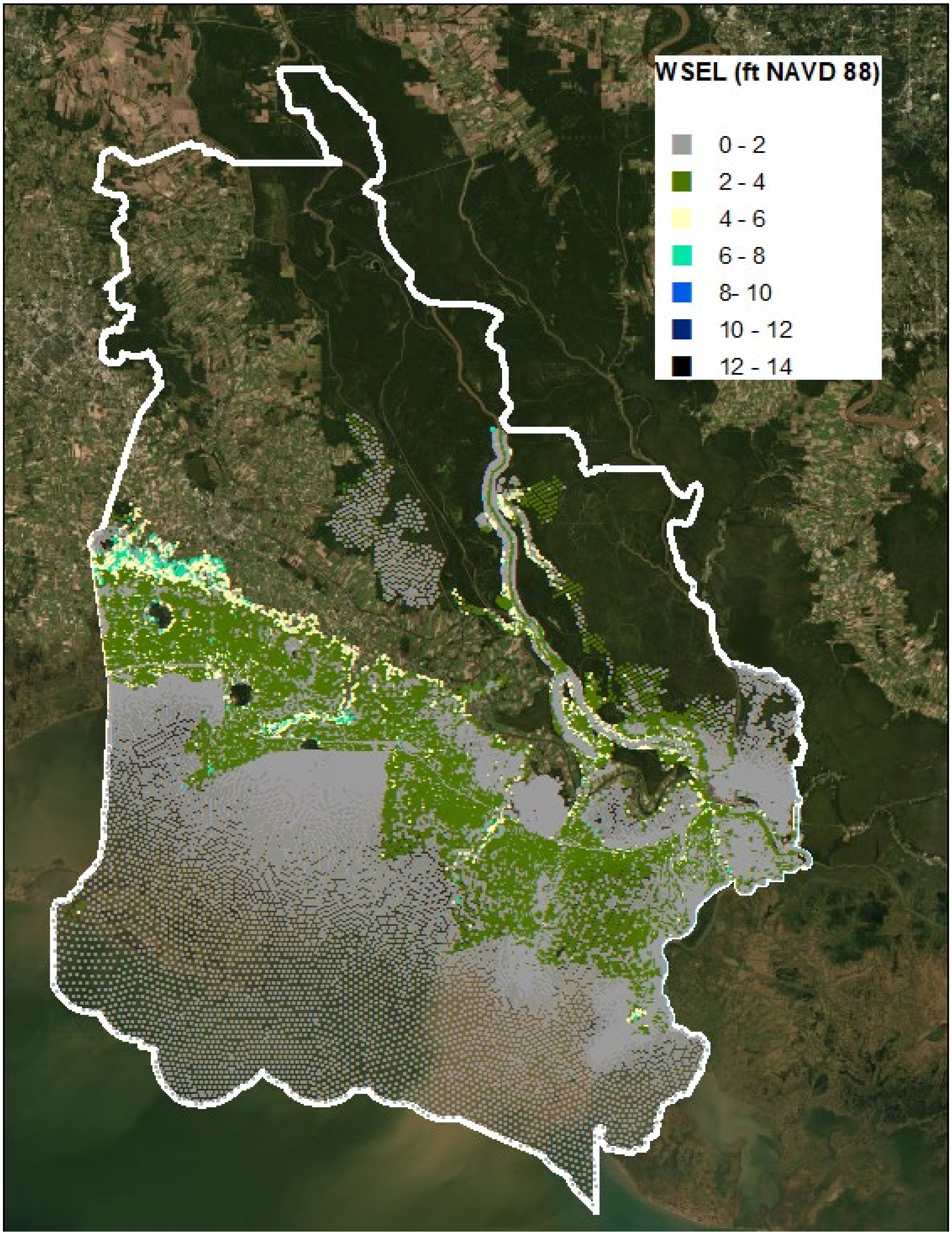

Figure 4. 20% AEP Storm Existing Conditions Water Surface Elevations (Ft. Navd88).

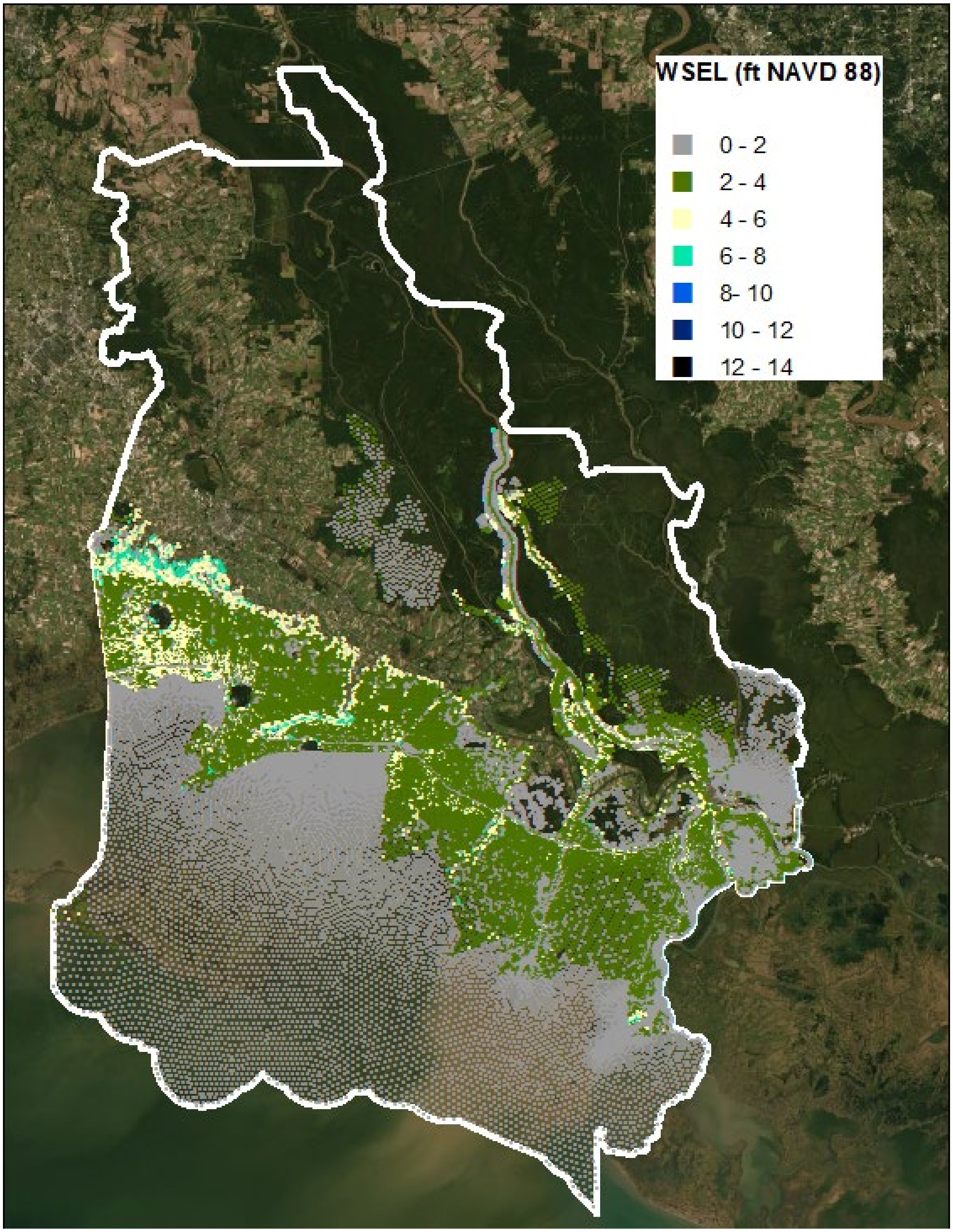

Figure 5. 10% AEP Storm Existing Conditions Water Surface Elevations (Ft. Navd88).

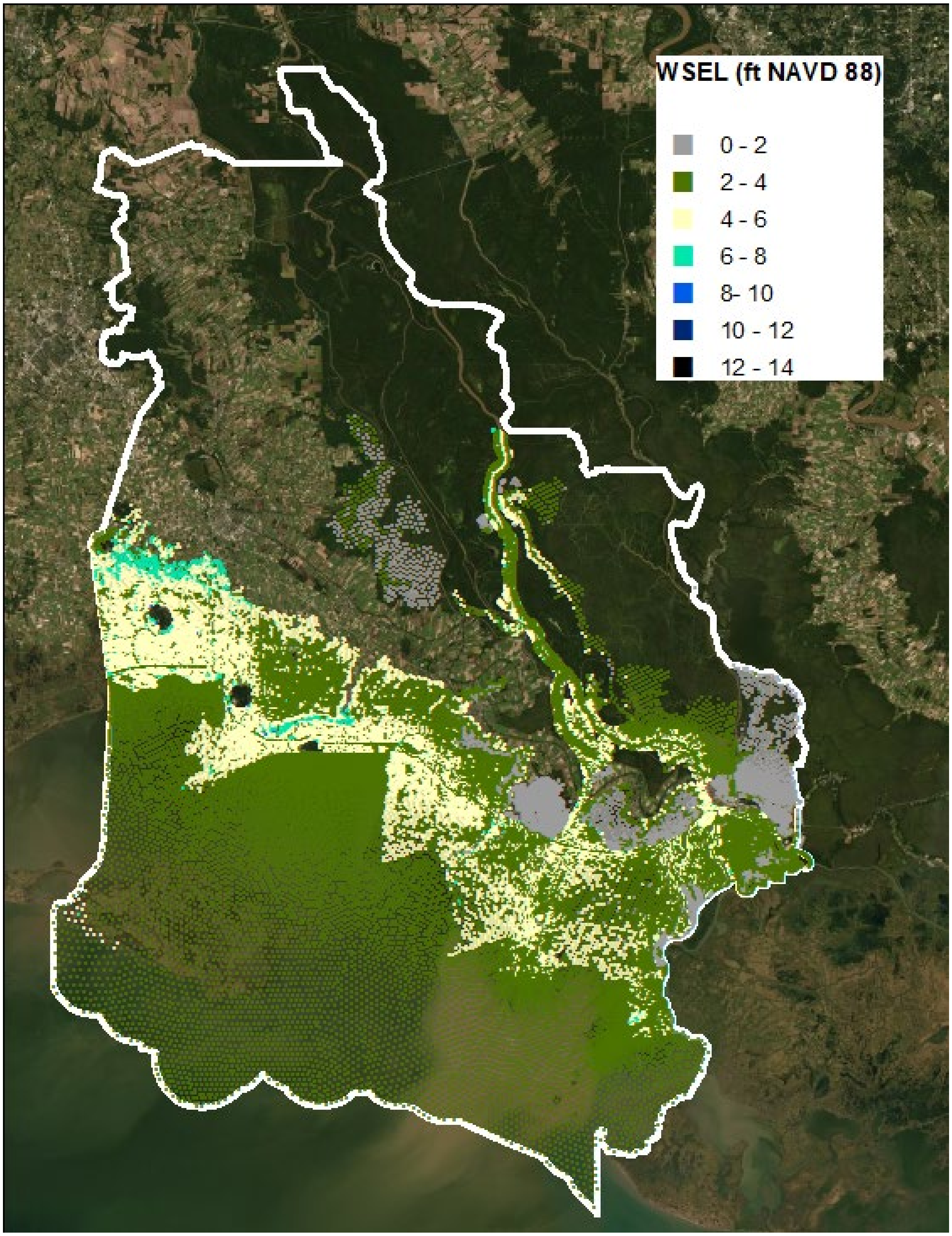

Figure 6. 5% AEP Storm Existing Conditions Water Surface Elevations (Ft. Navd88).

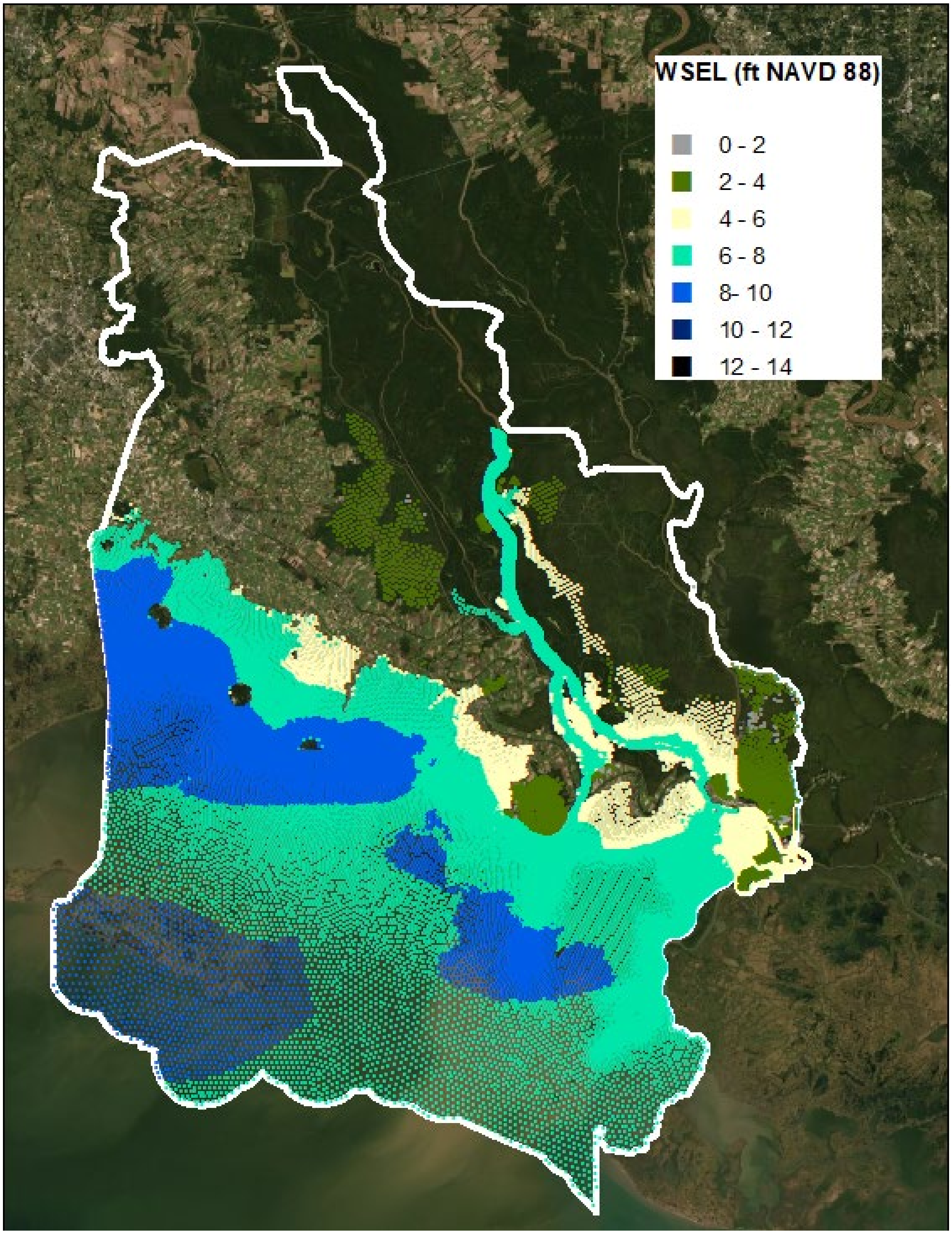

Figure 7. 2% AEP Storm Existing Conditions Water Surface Elevations (Ft. Navd88).

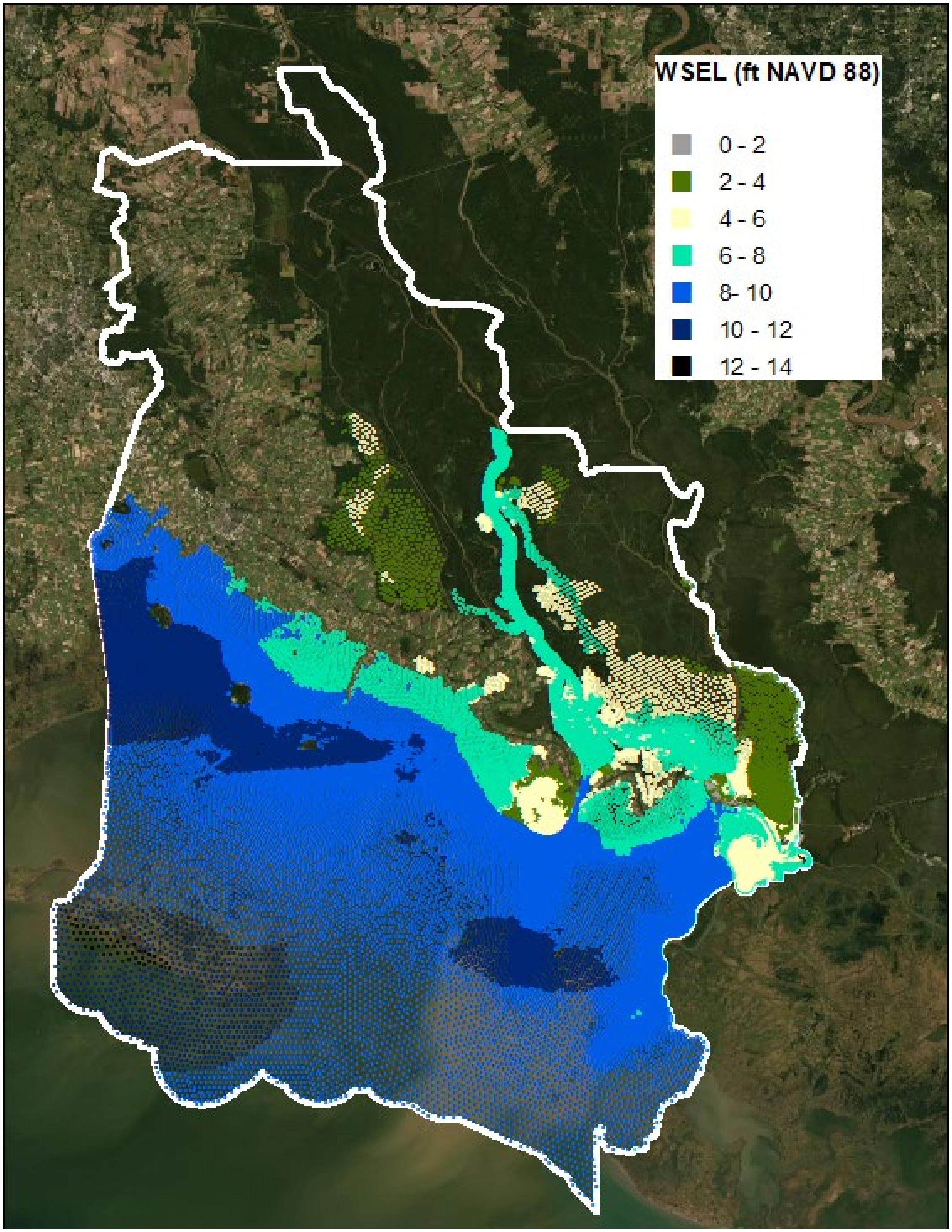

Figure 8. 1% AEP Storm Existing Conditions Water Surface Elevations (Ft. Navd88).

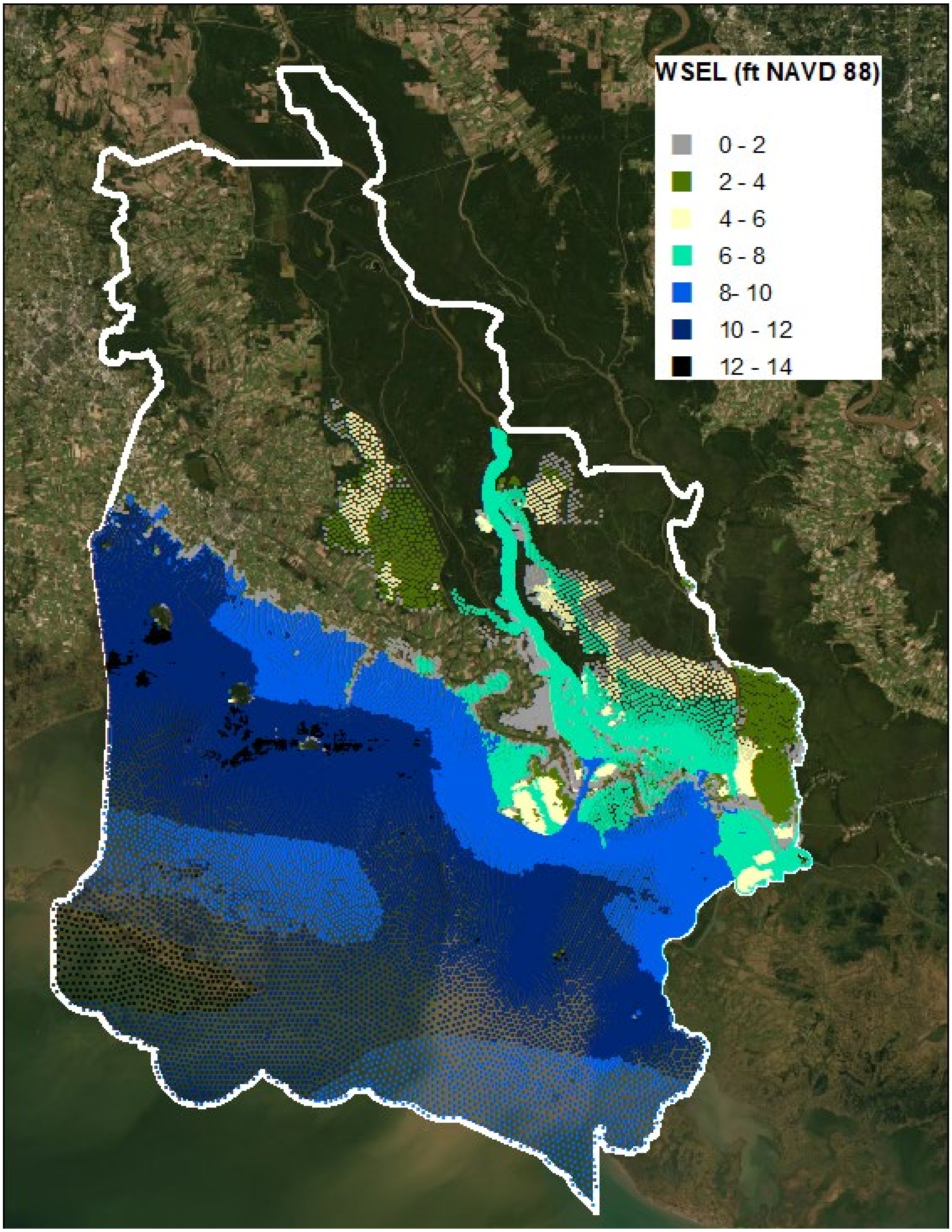

Figure 9. 0.5% AEP Storm Existing Conditions Water Surface Elevations (Ft. Navd88).

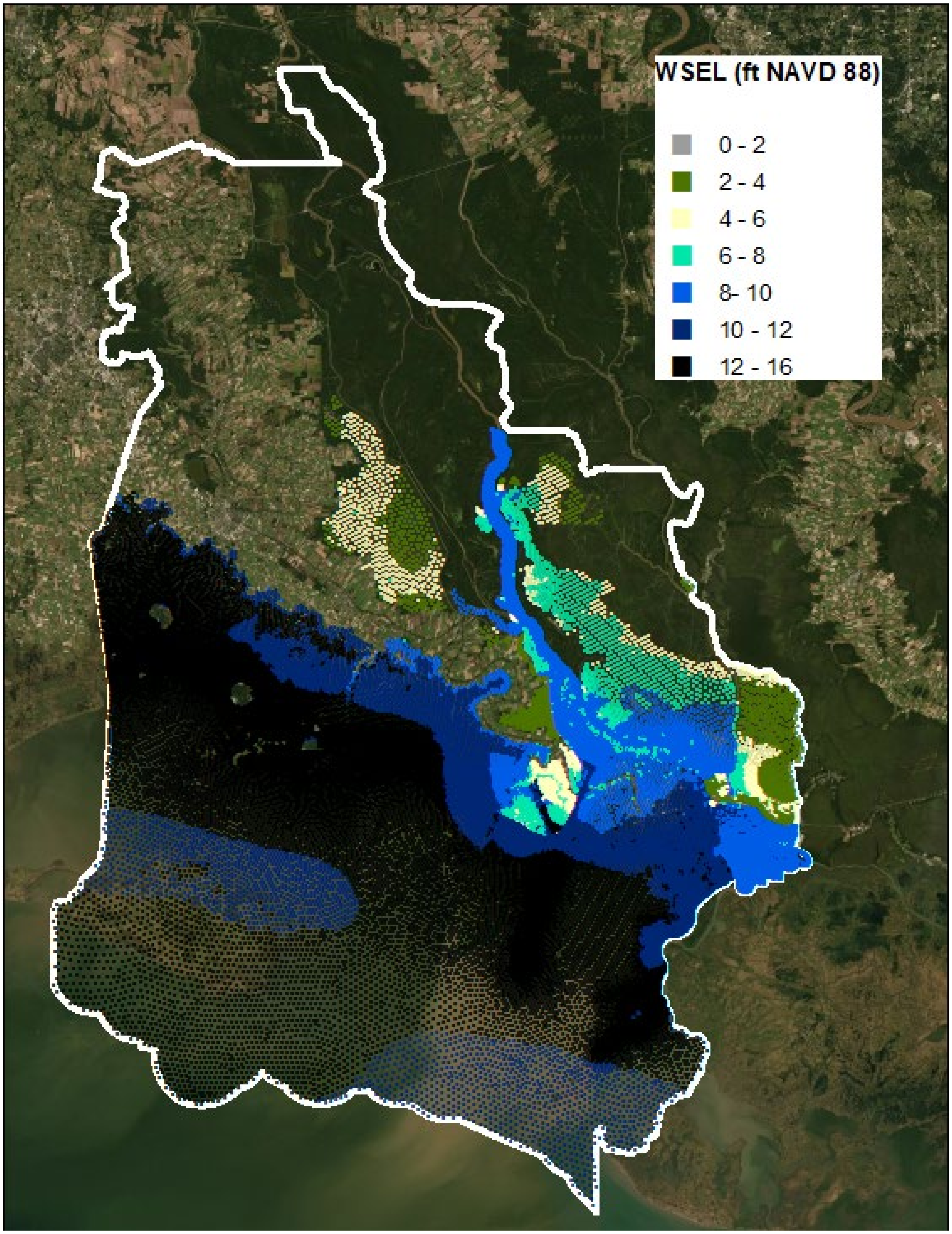

Figure 10. 0.2% AEP Storm Existing Conditions Water Surface Elevations (Ft. Navd88)

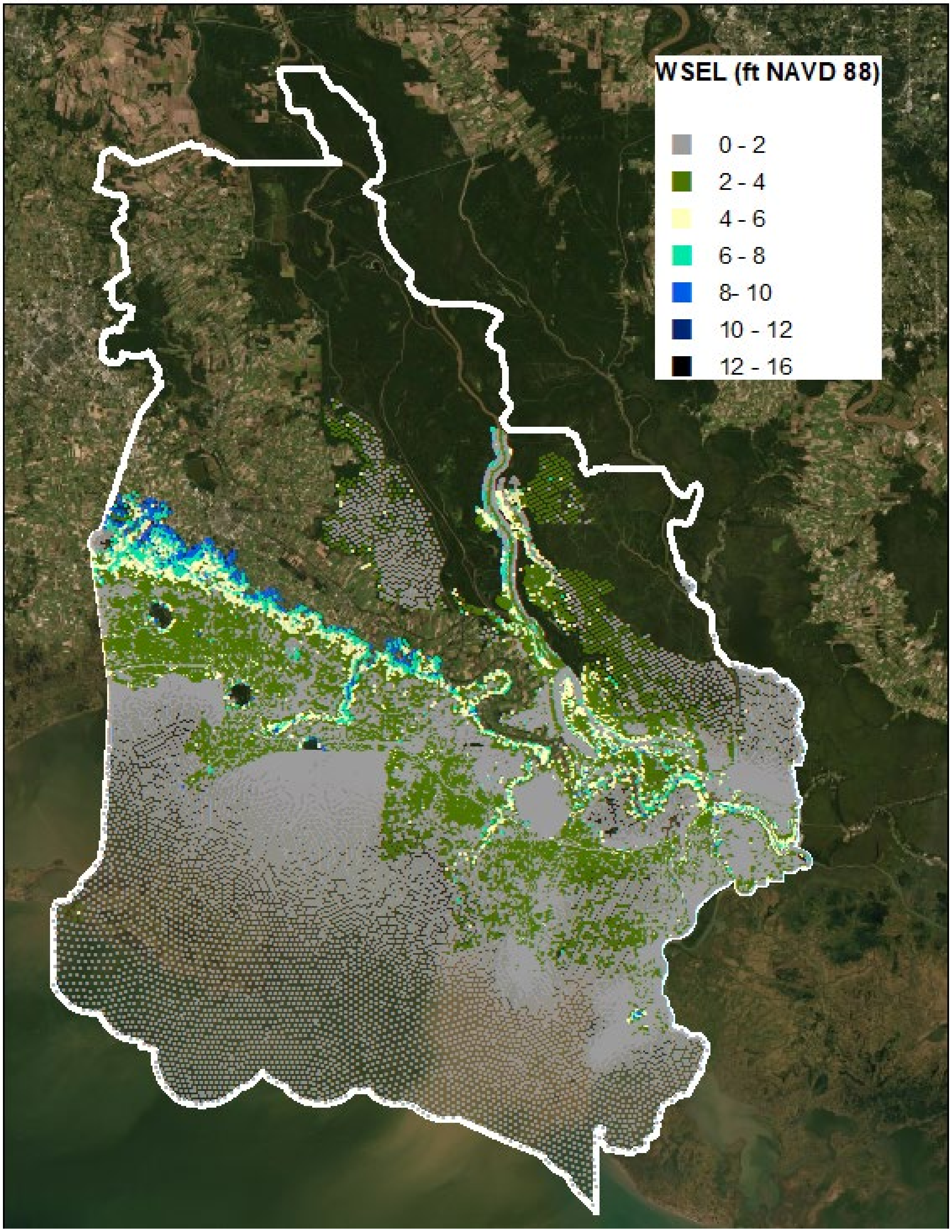

Figure 11. 50% AEP Storm Future Conditions Water Surface Elevations (Ft. Navd88).

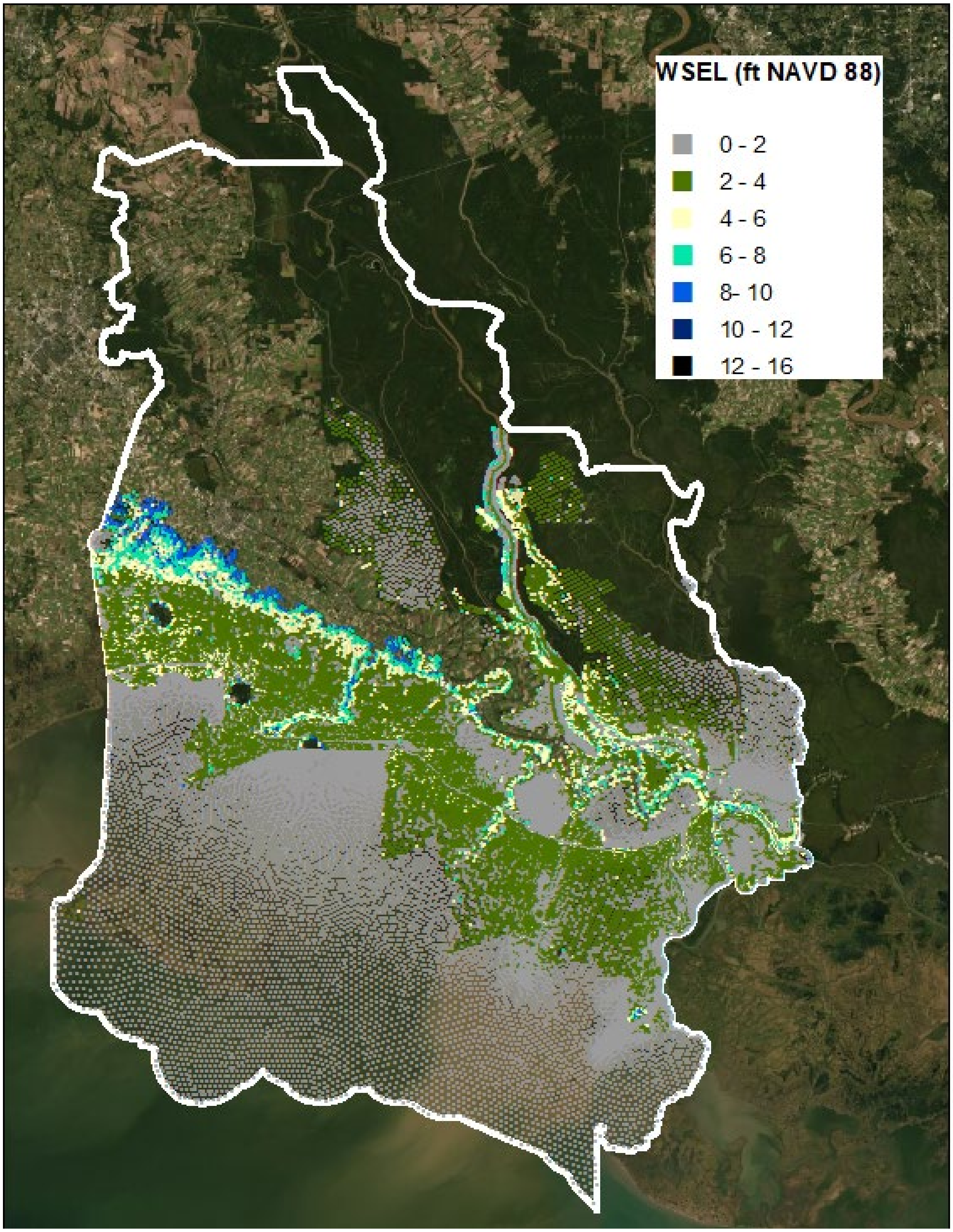

Figure 12. 20% AEP Storm Future Conditions Water Surface Elevations (Ft. Navd88).

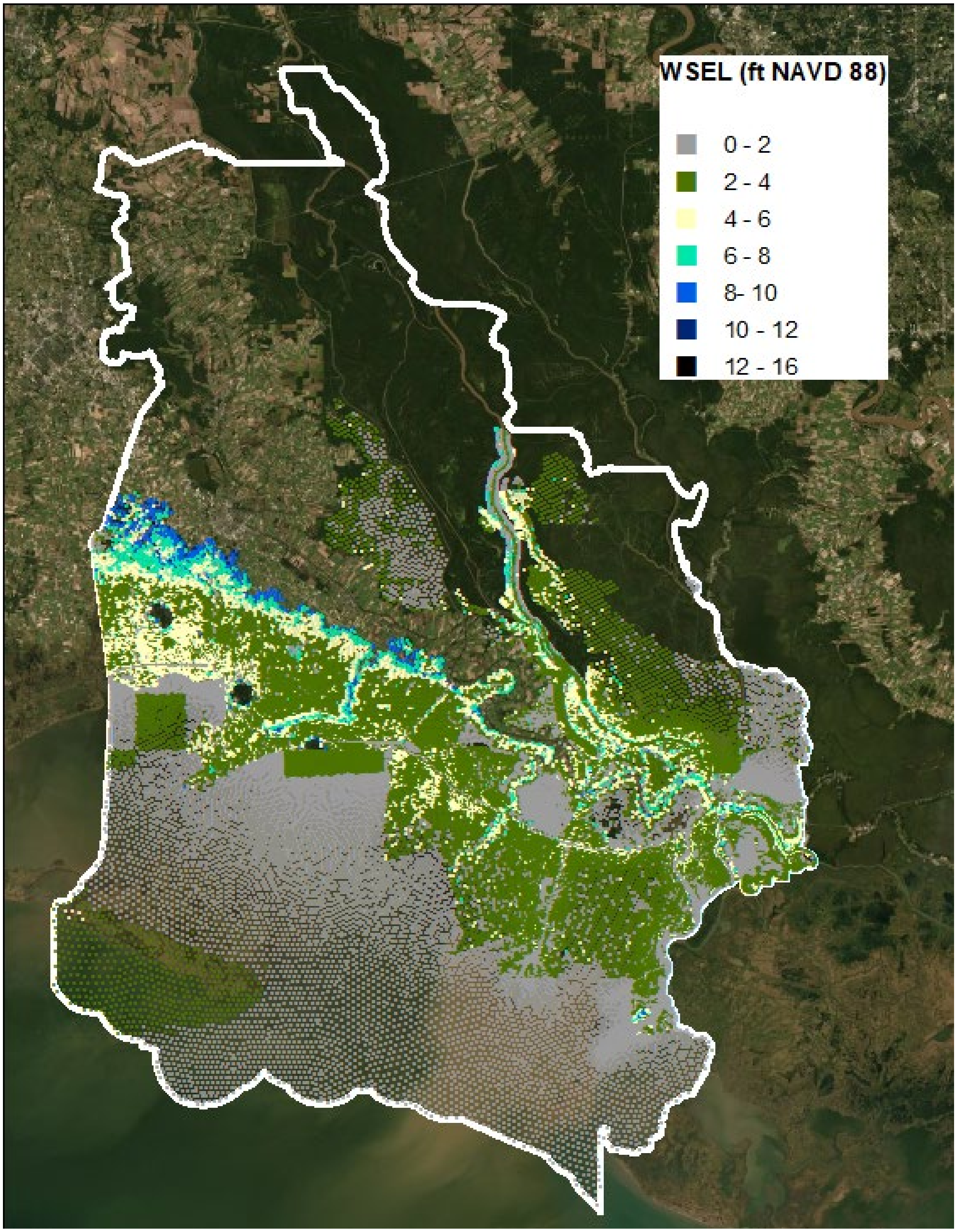

Figure 13. 10% AEP Storm Future Conditions Water Surface Elevations (Ft. Navd88).

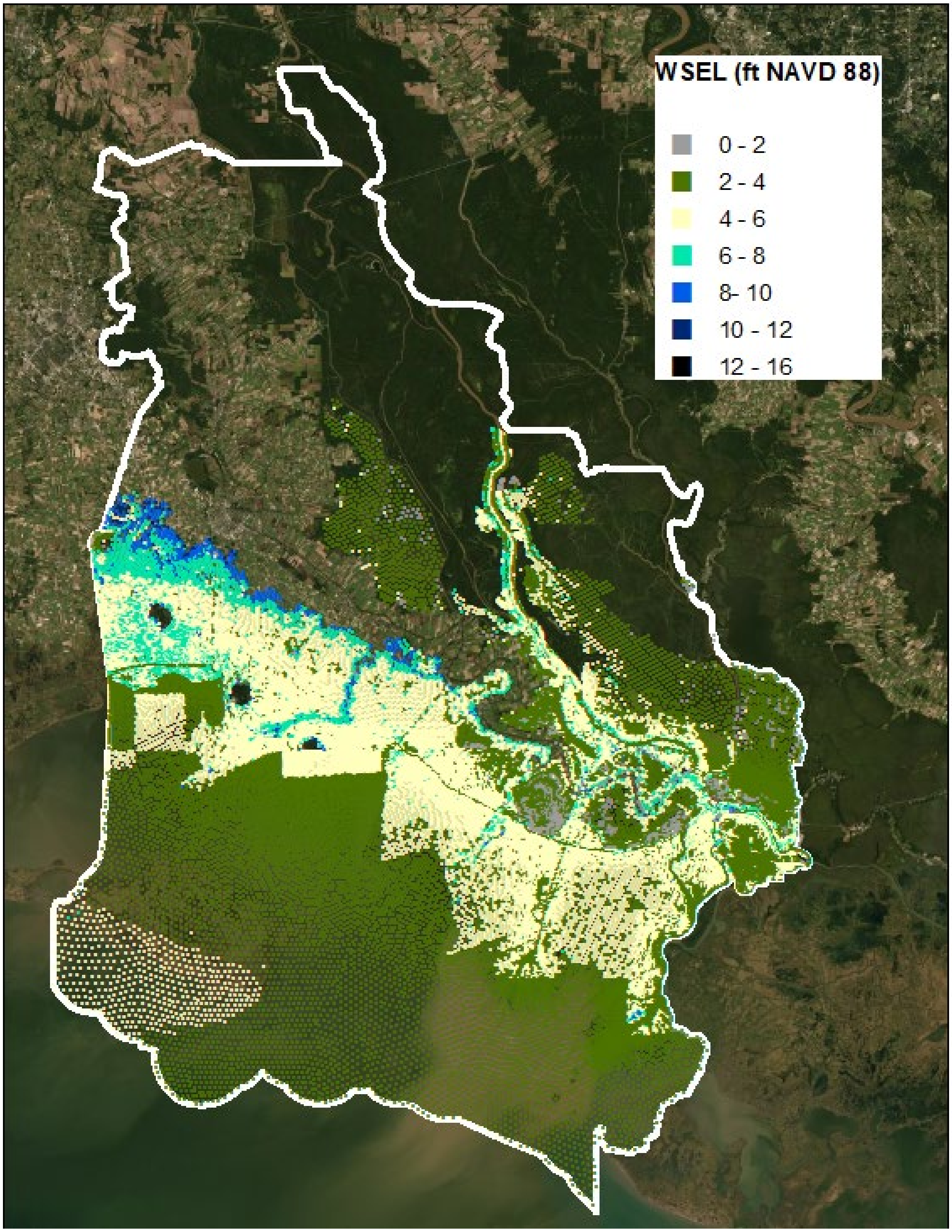

Figure 14. 5% AEP Storm Future Conditions Water Surface Elevations (Ft. Navd88).

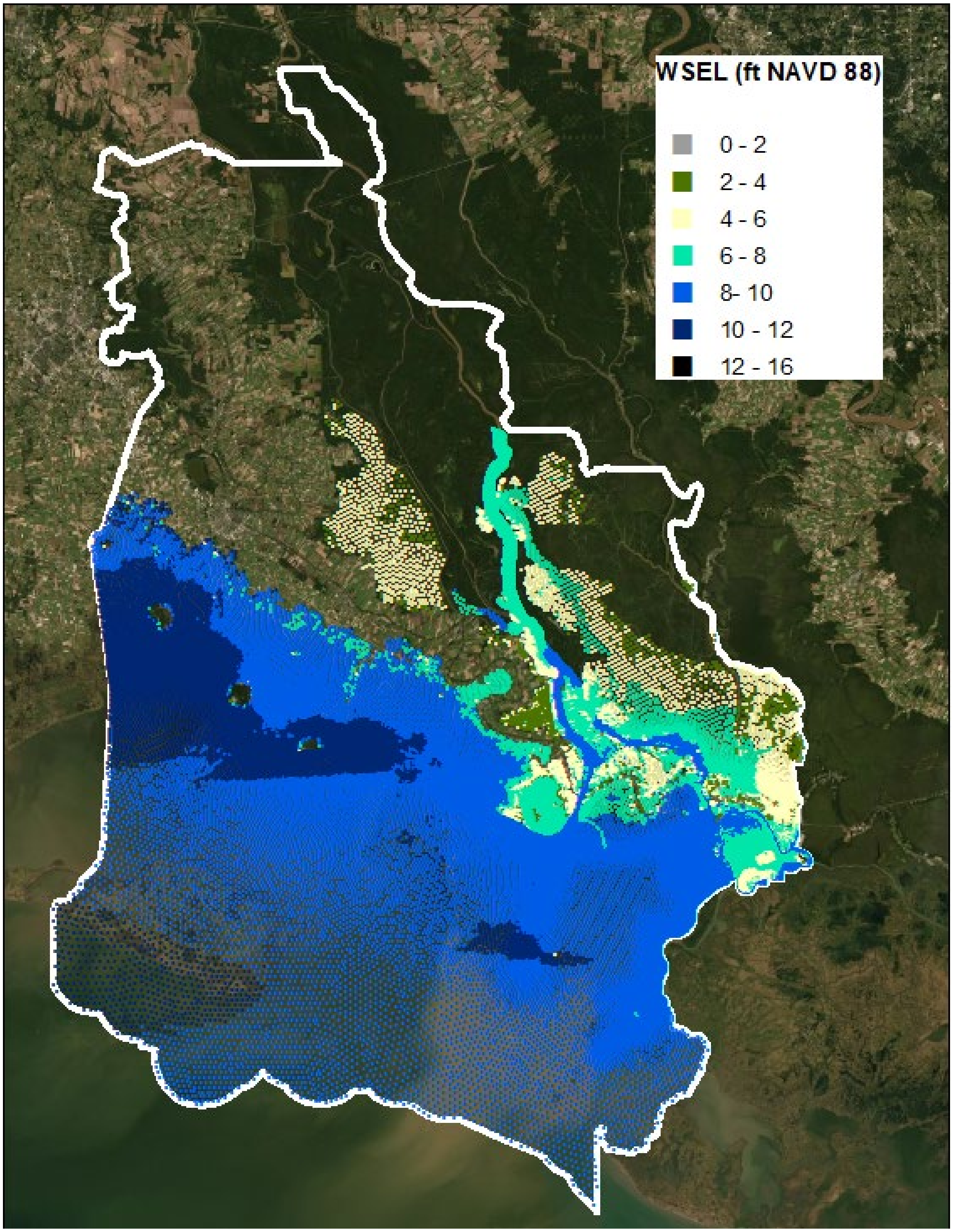

Figure 15. 2% AEP Storm Future Conditions Water Surface Elevations (Ft. Navd88).

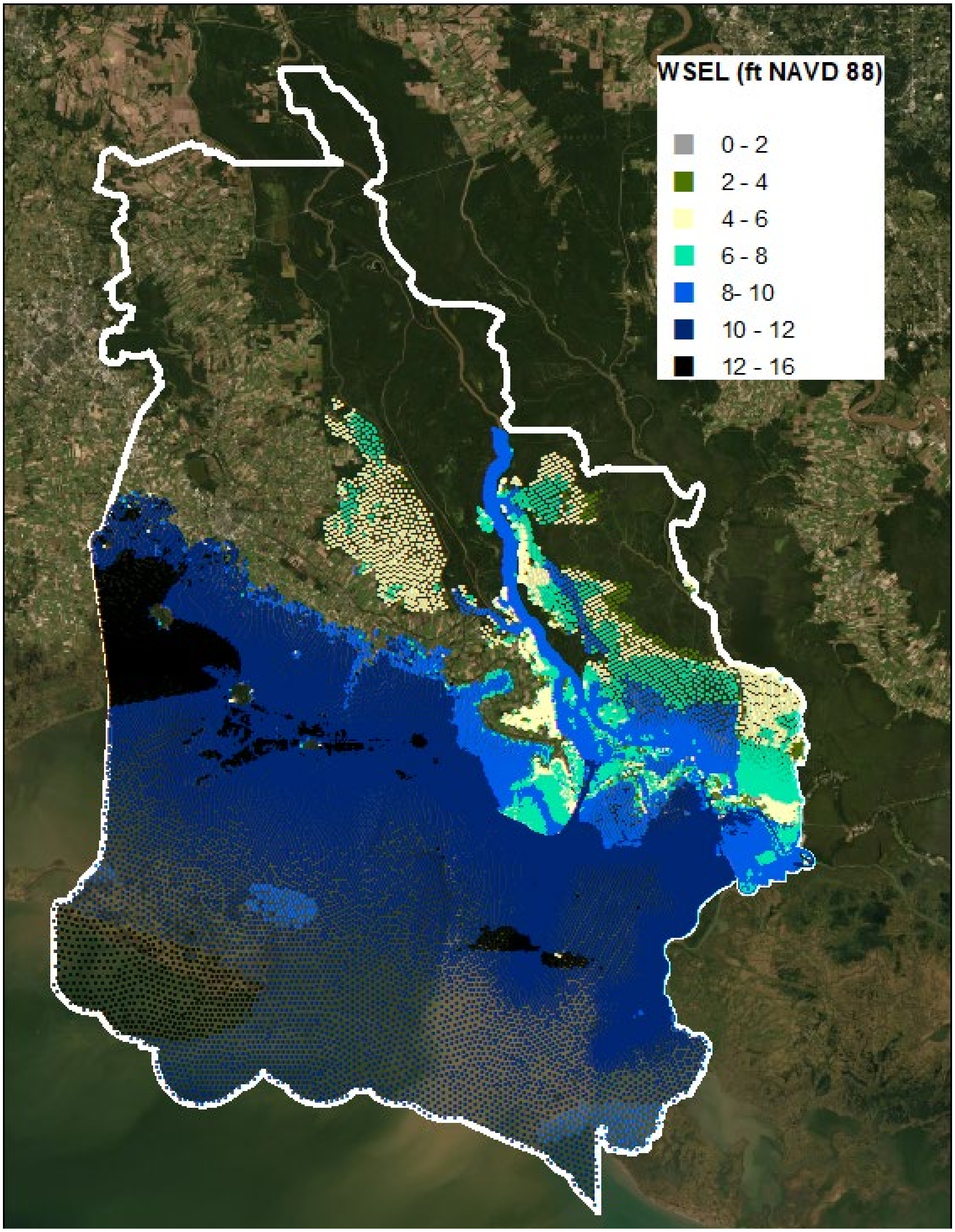

Figure 16. 1% AEP Storm Future Conditions Water Surface Elevations (Ft. Navd88).

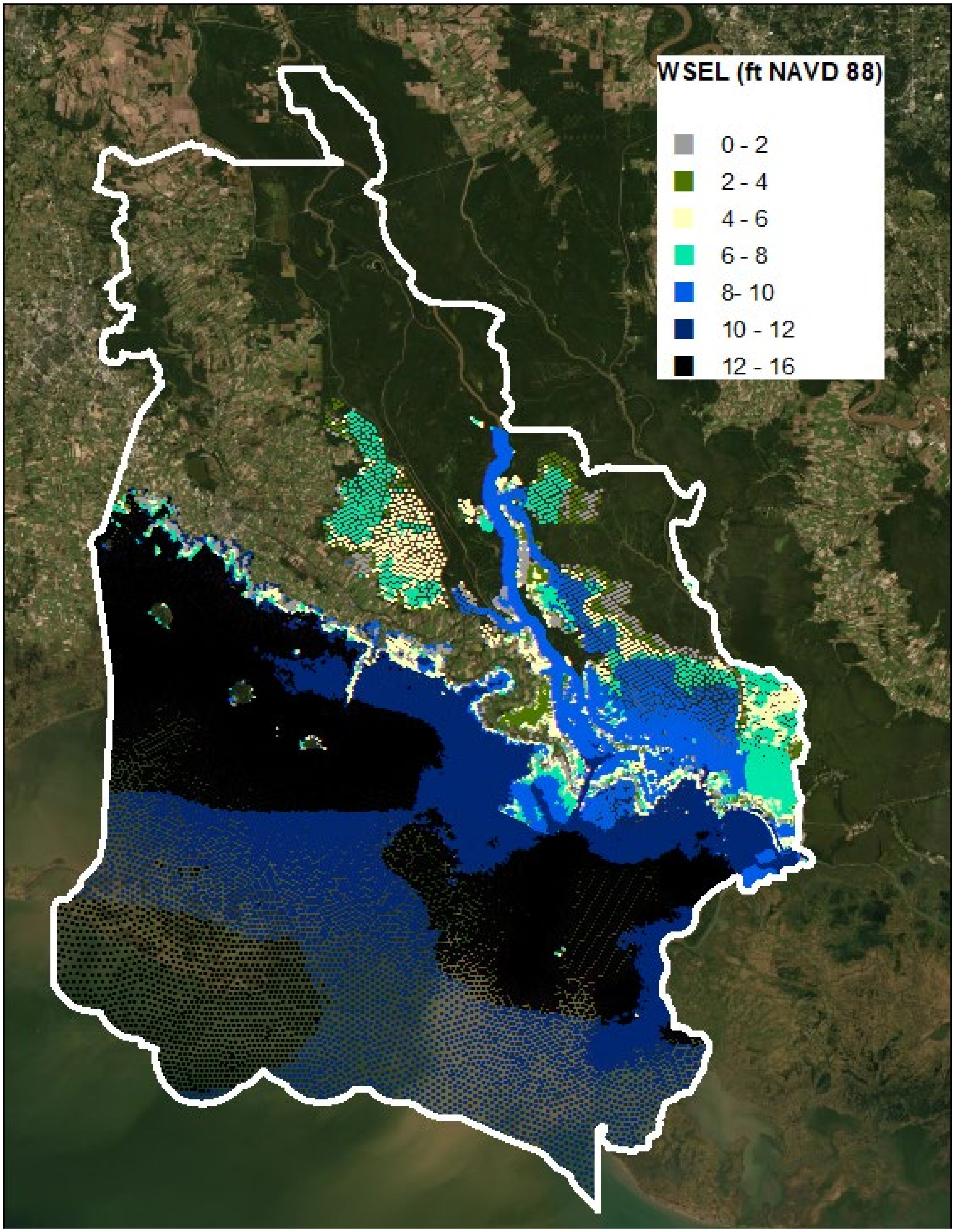

Figure 17. 0.5% AEP Storm Future Conditions Water Surface Elevations (Ft. Navd88).

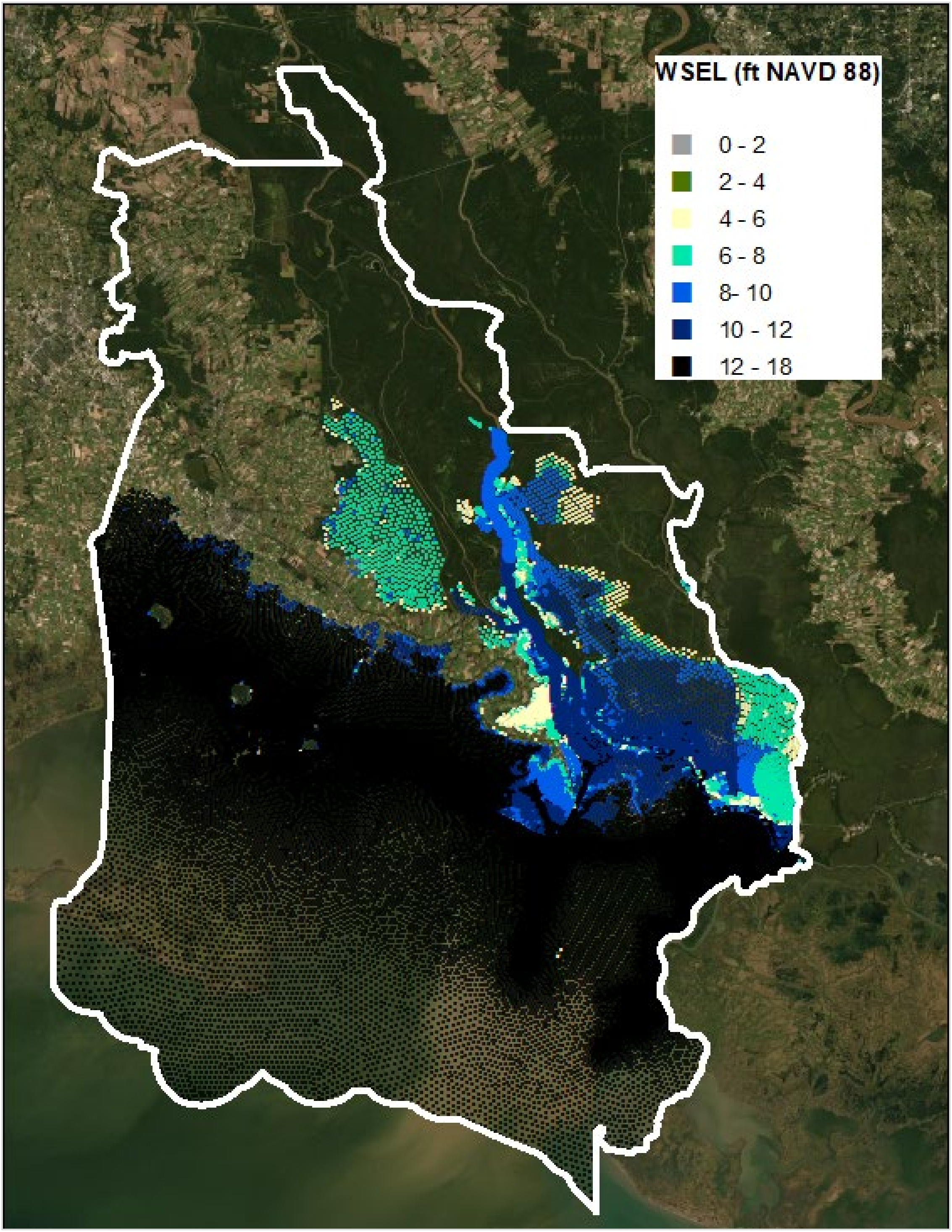

Figure 18. 0.2% AEP Storm Future Conditions Water Surface Elevations (Ft. Navd88).

3. Riverine

3.1 Model Setup

This model was expanded from the 2017 Atchafalaya flowline to include the area east of the Atchafalaya Basin levees and west of the Mississippi River levees and Bayou Lafourche as shown in Figure 19. The hydrologic impact of the Atchafalaya River on the project area was modeled using a combined 1-D:2-D domain in HEC-RAS version 5.0.7. The terrain was built from the datasets in Table 1. The 2-D area Manning's n values were mapped using the NCLD 2011 landcover dataset in Figure 19. Table 2 presents the manning's n values attributed to the project area using the landcover data.

The model consists of two flow boundaries. The Atchafalaya main stem is placed at Simmesport with the other boundary located at the Morganza spillway to account for any further contribution from the Mississippi River. The tail water is a stage boundary located in the Gulf of Mexico. The flow rates assigned to the boundary conditions are the predicted 30 percent latitude flow based on the Mississippi and Red River flows. The predicted flow frequency table and graph are presented in Table 3 and Figure 12 with the given confidence intervals and observed events.

The contribution from the Morganza spillway is based on both the 70% flow estimated to still be in the Mississippi river. The operation of Morganza is primarily operated using a flow rate trigger point of 1.5 million cfs downstream of the Old River Control Structure (ORCS). The boundary is assigned a flow calculated by subtracting 1.5 million cfs from the 70% latitude flow as long as it is a positive value. This results in Morganza only being operated for all frequencies of 2% AEP or lesser.

Table 1. Terrain Dataset Sources and Resolution

Terrain Data	Source	Spatial Resolution
Atchafalaya River Multibean SONAR 2010	USACE-MVN	2ft
Atchafalaya River Levee Lidar 2007	USACE-MVN	1ft
Atchafalaya LIDAR 2013	Northrop Grumman, Advanced GEOINT Solutions Operating Unit	1m
Northern G.O.M. Topobathy	Coastal National Elevation Dataset	1m-3m
USGS Topography	USGS	20ft

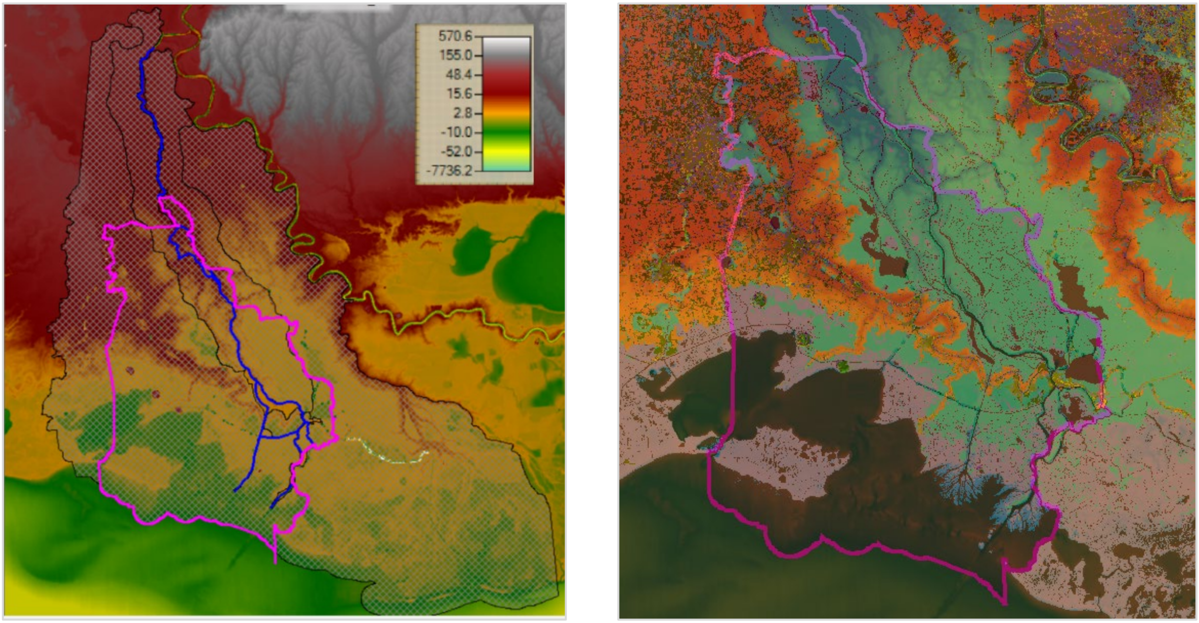

Figure 19. The Computational Domain Superimposed Onto The Terrain (Left), Project Area Superimposed Onto The Land Cover (Right).

Table 2. Manning's n Values Applied to HEC-RAS 2D Model

ID	Description	n-value
11	Open Water	0.022
21	Developed, Open Space	0.12
22	Developed, Low Intensity	0.121
23	Developed, Medium Intensity	0.05
24	Developed, High Intensity	0.05
31	Barren Land	0.04
41	Deciduous Forest	0.16
42	Evergreen Forest	0.18
43	Mixed Forest	0.17
52	Shrub/Scrub	0.07
71	Grassland/Herbaceous	0.035
81	Pasture/Hay	0.033
82	Cultivated Crops	0.04
90	Woody Wetlands	0.14
95	Emergent Herbaceous	0.035

Sixteen simulations runs for the riverine analysis of the project area. The eight existing condition runs used a downstream gulf boundary stage of 1.2 ft NAVD 88, while the eight future condition runs used a downstream gulf stage boundary of 3.0 ft. NAVD88 to account for the +1.8ft intermediate sea level rise scenario. The 50, 20, 10, 5% AEP frequencies were run with the Atchafalaya flow only. The 2, 1, 0.5, and 0.2% AEP frequencies included the contribution from the Morganza spillway. All were run for 2 months, allowing enough duration for the system to achieve steady state. The riverine bathymetry is considered to be static for all runs, assuming no scour or accretion in the channel. The steady state scenarios are presented graphically in Figure 21 and tabled in Table 4. Existing conditions results are presented in figures 22 through 29 and the Future conditions are presented in figures 30 through 37.

Table 3. Flow Frequency Chart For 30% Latitude Flow Into The Atchafalaya River

HEC-SSP 2.0 - 30 Percent of Total Latitude Flow

Frequency Curve for: 30% Latitude Flow-TOTAL-FLOW				
Percent Chance Exceedance	Computed Curve Flow in cfs	Expected Prob. Flow in cfs	Confidence Limits Flow in cfs	
			0.05	0.95
0.1	862.0	900.7	988.4	779.2
0.2	823.6	854.1	936.5	748.8
0.3333	795.0	820.1	898.2	726.0
0.5	771.9	793.4	867.7	707.5
0.6667	755.5	774.4	845.9	694.2
1.0	732.0	747.8	815.1	675.2
1.25	718.9	733.1	798.1	664.5
2.0	690.9	702.0	761.8	641.5
5.0	633.9	640.2	689.2	594.1
10.0	587.6	591.2	631.5	554.7
20.0	536.3	538.1	569.6	509.8
50.0	451.4	451.4	473.3	430.5
80.0	381.1	379.9	400.9	358.7
90.0	349.1	347.1	369.7	325.0
95.0	325.0	322.0	346.5	299.3
99.0	284.5	279.0	307.8	256.3

System Statistics	
Log Transform: Flow	
Statistic	Value
Mean	2.655
Standard Dev	0.088
Station Skew	0.116
Regional Skew	-0.100
Weighted Skew	0.059
Adopted Skew	0.059

Number of Events	
Event	Number
Historic Events	0
High Outliers	0
Low Outliers	0
Zero Or Missing	0
Systematic Events	51
Historic Period	

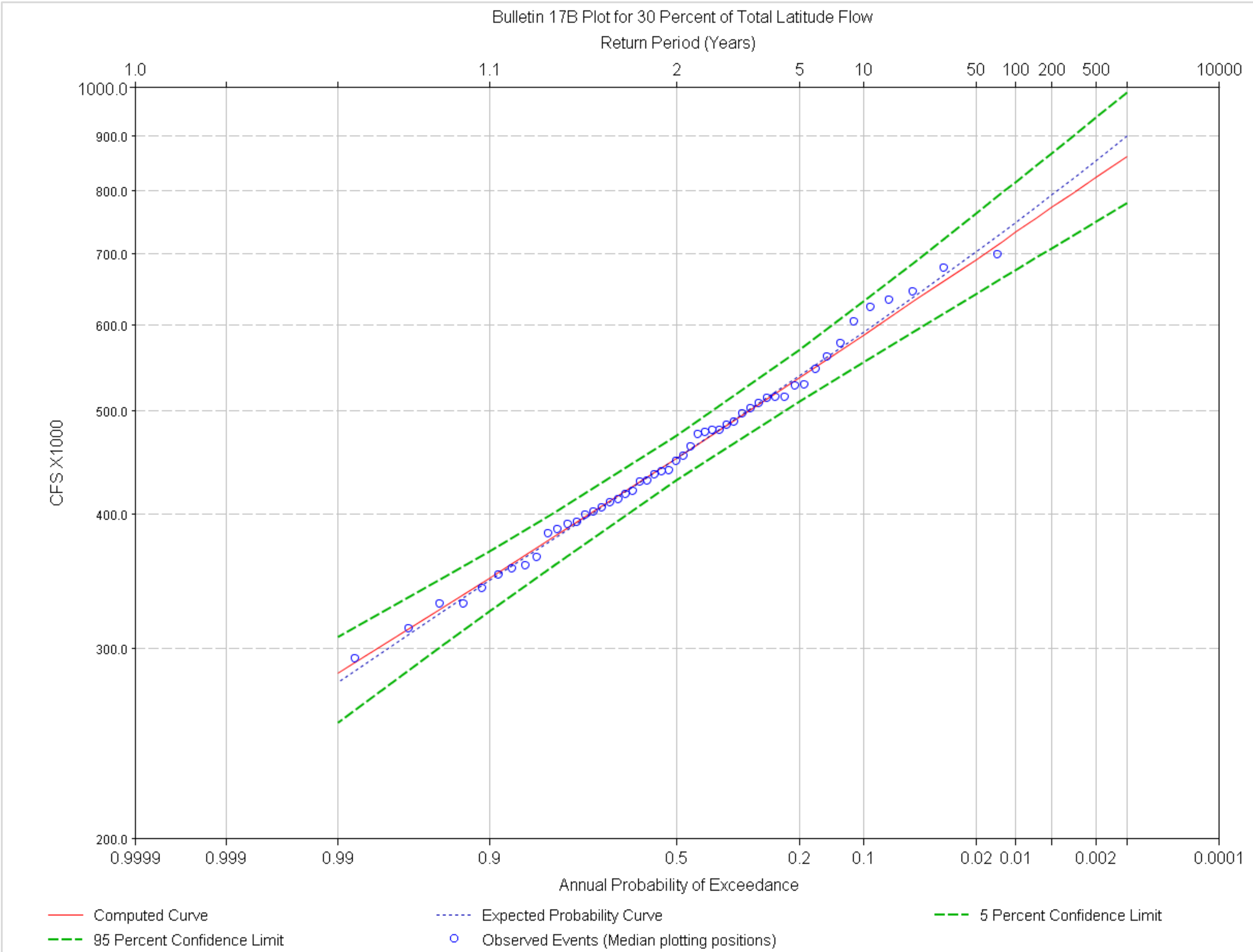

Figure 20. Graphical Representation Of The Estimated Flow Frequency Relationship At Simmesport (30% Latitudinal Flow)

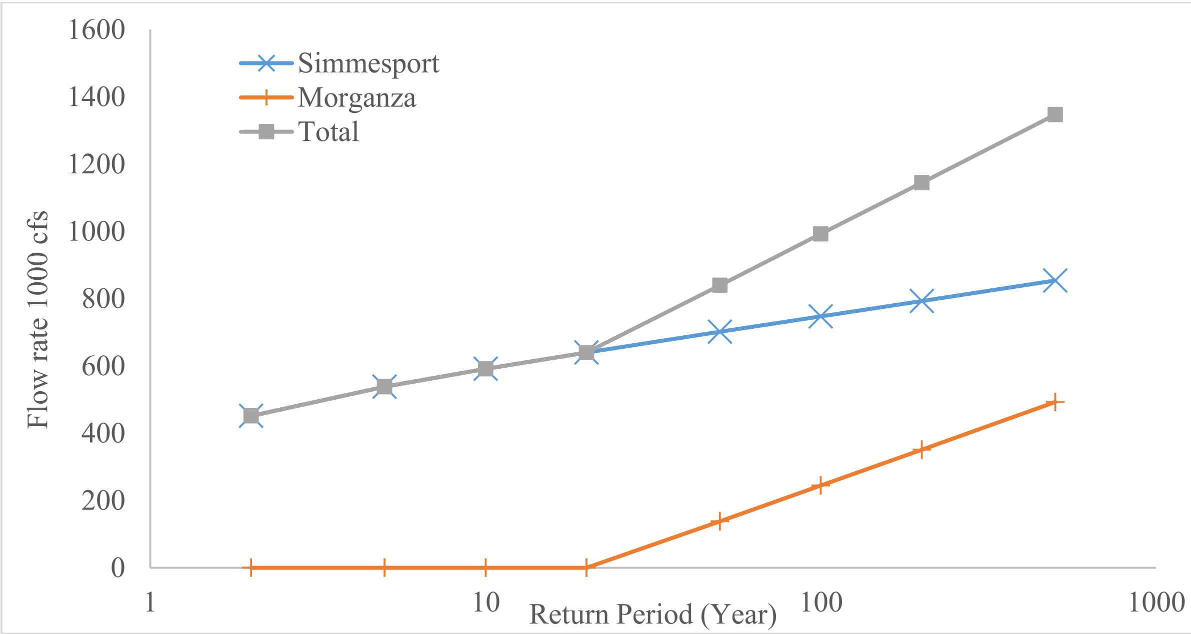

Figure 21. Flow Rates Vs Return Period For Riverine Boundaries (Simmesport And Morganza)

Table 4. 16 Modeled Scenarios For Riverine Analysis

Return (% AEP)	Simmesport (x1000 cfs)	Morganza (x1000 cfs)	Gulf stage (ft NAVD88)
0.2	854.1	492.9	1.2
0.5	793.4	351.3	1.2
1	747.8	244.9	1.2
2	702	138.0	1.2
50	640.2	0.0	1.2
10	591.2	0.0	1.2
20	538.1	0.0	1.2
5	451.4	0.0	1.2
0.2	854.1	492.9	1.8
0.5	793.4	351.3	1.8
1	747.8	244.9	1.8
2	702	138.0	1.8
25	640.2	0.0	1.8
10	591.2	0.0	1.8

20	538.1	0.0	1.8
50	451.4	0.0	1.8

3.2 Existing Conditions Results

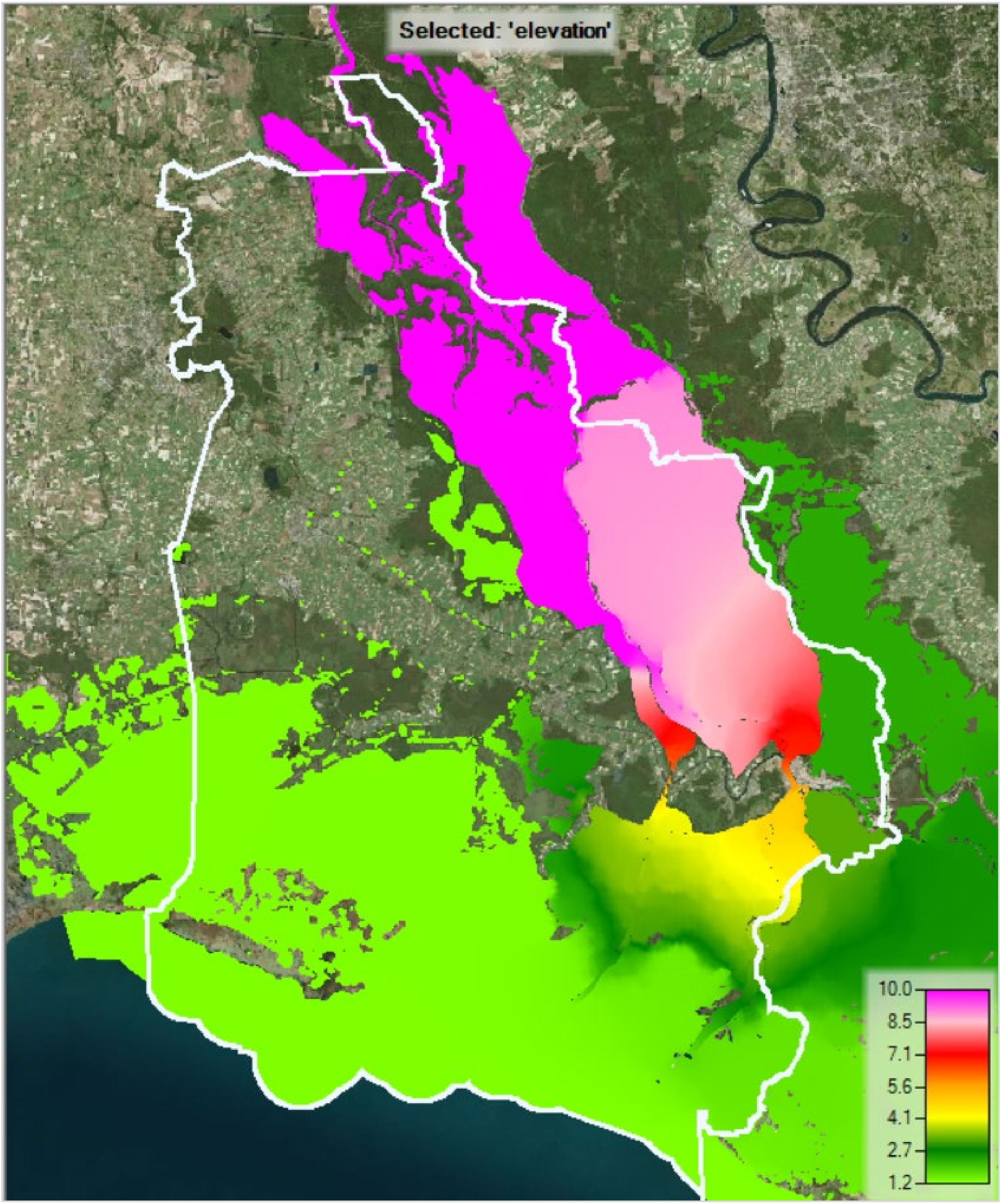

Figure 22. 50% AEP Existing Conditions Max Steady State Riverine Water Levels In Ft. Navd88.

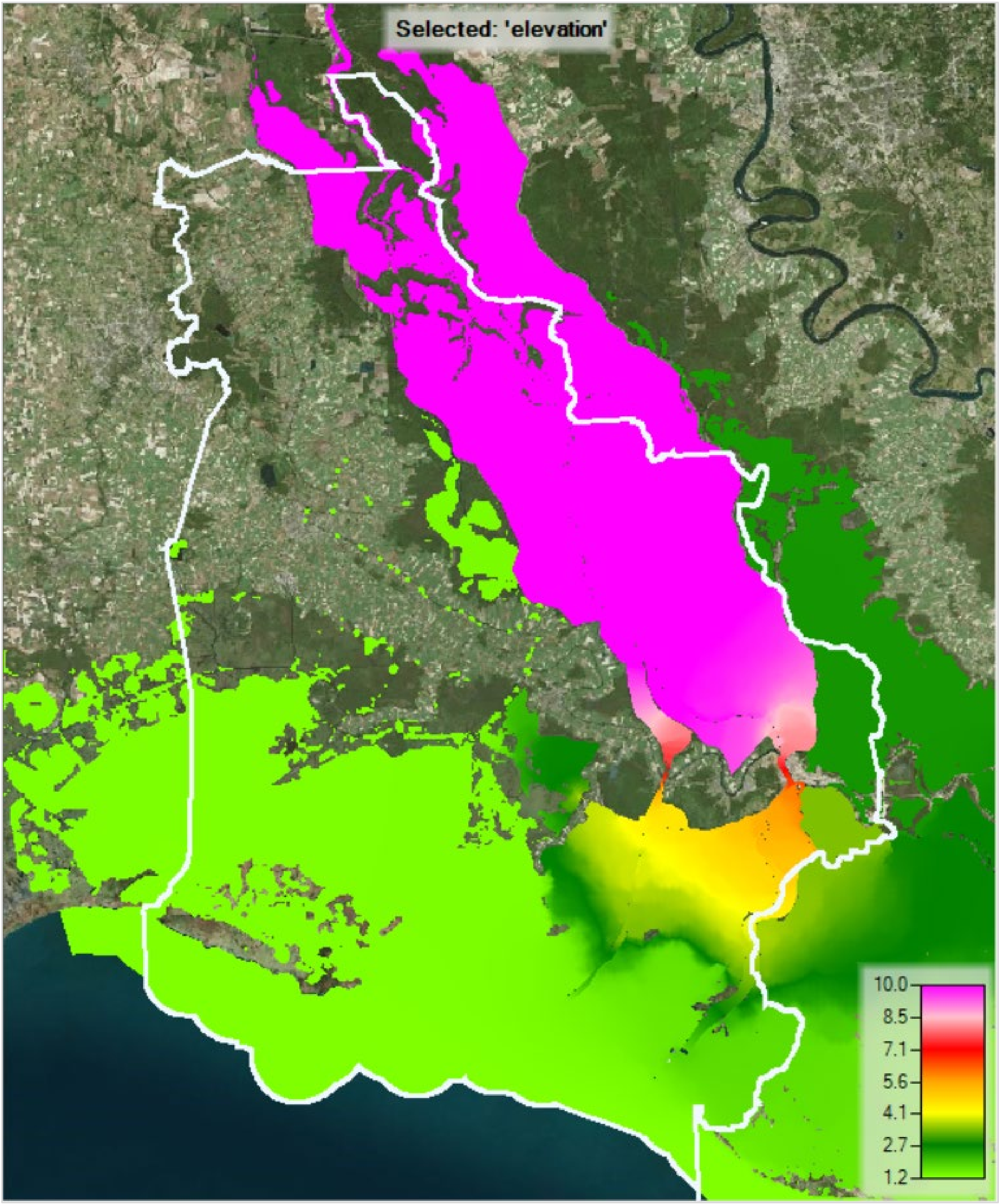

Figure 23. 20% AEP Existing Conditions Max Steady State Riverine Water Levels In Ft. Navd88.

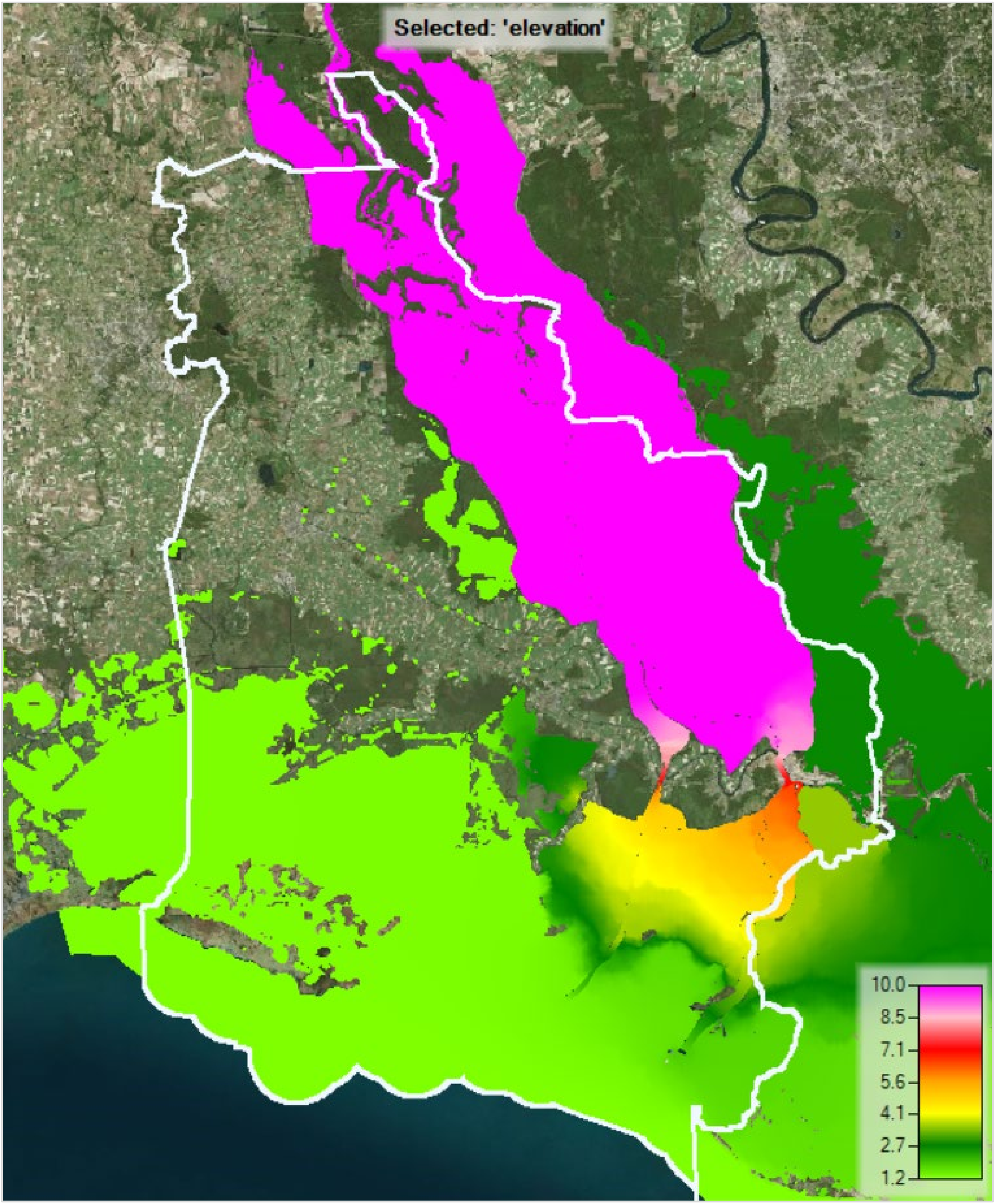

Figure 24. 10% AEP Existing Conditions Max Steady State Riverine Water Levels In Ft. Navd88.

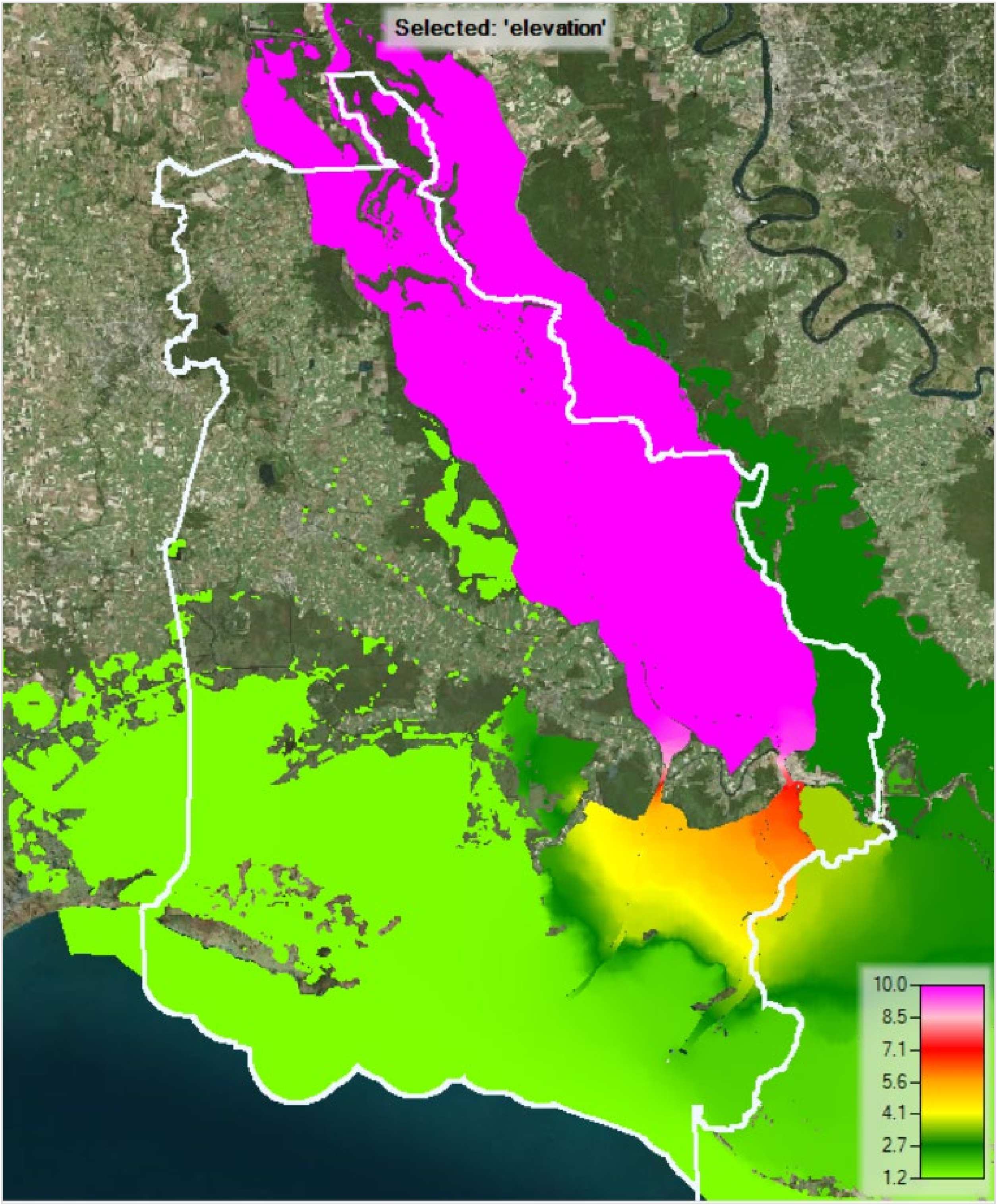

Figure 25. 5% AEP Existing Conditions Max Steady State Riverine Water Levels In Ft. Navd88.

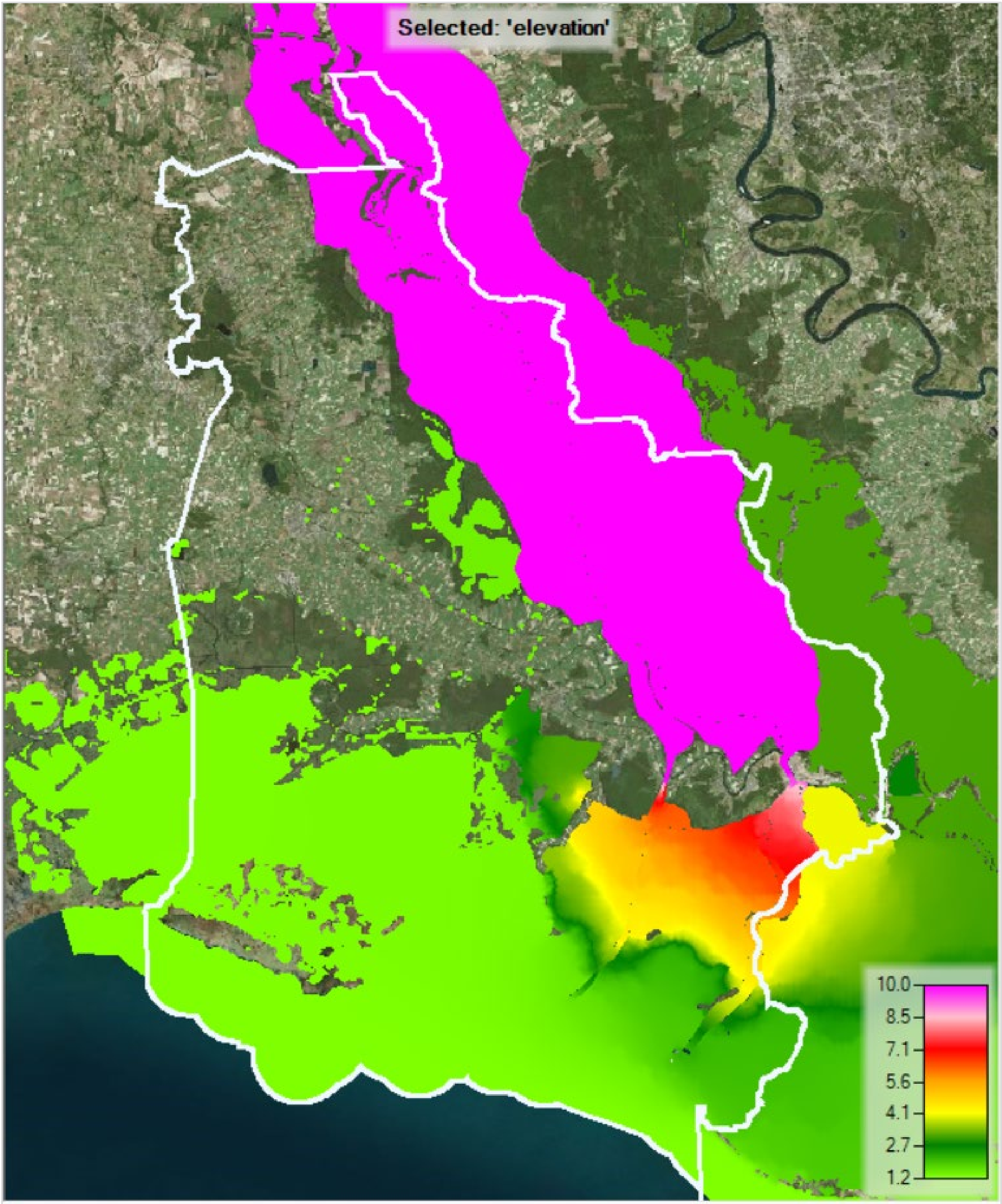

Figure 26. 2% AEP Existing Conditions Max Steady State Riverine Water Levels In Ft. Navd88.

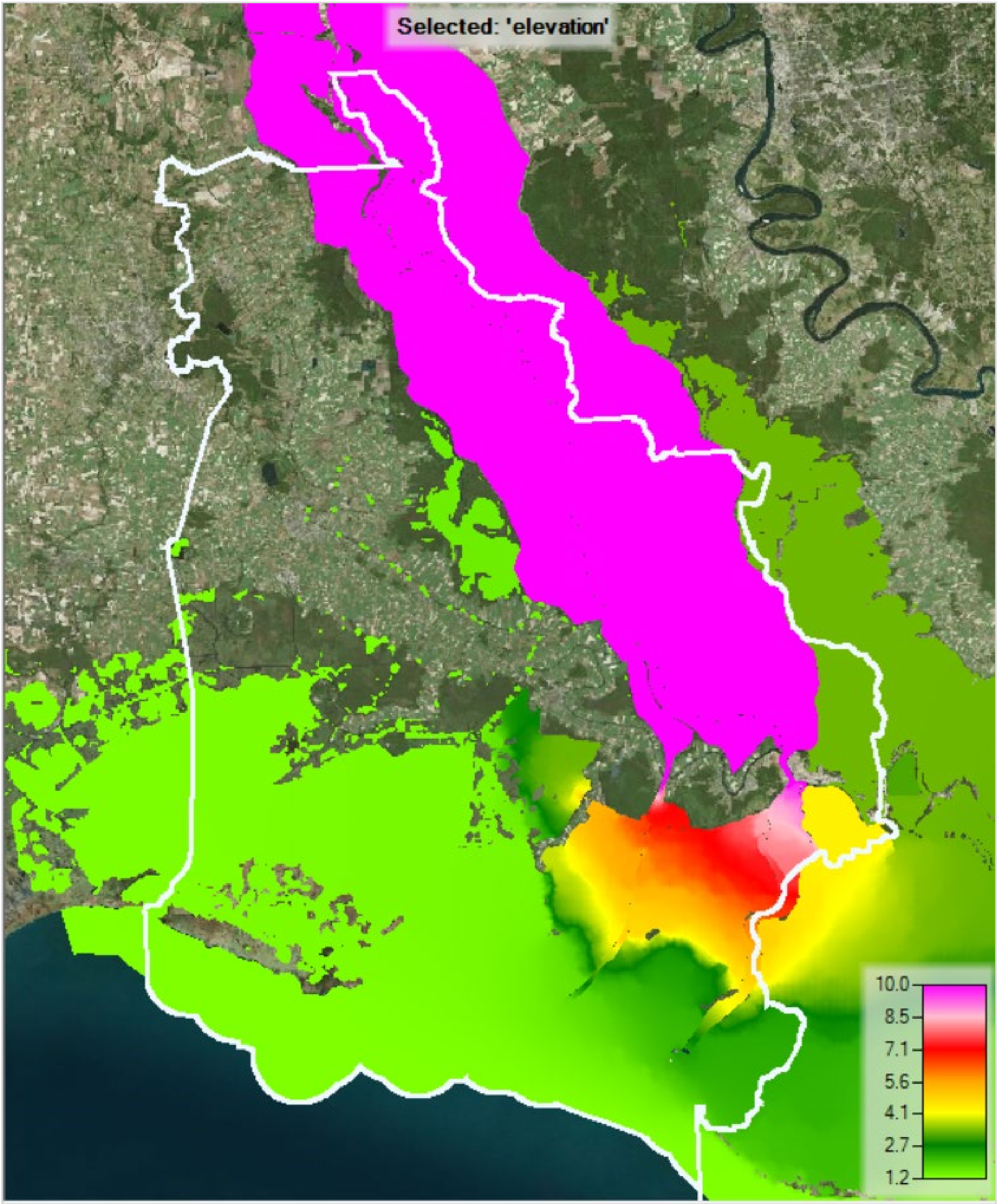

Figure 27. 1% AEP Existing Conditions Max Steady State Riverine Water Levels In Ft. Navd88.

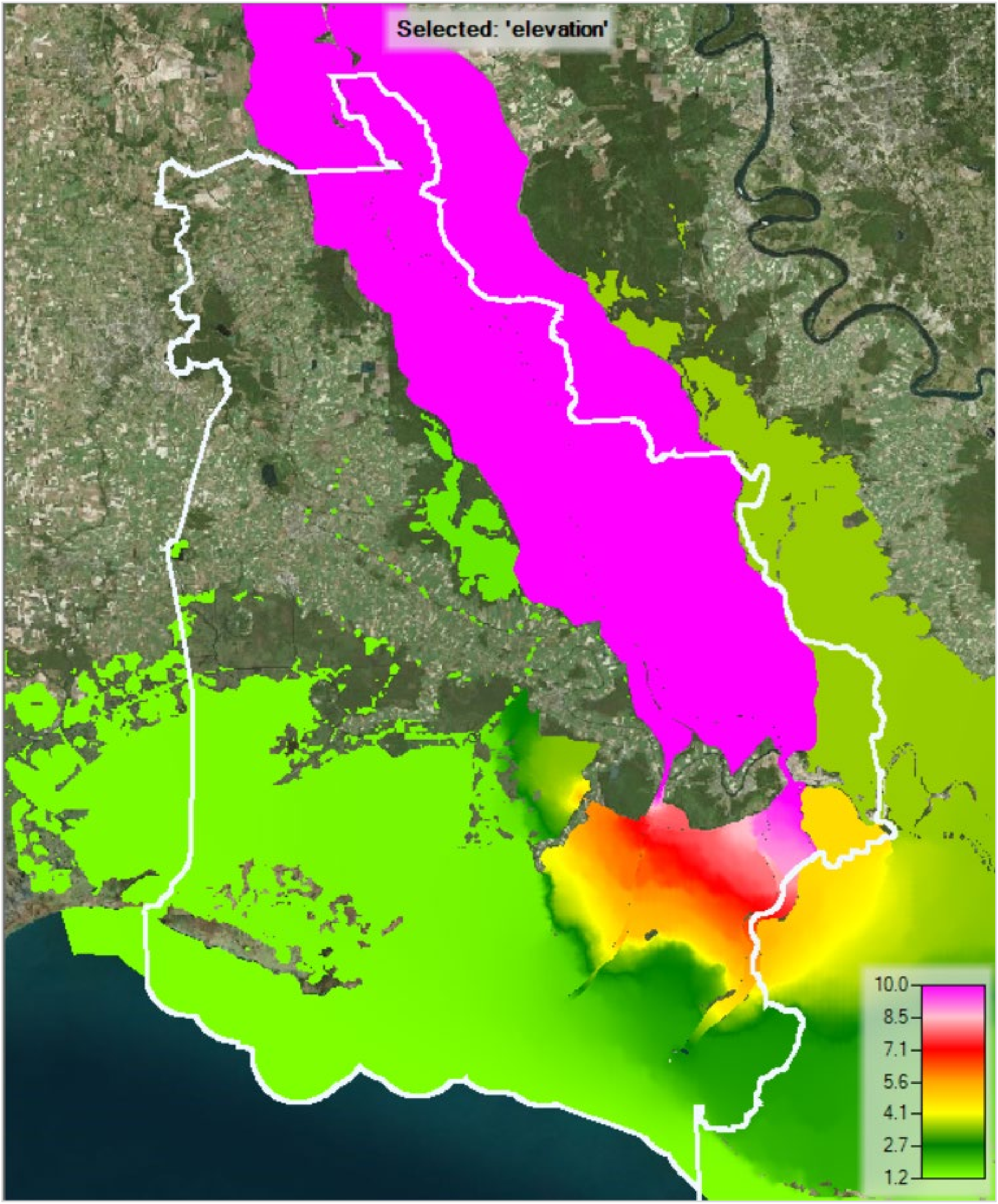

Figure 28. 0.5% AEP Existing Conditions Max Steady State Riverine Water Levels In Ft. Navd88.

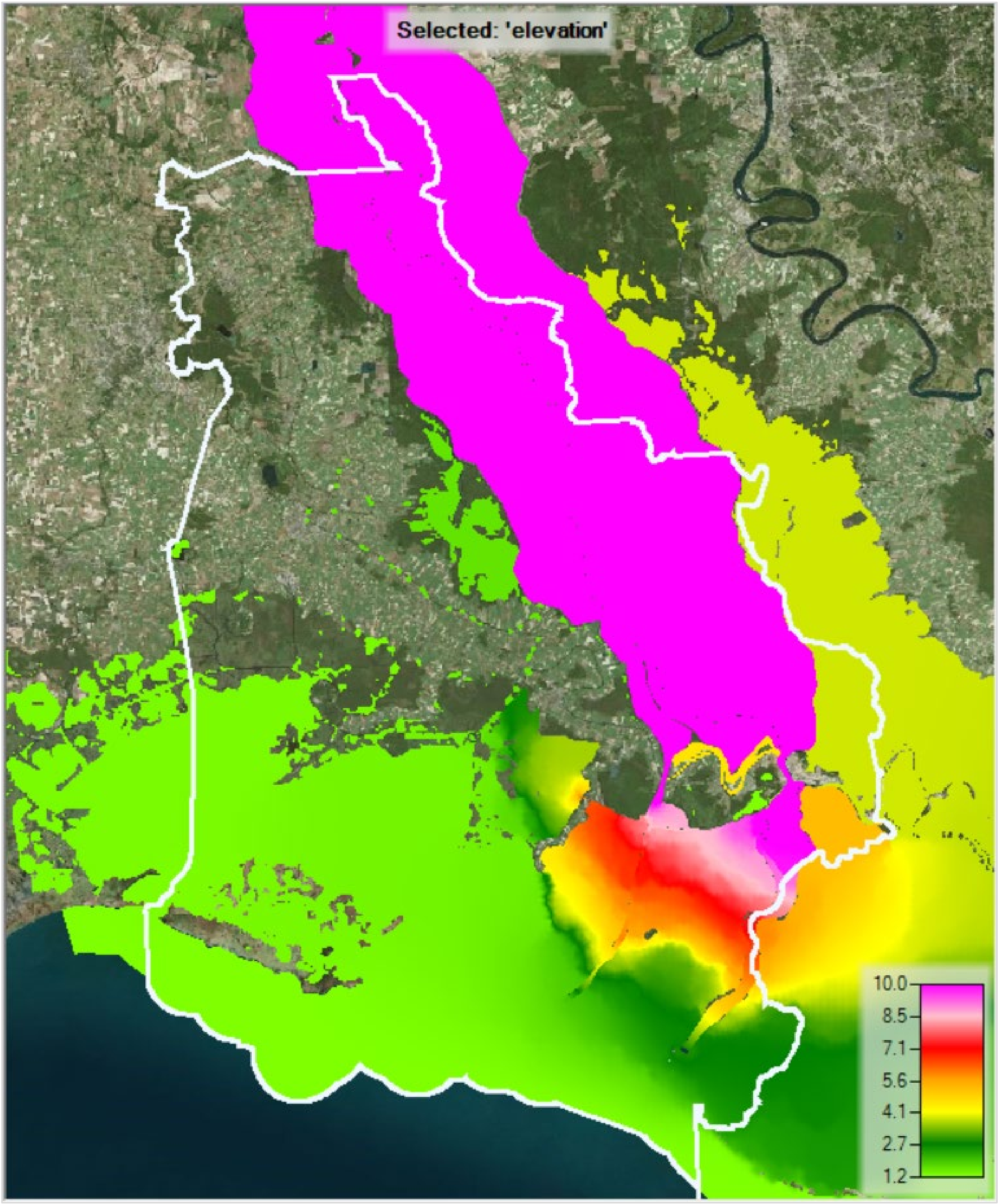

Figure 29. 0.2% AEP Existing Conditions Max Steady State Riverine Water Levels In Ft. Navd88.

3.3 Future Conditions Results

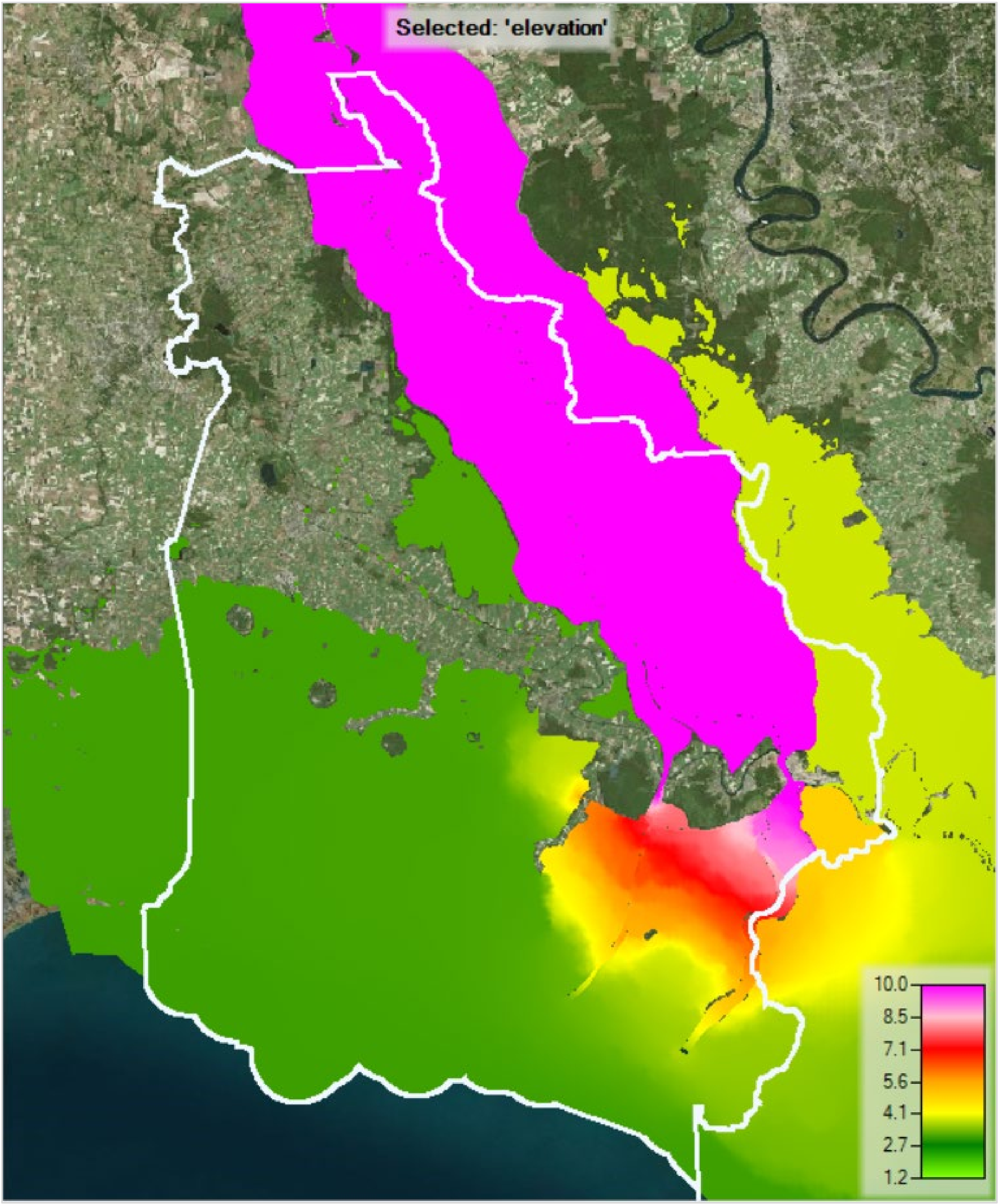

Figure 30. 50% AEP Future Conditions Max Steady State Riverine Water Levels In Ft. Navd88.

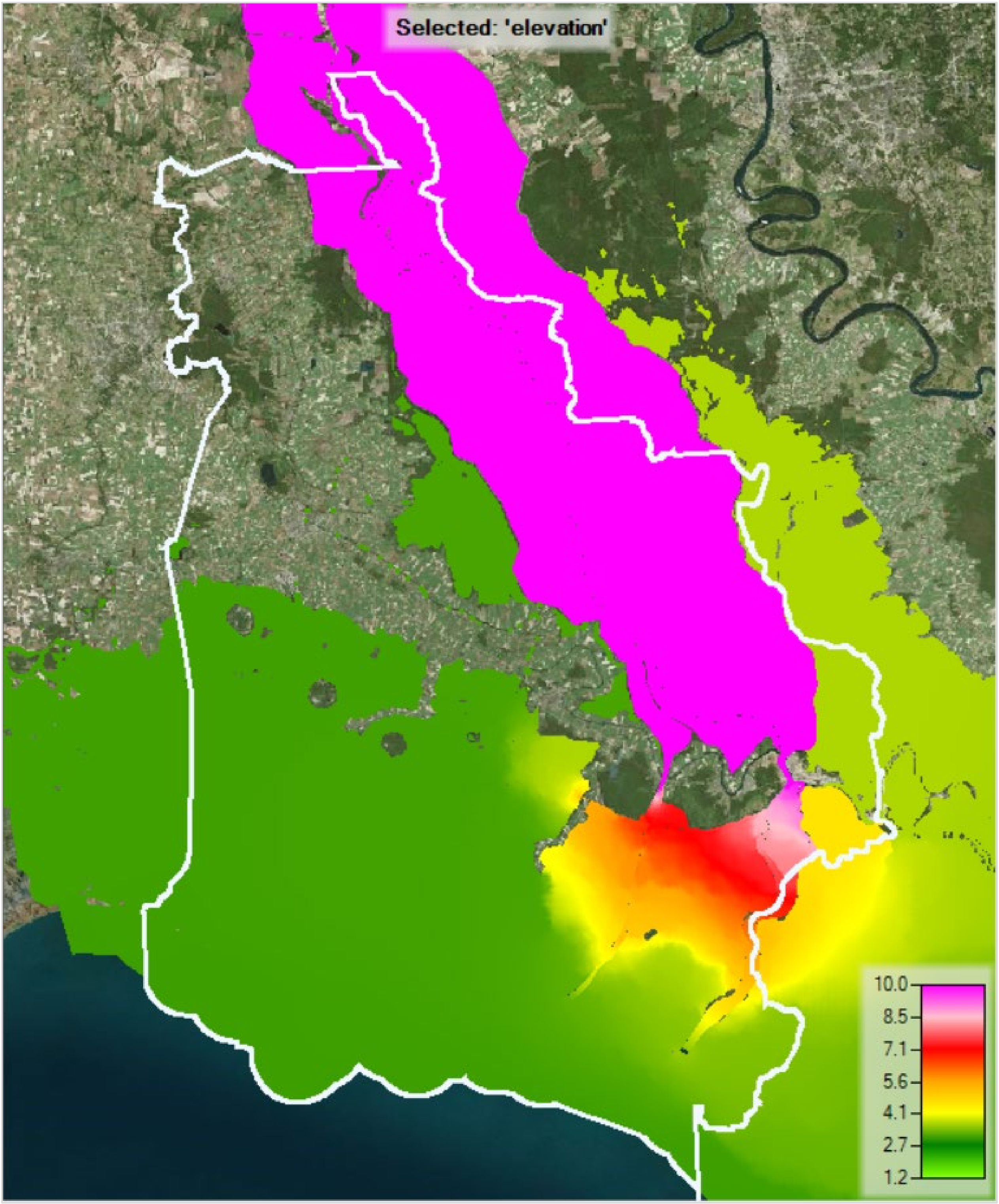

Figure 31. 20% AEP Future Conditions Max Steady State Riverine Water Levels In Ft. Navd88.

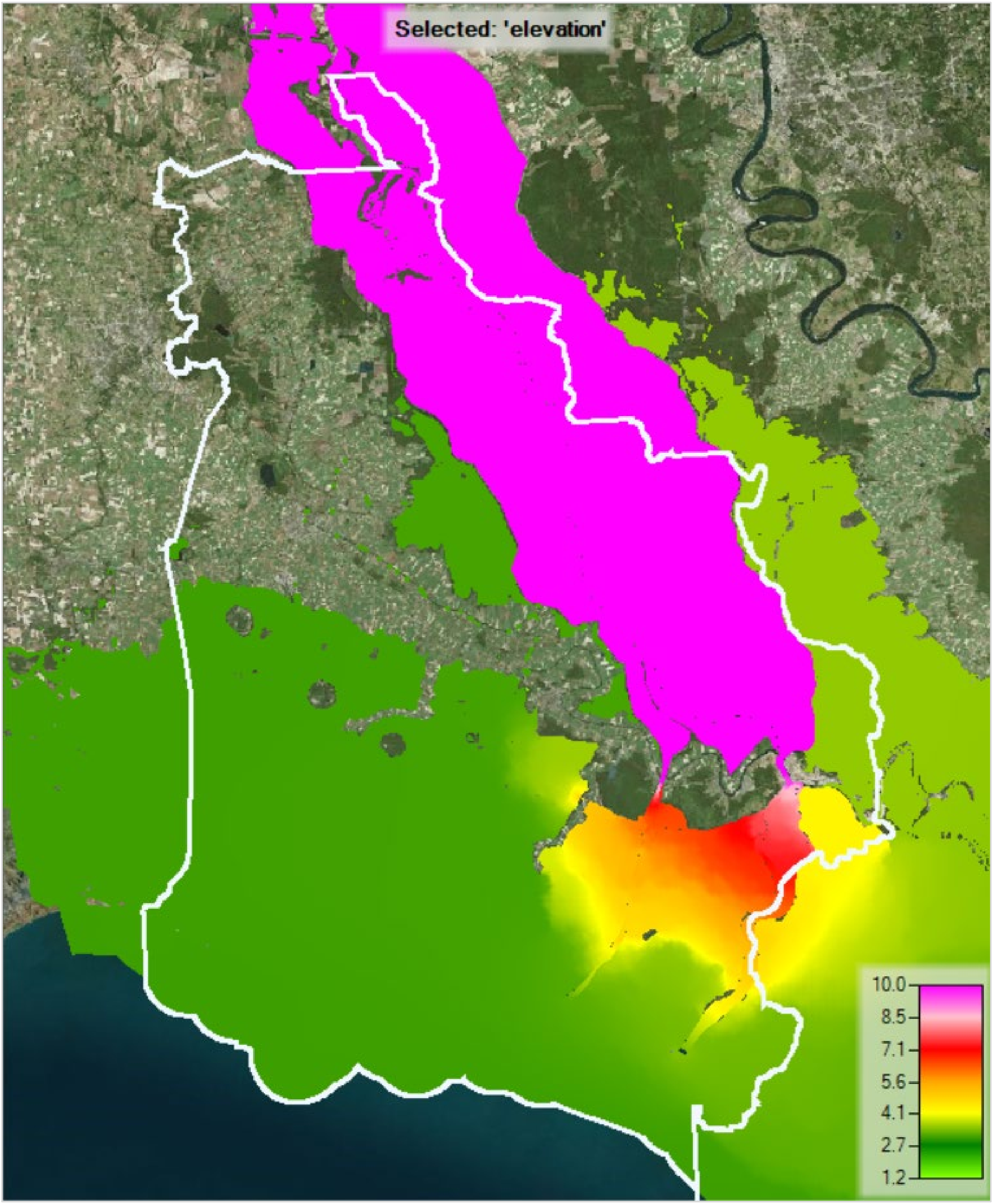

Figure 32. 10% AEP future conditions max steady state riverine water levels in ft. NAVD88.

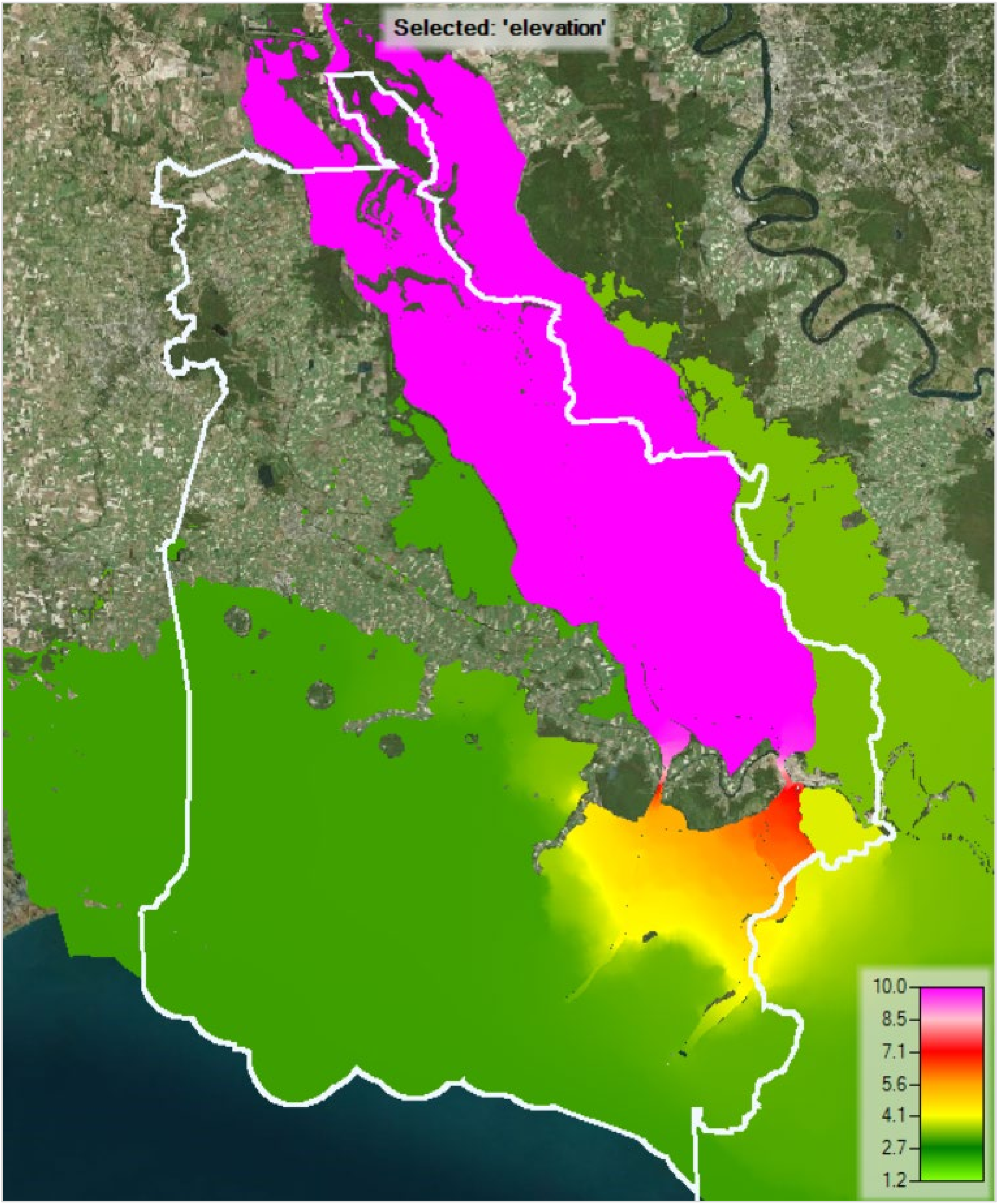

Figure 33. 5% AEP Future Conditions Max Steady State Riverine Water Levels In Ft. Navd88.

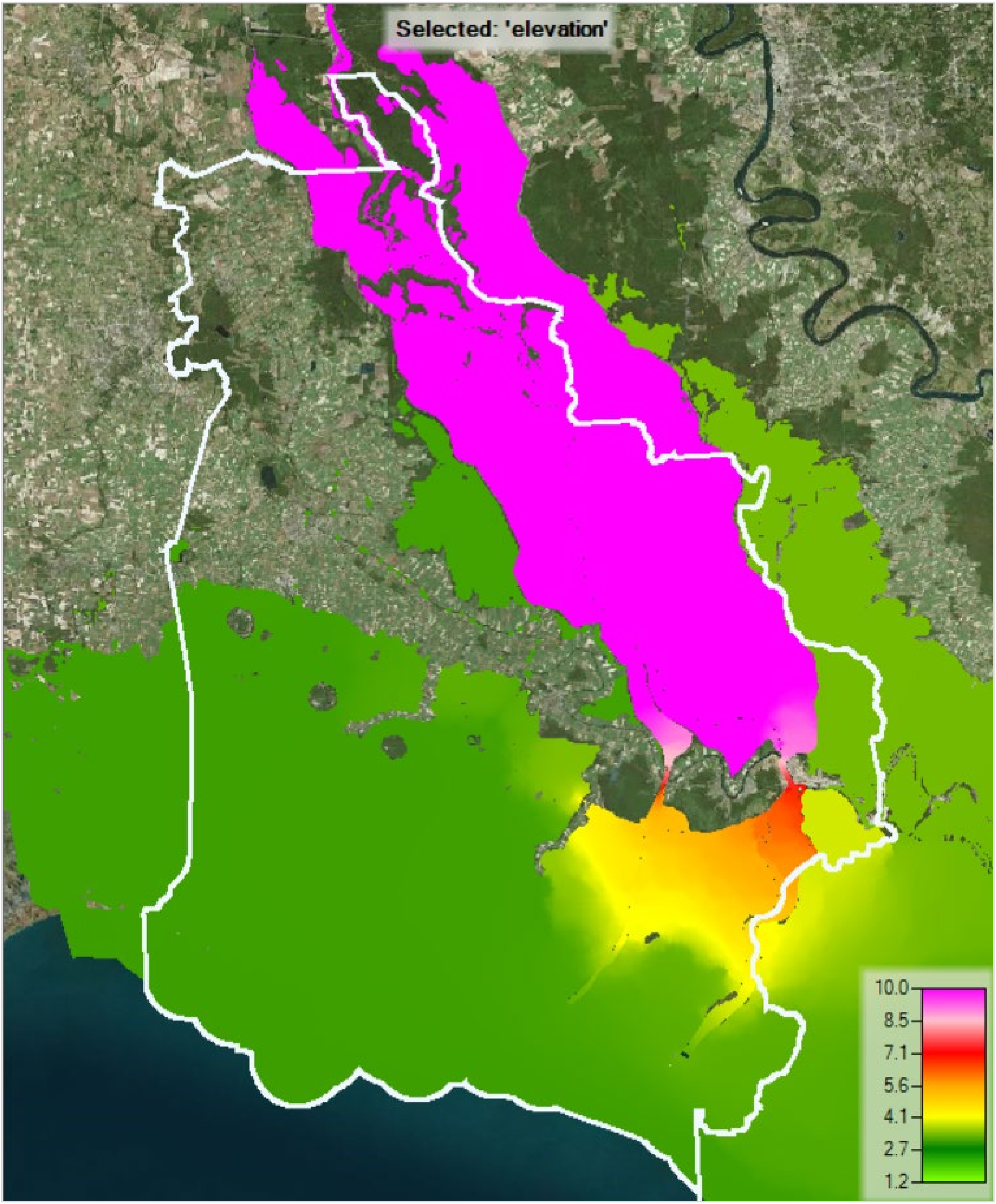

Figure 34. 2% AEP Future Conditions Max Steady State Riverine Water Levels In Ft. Navd88.

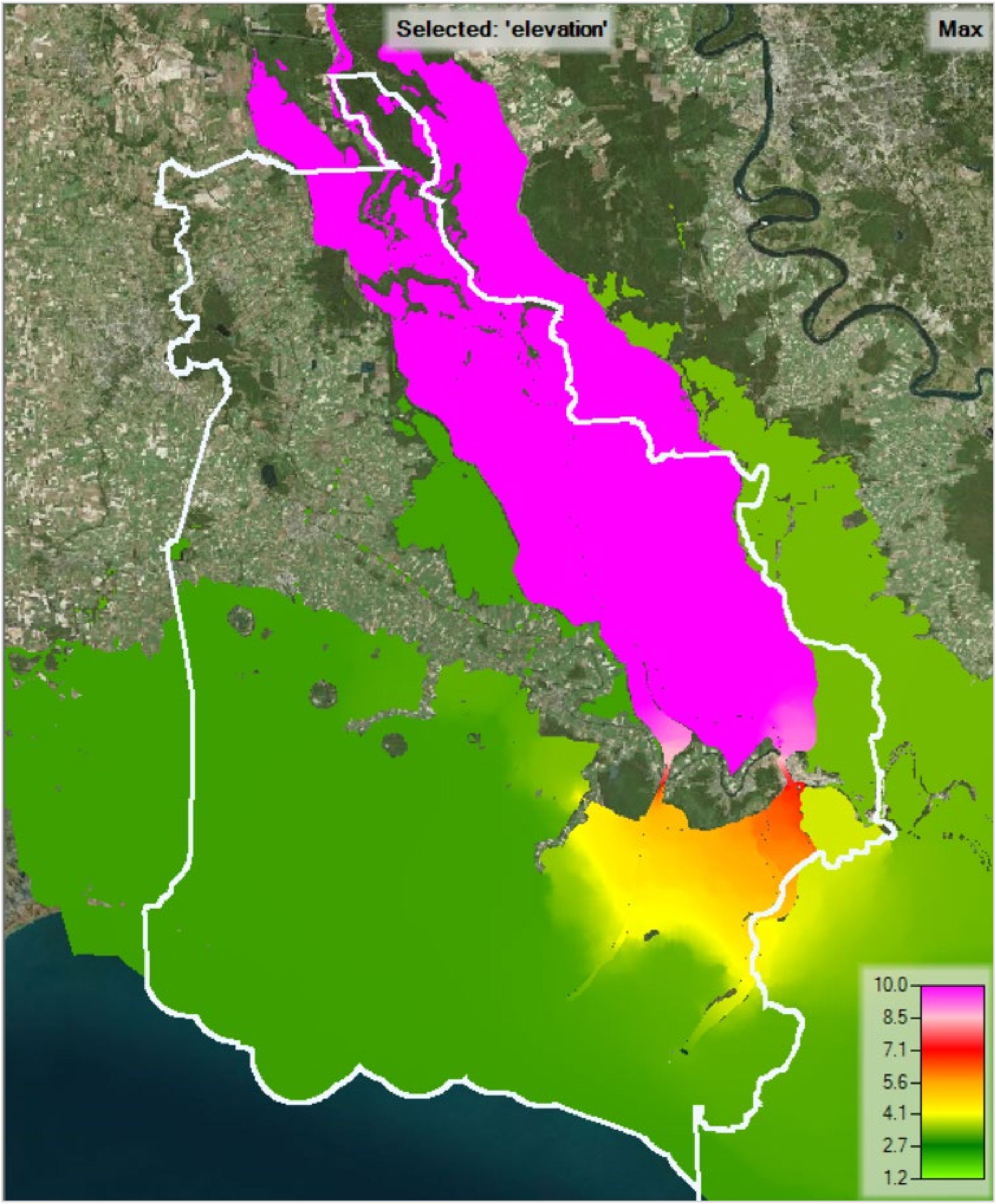

Figure 35. 1% AEP Future Conditions Max Steady State Riverine Water Levels In Ft. Navd88.

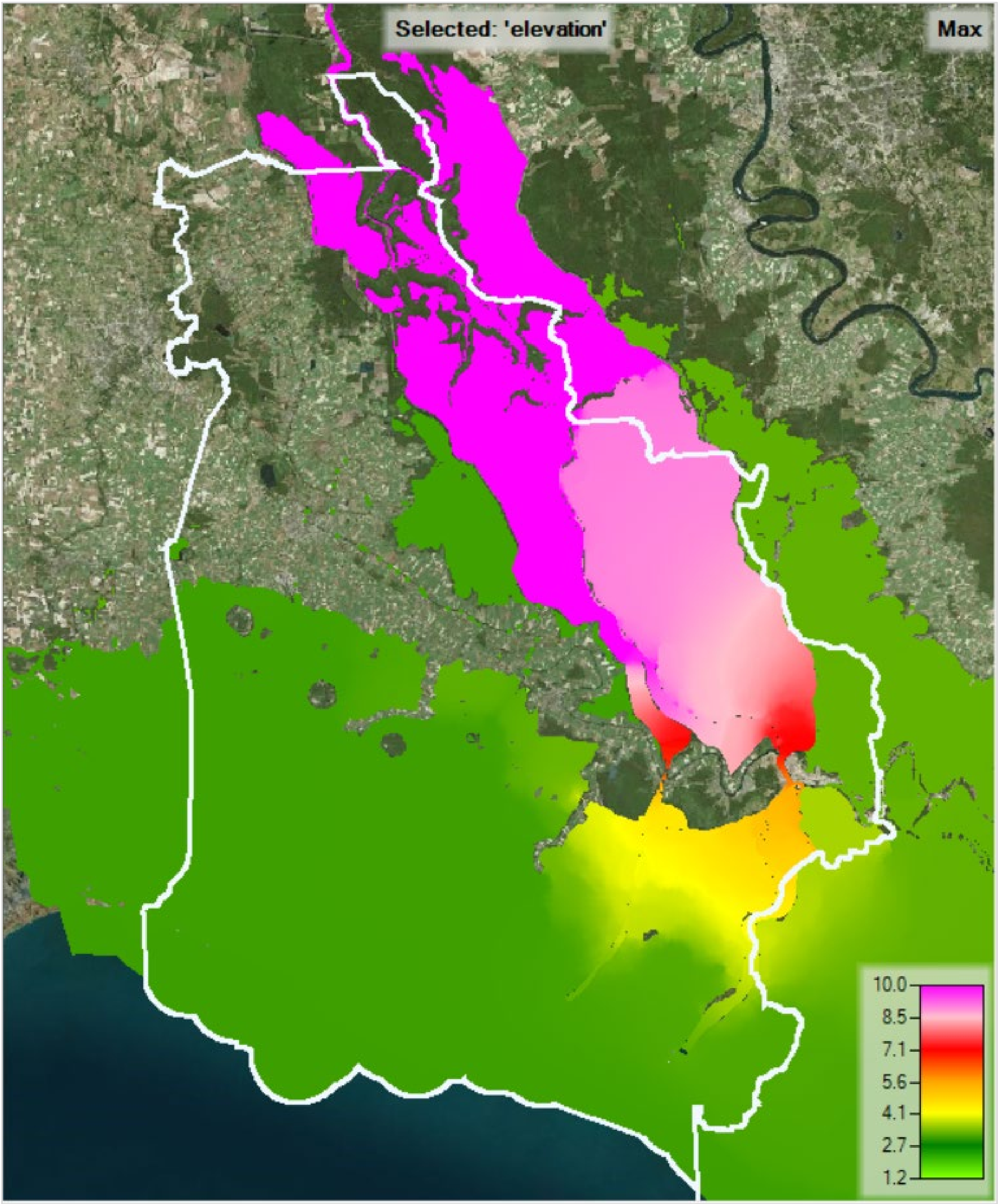

Figure 36. 0.5% AEP Future Conditions Max Steady State Riverine Water Levels In Ft. Navd88.

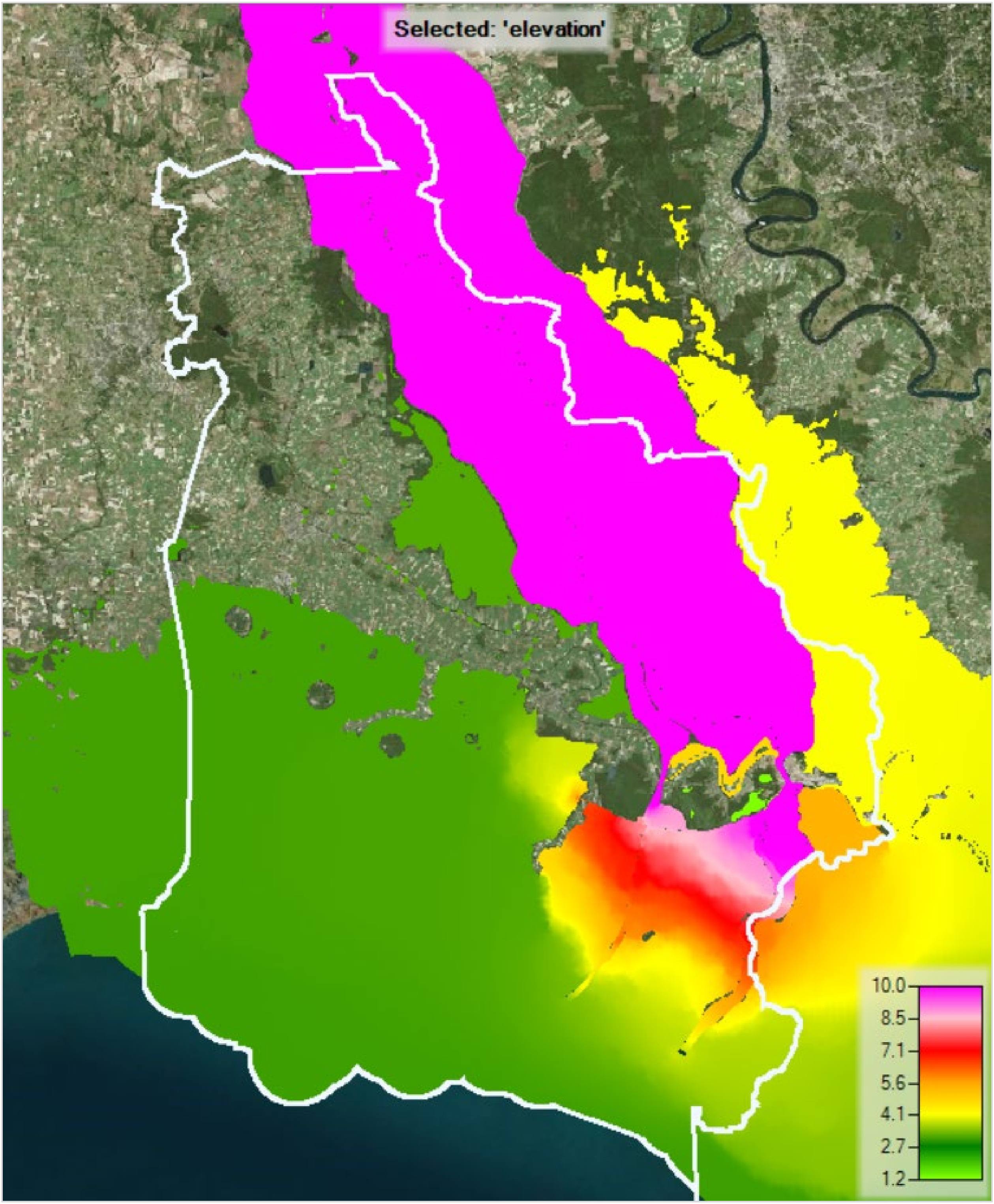

Figure 37. 0.2% AEP Future Conditions Max Steady State Riverine Water Levels In Ft. Navd88.

3.4 Conclusions

The impact of riverine flooding on the proposed levee alternatives is considered to be negligible as these levees are too far west of the hydraulic area of influence. The levees west of Berwick and the Bayou Sale levee choke the flow traveling west out of the Wax Lake delta through the GIWW. The stages reach near gulf level quickly beyond Morgan City and the Wax Lake outlet. The extent of this flooding is presented in Figure 38. The proposed levee alignments are pictured in the west side of the authorization zone (black line).

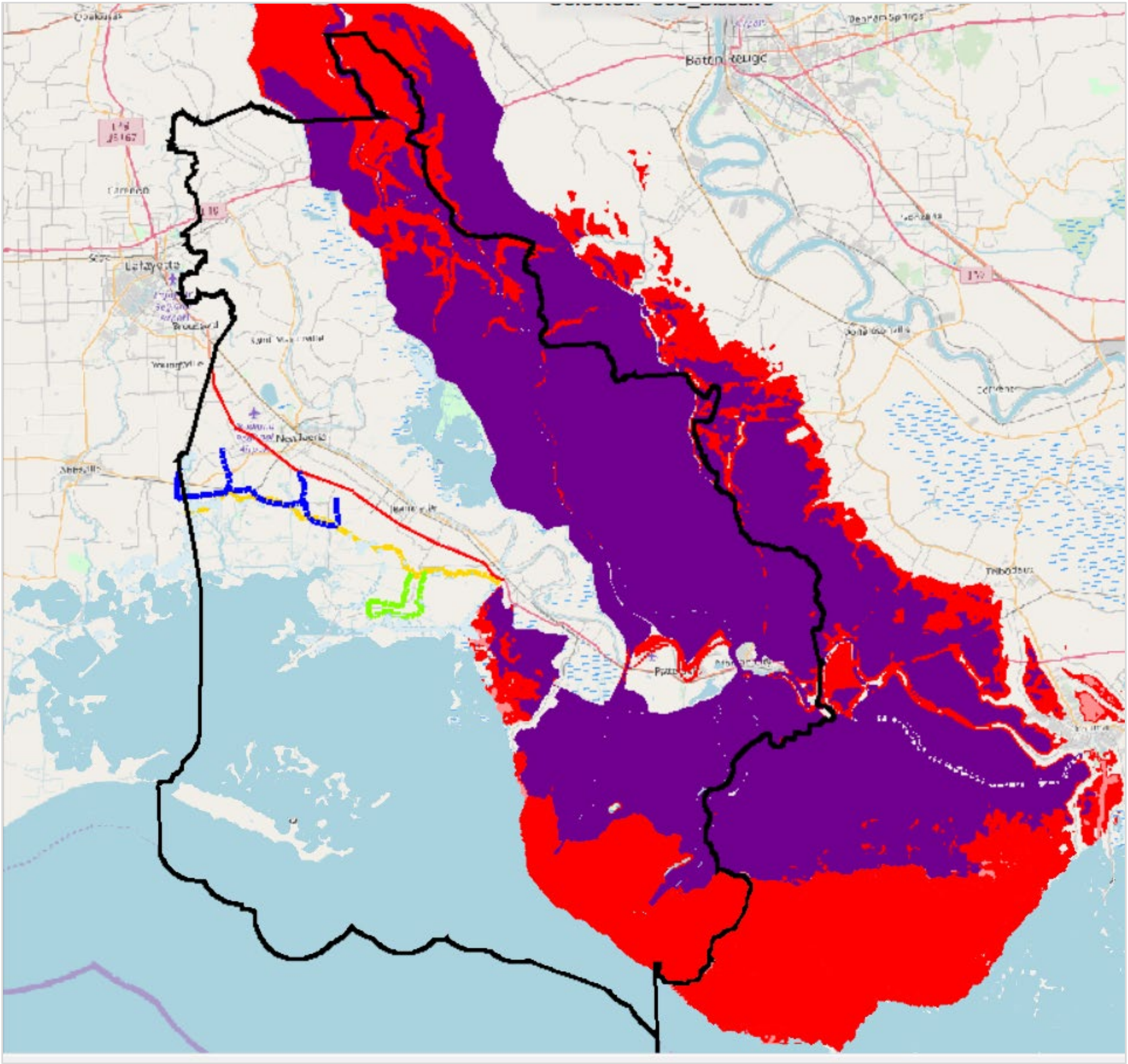

Figure 38. Extent Of Riverine Flooding Greater Than 0.5ft Above G.O.M Stage For 50 % (Purple) And 0.2% AEP (Red) Existing.

4. Levee Heights

The existing (2025) and future (2075) 2% and 1% hydraulic boundary conditions were used to compute the 2%, and 1% annual exceedence levee design elevations. All levees were designed using a slope of 1 on 4. The design criteria for the levees are as follows:

For the design still water, wave height and wave period, the maximum allowable average wave overtopping of 0.1 cubic feet per second per foot (cfs/ft) at 90% level of assurance and 0.01 cfs/ft at 50% level of assurance for grass-covered levees; No minimum freeboard required.

The application of a Monte Carlo analysis was used to determine the levee design elevation. In the Monte Carlo analysis, the overtopping algorithm is repeated to compute the overtopping rate many times. Based on these outputs, a statistical distribution can be derived from the resulting overtopping rates. The parameters that are included in the Monte Carlo analysis are the surge elevation, wave height and wave period.

To determine the overtopping rate in the Monte Carlo analysis, the probabilistic overtopping formulations from Van der Meer (TAW, 2002) are applied for levees (see Figure 39). Along with the geometric parameters (levee height and slope), hydraulic input parameters for determination of the overtopping rate in Equations 1 and 2 are the water elevation (ζ), the significant wave height (H_s) and the peak wave period (T_p).

Figure 40 graphically shows the overtopping for a levee situation including the most relevant parameters. In the design process, we use the best estimate 2% and 1% values for these parameters from the JPM-OS method (Resio, 2007); uncertainty in these values exists. Resio (2007) has provided a method to derive the standard deviation in the 2% and 1% surge elevations. Standard deviation values of 10% of the average significant wave height and 20% of the peak period were used (Smith, 2006, pers. comm.). In the absence of data, all uncertainties are assumed to be normally distributed.

Van der Meer overtopping formulations

The overtopping formulation from Van der Meer reads (TAW, 2002):

$$\frac{q}{\sqrt{gH_{m0}^3}} = \frac{0.067}{\sqrt{\tan\alpha}}\gamma_b\xi_0 \exp\left(-4.75\frac{R_c}{H_{m0}}\frac{1}{\xi_0\gamma_b\gamma_f\gamma_\beta\gamma_v}\right)$$

$$\text{with}\quad \max imum: \quad \frac{q}{\sqrt{gH_{m0}^3}} = 0.2\exp\left(-2.6\frac{R_c}{H_{m0}}\frac{1}{\gamma_f\gamma_\beta}\right) \qquad (1)$$

With:

q : average overtopping rate [cfs/ft]
g : gravitational acceleration [ft/s^2]
H_{m0} : wave height at toe of the structure [ft]
ξ_0: surf similarity parameter [-]
α : slope [-]
R_c : freeboard [ft]
γ : coefficient for presence of berm (b), friction (f), wave incidence (β), vertical wall (v)

The surf similarity parameter ξ0 is defined herein as $\xi_0 = \tan\alpha / \sqrt{s_0}$ with α the angle of slope and s_0 the wave steepness. The wave steepness follows from $s0 = 2\pi H_{m0} / (g\, T_{m\text{-}10}^2)$. The coefficients -4.75 and -2.6 in Equation 1 are the mean values. The standard deviations of these coefficients are equal to 0.5 and 0.35, respectively and these errors are normally distributed (TAW, 2002). The reader is referred to TAW (2002) for definitions of the various coefficients for presence of berm, friction, wave incidence, vertical wall.

Equation 1 is valid for $\xi_0 < 5$ and slopes steeper than 1:8. For values of $\xi_0 > 7$ the following equation is proposed for the overtopping rate:

$$\frac{q}{\sqrt{gH_{m0}^3}} = 10^{-0.92}\exp\left(-\frac{R_c}{\gamma_f\gamma_\beta H_{m0}(0.33+0.022\xi_0)}\right) \qquad (2)$$

The overtopping rates for the range $5 < \xi_0 < 7$ are obtained by linear interpolation of Equation 1 and 2 using the logarithmic value of the overtopping rates. For slopes between 1:8 and 1:15, the solution should be found by iteration. If the slope is less than 1:15, it should be considered as a berm or a foreshore depending on the length of the section compared to the deep water wavelength. The coefficients -0.92 is the mean value. The standard deviation of this coefficient is equal to 0.24 and the error is normally distributed (TAW, 2002).

Figure 39 - Van der Meer Overtopping Formula

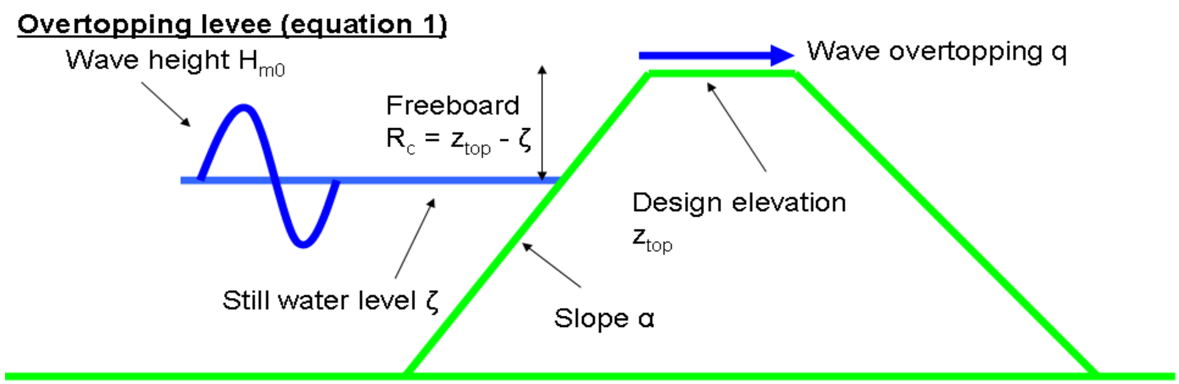

Figure 40. - Definition for Overtopping for Levee

The Monte Carlo Analysis is executed as follows:

1. Draw a random number between 0 and 1 to set the exceedence probability (p).
2. Compute the water elevation from a normal distribution using the mean 1% surge elevation and standard deviation as parameters and with an exceedence probability (p).
3. Draw a random number between 0 and 1 to set the exceedence probability (p).
4. Compute the wave height and wave period from a normal distribution using the mean 1% wave height/wave period and the associated standard deviation and with an exceedence probability (p).
5. Repeat step 3 and 4 for the three overtopping coefficients independently.
6. Compute the overtopping rate for these hydraulic parameters and overtopping coefficients determined in step 2, 4 and 5 using the Van der Meer overtopping formulations for levees or the Franco & Franco equation for floodwalls (see Equations 1 and 2 in the textbox).
7. Repeat the Step 1 through 5 a large number of times. (N)
8. Compute the 50% and 90% confidence limit of the overtopping rate. (i.e. q_{50} and q_{90})

The procedure is implemented in the numerical software package MATLAB because it is a computationally intensive procedure. MATLAB is a high-level technical computing language and interactive environment for algorithm development, data visualization, data analysis, and numeric computation.

The results were compiled for the 2% and 1% elevations for existing and future conditions. The segments for each levee alignment are presented in figures 41 through 44 and the data is tabulated in tables 5 – 20.

Hydraulic Reach	SWE (ft)	Std. Dev.	Hs (ft)	Tp (s)	Levee Elevation (ft) NAVD88(2004.65)
1	8.7	1.2	3.0	7.0	15.0
2	8.4	1.2	2.0	7.0	12.5
3	7.7	1.2	3.0	7.0	14.0
4	7.4	1.2	2.0	7.0	11.5
5	6.5	1.2	2.0	7.0	10.5
6	6.0	1.2	1.5	5.0	8.5
7	5.9	1.2	1.5	5.0	8.5
8	6.1	1.2	3.0	5.0	10.5
9	6.5	1.2	1.5	8.0	9.0
10	6.3	1.2	3.0	7.0	11.5

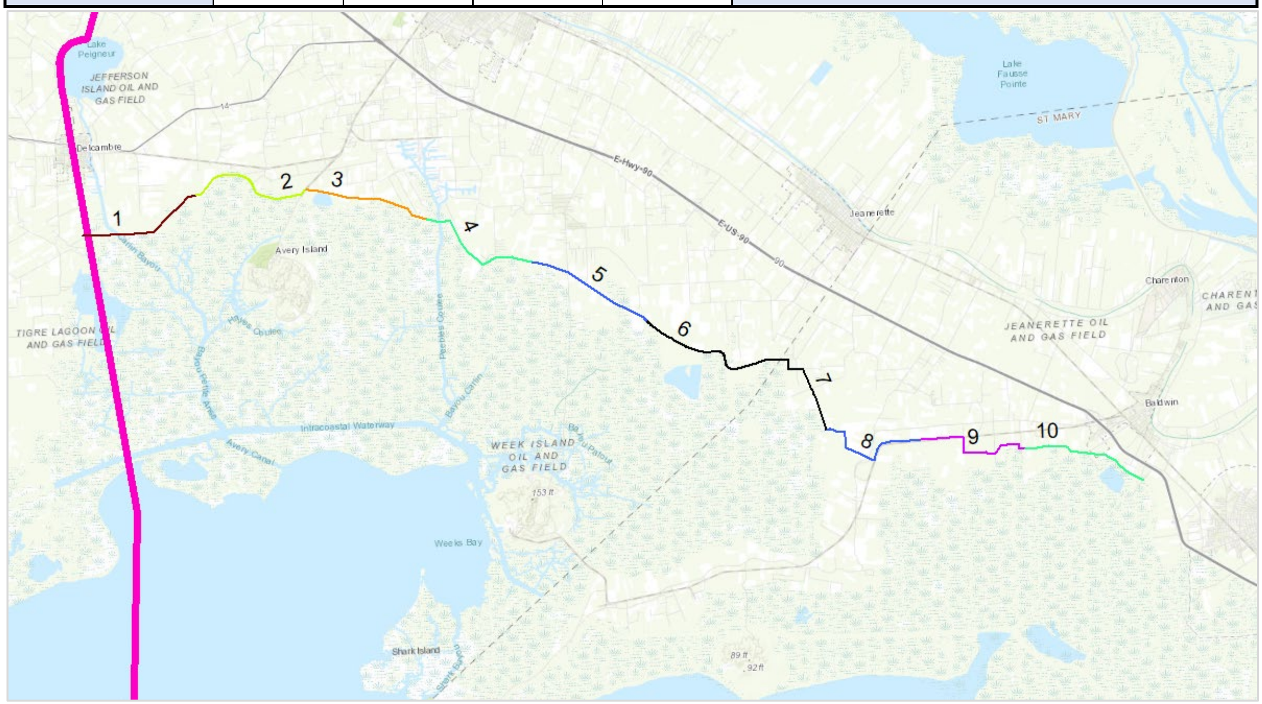

Figure 41. Segments Of The CLA

Table 5. Existing Conditions 2% Surge, Wave Parameters & Levee Elevations For The Comprehensive Levee Alignment.

Table 6. Existing Conditions 1% Surge And Wave Parameters With Levee Elevations For The Comprehensive Levee Alignment.

Hydraulic Reach	SWE (ft)	Std. Dev.	Hs (ft)	Tp (s)	Levee Elevation (ft) NAVD88(2004.65)
1	10.3	1.2	4.0	8.0	19.5
2	9.9	1.2	3.0	8.0	16.5
3	9.3	1.2	4.0	8.0	17.5
4	9.0	1.2	3.0	8.0	15.5
5	8.3	1.2	3.0	8.0	15.0
6	8.0	1.2	2.0	7.0	12.0
7	7.8	1.2	2.0	8.0	11.5
8	7.8	1.2	4.0	7.0	14.5
9	8.0	1.2	4.0	8.0	15.0
10	7.8	1.2	4.0	8.0	15.0

Table 7. Future Conditions 2% Surge And Wave Parameters With Levee Elevations For The Comprehensive Levee Alignment

Hydraulic Reach	SWE (ft)	Std. Dev.	Hs (ft)	Tp (s)	Levee Elevation (ft) NAVD88(2004.65)
1	11.1	1.2	4.0	7.0	20.0
2	10.8	1.2	3.5	7.0	18.5
3	10.2	1.2	3.5	7.0	18.0
4	9.9	1.2	3.0	7.0	16.5
5	9.1	1.2	3.0	7.0	15.5
6	8.8	1.2	1.5	7.0	11.5
7	8.6	1.2	1.5	7.0	11.5
8	8.6	1.2	3.5	7.0	16.0
9	9.0	1.2	4.0	7.0	17.0
10	8.6	1.2	3.0	8.0	15.0

Table 8. Future Condition 1% Surge And Wave Parameters With Levee Elevations For The Comprehensive Levee Alignment.

Hydraulic Reach	SWE (ft)	Std. Dev.	Hs (ft)	Tp (s)	Levee Elevation (ft) NAVD88(2004.65)
1	12.7	1.2	5.5	8.0	24.5
2	12.5	1.2	4.5	8.0	23.0
3	12.0	1.2	4.5	8.0	22.5
4	11.7	1.2	4.0	8.0	21.0
5	11.1	1.2	4.0	8.0	20.5
6	10.9	1.2	2.5	7.0	16.0
7	10.7	1.2	2.5	8.0	16.0
8	10.4	1.2	4.5	7.0	19.5
9	10.6	1.2	5.0	8.0	20.5
10	10.2	1.2	4.0	8.0	19.5

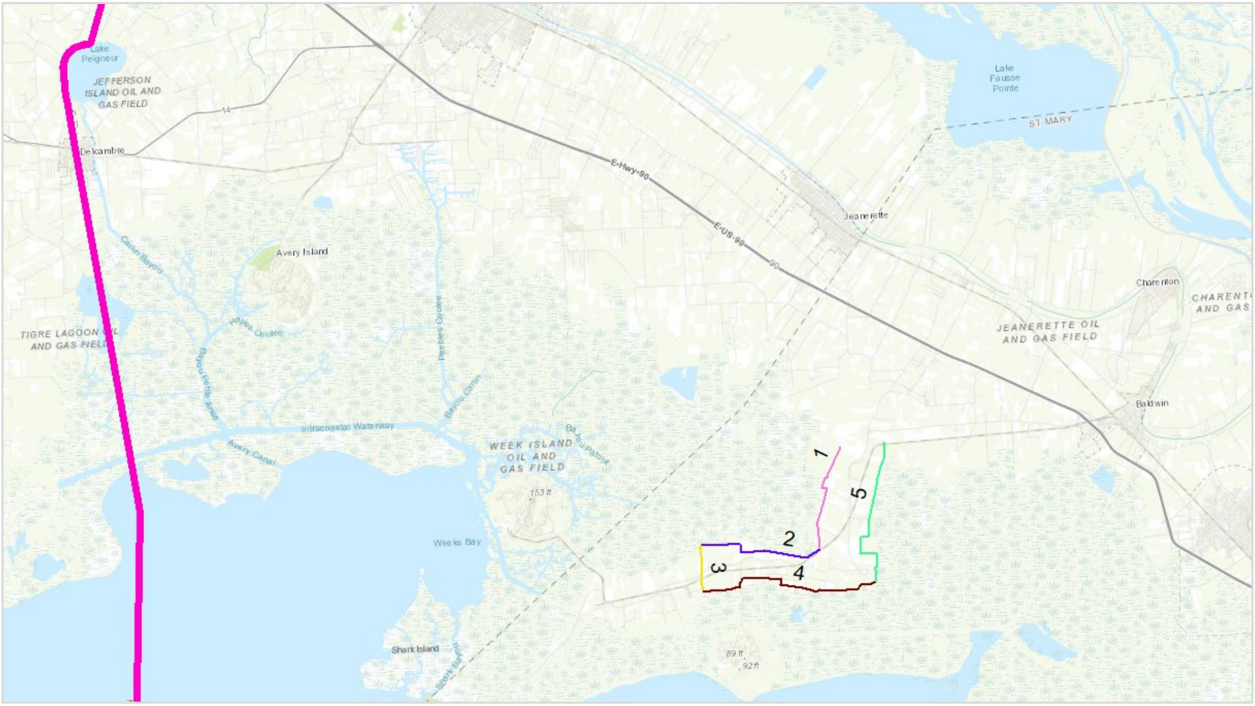

Figure 42. Segments Of The Proposed State Alignment HWY 83 EXT

Table 9. Existing Conditions 2% Surge And Wave Parameters With Levee Elevations For The HWY 83 EXT Alignment.

Hydraulic Reach	SWE (ft)	Std. Dev.	Hs (ft)	Tp (s)	Levee Elevation (ft) NAVD88(2004.65)
1	6.3	1.2	1.5	5.0	9.0
2	7.1	1.2	1.5	7.0	10.0
3	7.8	1.2	3.0	7.0	14.0
4	8.7	1.2	3.0	7.0	15.0
5	7.5	1.2	3.0	5.0	12.5

Table 10. Existing Conditions 1% Surge And Wave Parameters With Levee Elevations For The HWY 83 EXT Alignment.

Hydraulic Reach	SWE (ft)	Std. Dev.	Hs (ft)	Tp (s)	Levee Elevation (ft) NAVD88(2004.65)
1	8.2	1.2	2.0	7.0	12.0
2	9.2	1.2	2.0	7.0	13.0
3	9.6	1.2	5.0	8.0	19.0
4	10.3	1.2	5.0	7.0	20.0
5	9.0	1.2	5.0	9.0	18.0

Table 11. Future Conditions 2% Surge And Wave Parameters With Levee Elevations For The HWY 83 EXT Alignment.

Hydraulic Reach	SWE (ft)	Std. Dev.	Hs (ft)	Tp (s)	Levee Elevation (ft) NAVD88(2004.65)
1	8.6	1.2	1.5	5.0	11.5
2	9.4	1.2	1.5	7.0	12.0
3	9.8	1.2	3.5	7.0	17.5
4	10.4	1.2	5.5	8.0	20.5
5	9.4	1.2	5.0	8.0	18.0

Table 12. Future Conditions 1% Surge And Wave Parameters With Levee Elevations For The HWY 83 EXT Alignment.

Hydraulic Reach	SWE (ft)	Std. Dev.	Hs (ft)	Tp (s)	Levee Elevation (ft) NAVD88(2004.65)
1	10.6	1.2	2.5	7.0	16.0
2	11.4	1.2	2.5	7.0	16.5
3	11.6	1.2	5.0	8.0	22.5
4	12.0	1.2	6.5	7.0	22.0
5	11.1	1.2	6.0	9.0	22.0

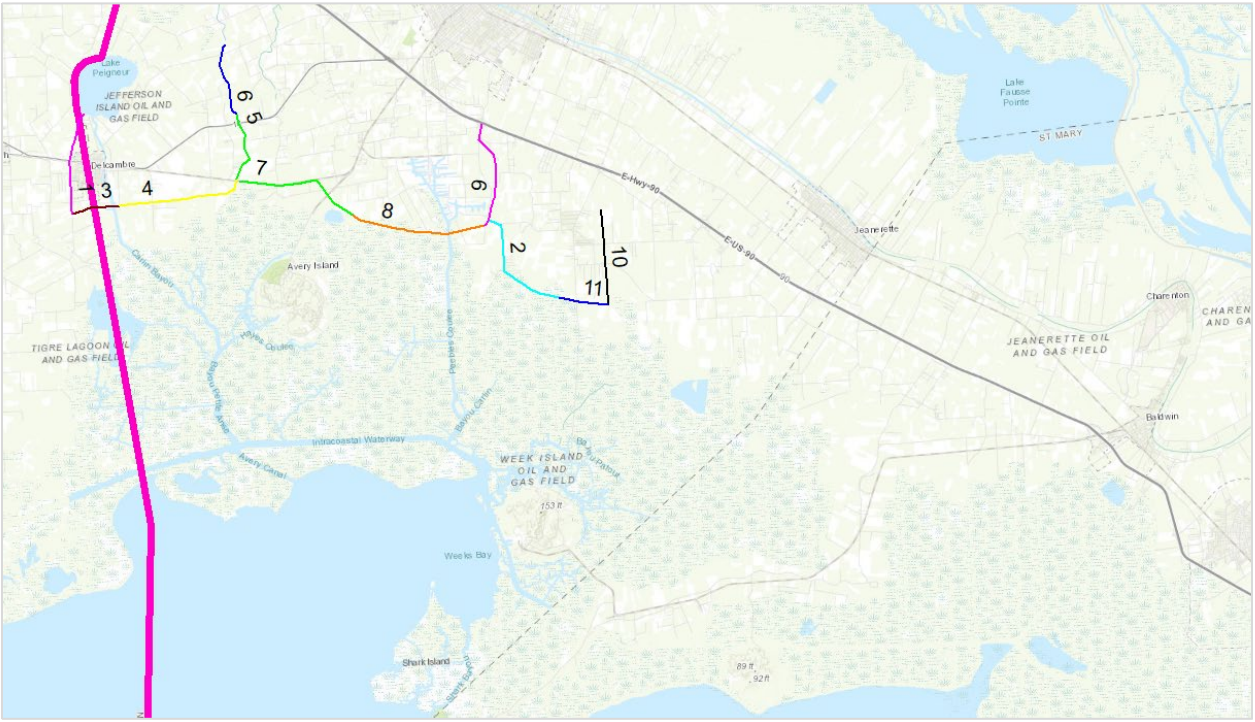

Figure 43. Segments Of The Proposed West Ring Levees

Table 13. 2025 2% Surge And Wave Parameters With Levee Elevations For The West Ring Levees

Hydraulic Reach	SWE (ft)	Std. Dev.	Hs (ft)	Tp (s)	Levee Elevation (ft) NAVD88(2004.65)
1	7.0	1.2	3.0	3.0	9.5
2	7.2	1.2	2.0	7.0	11.0
3	9.0	1.2	3.0	6.0	15.0
4	8.7	1.2	2.0	7.0	12.5
5	8.3	1.2	2.0	7.0	12.0
6	6.7	1.2	2.0	7.0	10.5
7	8.2	1.2	2.0	7.0	12.0
8	7.5	1.2	3.0	7.0	13.5
9	7.0	1.2	1.5	7.0	9.5
10	6.3	1.2	1.5	4.0	8.5
11	6.6	1.2	2.0	7.0	10.5

Table 14. Existing Conditions 1% Surge And Wave Parameters With Levee Elevations For The West Ring Levees

Hydraulic Reach	SWE (ft)	Std. Dev.	Hs (ft)	Tp (s)	Levee Elevation (ft) NAVD88(2004.65)
1	9.3	1.2	4.0	7.0	17.5
2	8.7	1.2	3.0	8.0	15.0
3	10.7	1.2	4.0	7.0	19.5
4	10.3	1.2	4.0	7.0	19.0
5	10.0	1.2	3.0	8.0	16.5
6	9.0	1.2	3.0	8.0	15.5
7	9.8	1.2	3.0	8.0	16.5
8	9.2	1.2	4.0	8.0	17.5
9	8.3	1.2	2.0	8.0	12.0
10	8.0	1.2	3.0	8.0	14.5
11	8.4	1.2	3.0	8.0	15.0

Table 15. Future Conditions 2% Surge And Wave Parameters With Levee Elevations For The West Ring Levees

Hydraulic Reach	SWE (ft)	Std. Dev.	Hs (ft)	Tp (s)	Levee Elevation (ft) NAVD88(2004.65)
1	9.6	1.2	3.0	6.0	15.5
2	9.7	1.2	3.0	7.0	16.0
3	11.3	1.2	3.5	7.0	19.0
4	11.1	1.2	4.0	7.0	20.0
5	10.4	1.2	3.0	7.0	17.0
6	9.0	1.2	3.0	7.0	15.5
7	10.6	1.2	3.5	7.0	18.5
8	10.0	1.2	3.5	7.0	17.5
9	9.2	1.2	2.5	7.0	14.5
10	8.6	1.2	2.5	7.0	14.0
11	9.2	1.2	3.0	7.0	15.5

Hydraulic Reach	SWE (ft)	Std. Dev.	Hs (ft)	Tp (s)	Levee Elevation (ft) NAVD88(2004.65)
1	12.0	1.2	4.0	8.0	21.5
2	11.4	1.2	4.0	8.0	20.5
3	13.1	1.2	5.0	8.0	25.0
4	12.8	1.2	5.0	8.0	24.5
5	12.4	1.2	4.0	8.0	21.5
6	11.6	1.2	4.0	8.0	21.0
7	12.4	1.2	4.5	8.0	23.0
8	11.9	1.2	5.0	8.0	23.0
9	10.8	1.2	4.0	8.0	20.0
10	10.6	1.2	3.0	8.0	17.0
11	11.2	1.2	4.0	8.0	20.5

Table 16. 2075 1% Surge And Wave Parameters With Levee Elevations For The West Ring Levees

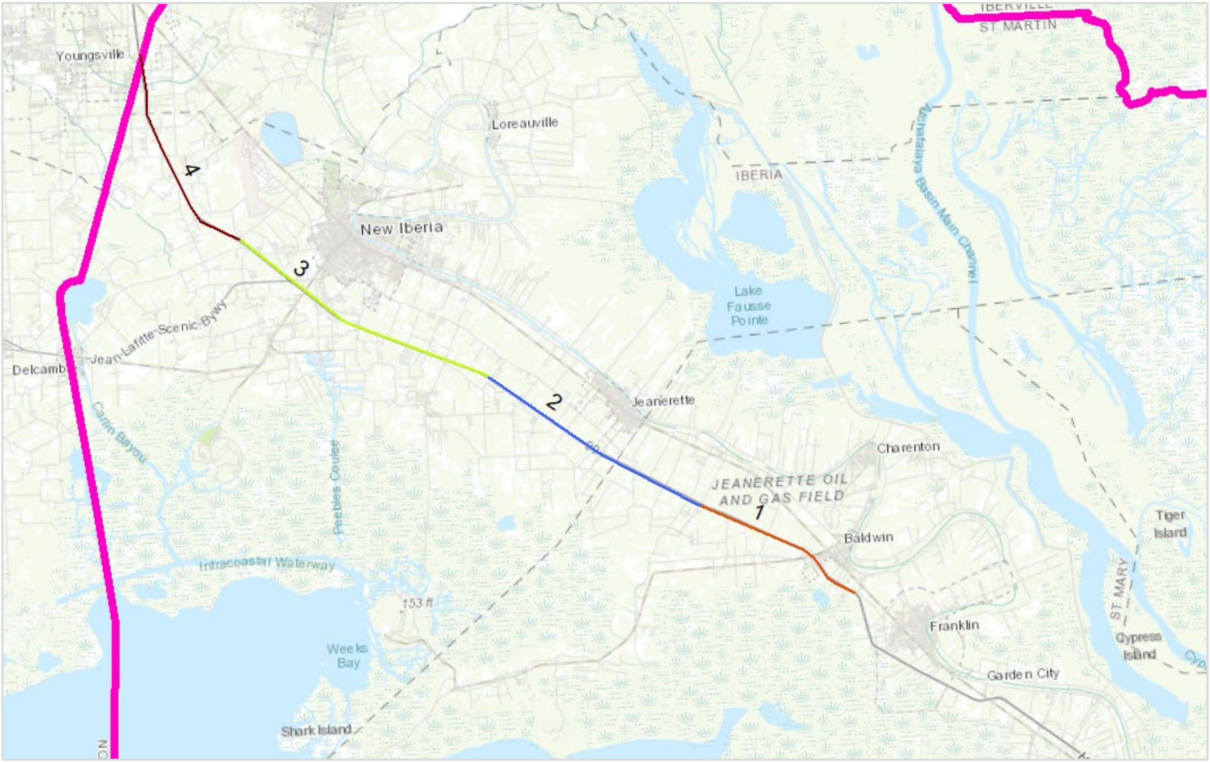

Figure 44. Segments Of The Proposed HWY90 Alignment

Table 17. Existing Conditions 2% Surge And Wave Parameters With Levee Elevations For HWY90 Alignment

Hydraulic Reach	SWE (ft)	Std. Dev.	Hs (ft)	Tp (s)	Levee Elevation (ft) NAVD88(2004.65)
1	6.0	1.2	3.0	6.0	11.0
2	5.9	1.2	1.5	5.0	8.5
3	7.1	1.2	2.0	7.0	11.0
4	6.3	1.2	1.5	3.0	8.0

Table 18. Existing Conditions 1% Surge And Wave Parameters With Levee Elevations For HWY90 Alignment

Hydraulic Reach	SWE (ft)	Std. Dev.	Hs (ft)	Tp (s)	Levee Elevation (ft) NAVD88(2004.65)
1	7.4	1.2	3.0	7.0	13.5
2	7.8	1.2	2.0	7.0	11.5
3	8.8	1.2	3.0	8.0	15.5
4	8.7	1.2	2.0	4.0	11.5

Table 19. Future Conditions 2% Surge And Wave Parameters With Levee Elevations For HWY90 Alignment

Hydraulic Reach	SWE (ft)	Std. Dev.	Hs (ft)	Tp (s)	Levee Elevation (ft) NAVD88(2004.65)
1	8.7	1.2	4.0	8.0	17.0
2	8.4	1.2	3.0	7.0	15.0
3	9.8	1.2	3.0	7.0	16.5
4	8.0	1.2	2.0	6.0	12.0

Table 20. Future Conditions 1% Surge And Wave Parameters With Levee Elevations For HWY90 Alignments

Hydraulic Reach	SWE (ft)	Std. Dev.	Hs (ft)	Tp (s)	Levee Elevation (ft) NAVD88(2004.65)
1	9.6	1.2	5.0	8.0	19.0
2	9.7	1.2	4.0	8.0	18.5
3	10.6	1.2	3.5	7.0	18.5
4	10.7	1.2	2.5	7.0	16.0

5. Subunits

The previous hydraulic subunits near this study are were developed from census blocks and the land-water boundary. For this analysis the PDT requested subunits that were more hydraulics dependent in delineation. Below is the methodology by which this was performed.

1. The project study boundary identified the outer boundary for the subunits.

2. Next, a land water boundary layer was used to determine the extent of the Gulf of Mexico into the project area.

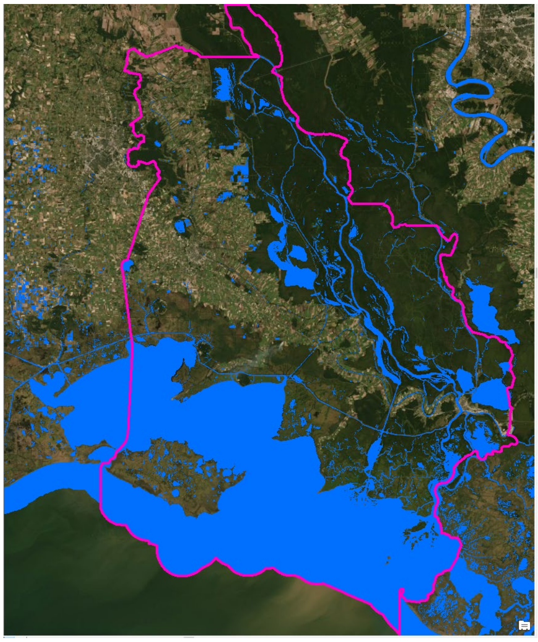

3. The zone was sliced along this coastal boundary, preserving the inland riverine regions.

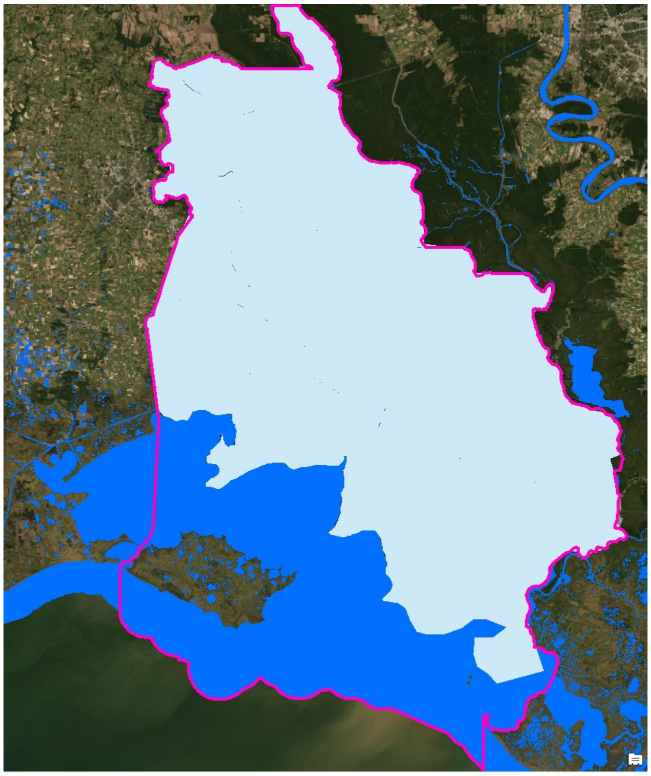

4. 1% AEP surge elevation heights were converted into polygons delineated with 0.5ft contoured bins

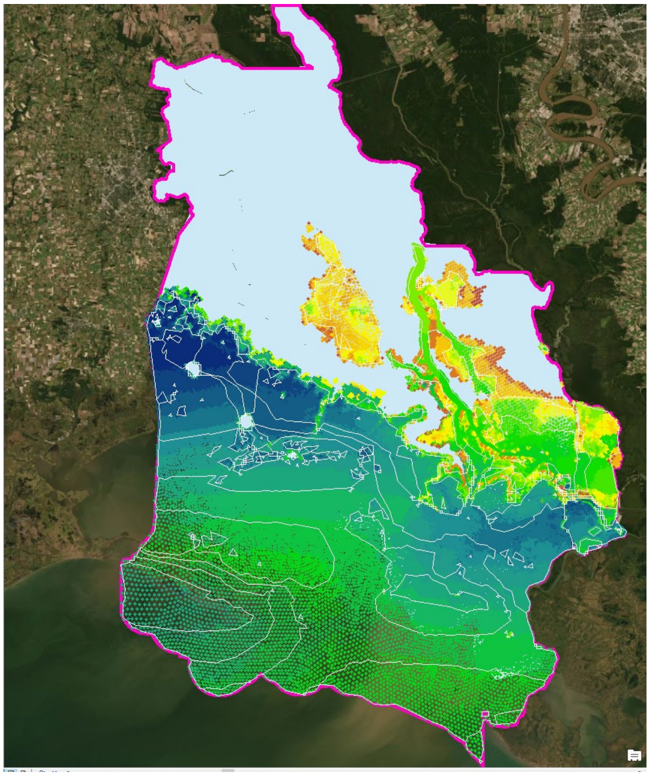

5. After a union was performed on the shape, those polygons were sliced with existing levees

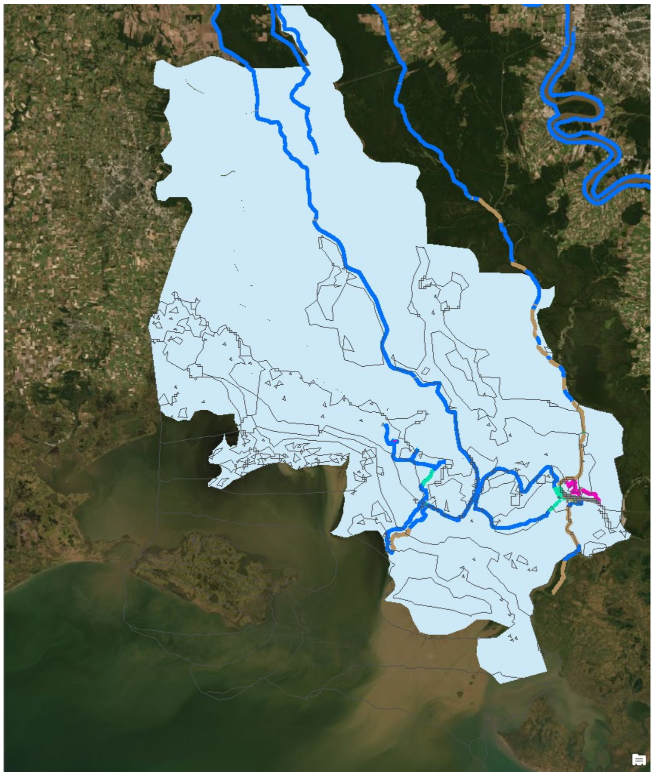

6. Next, the subunits shape was sliced with proposed SCCL levee alternatives.

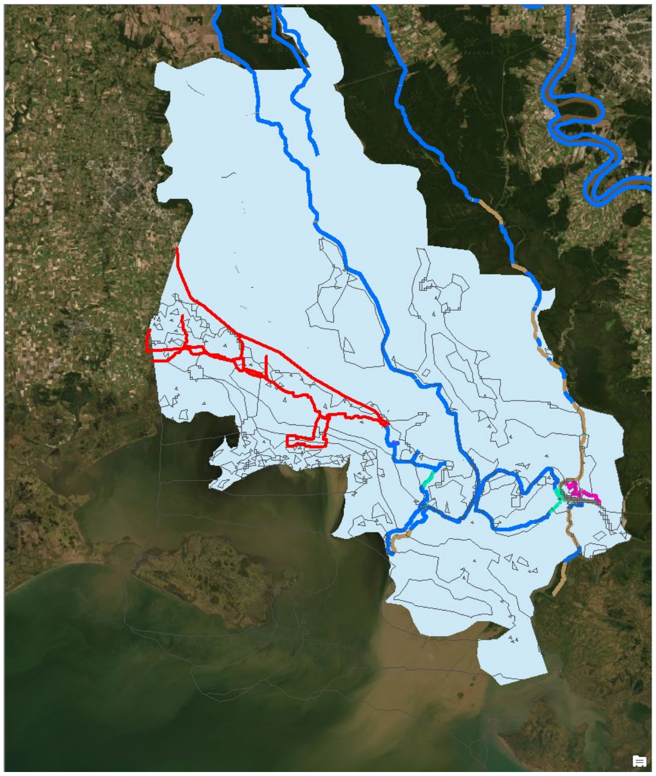

7. Then, the units were sliced with additional features like Bayou Teche, major roads, and high ground.

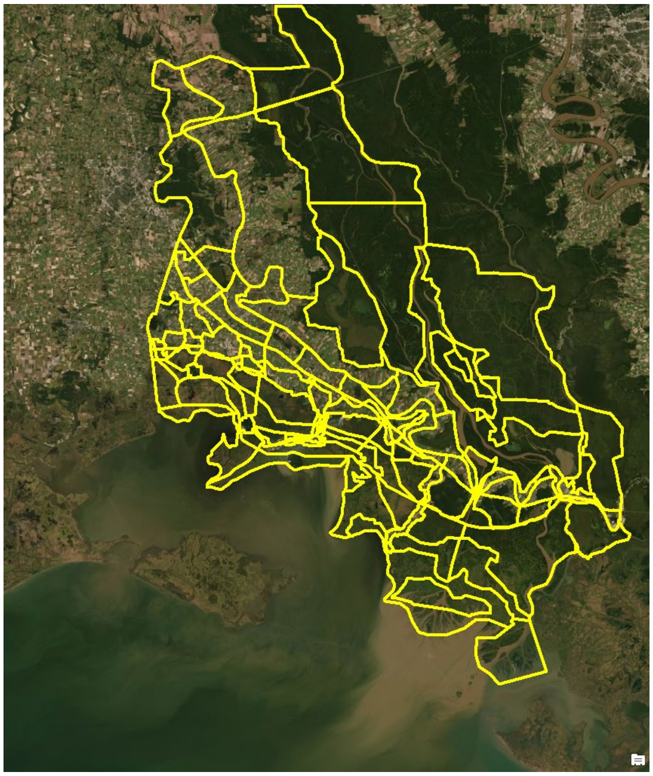

6. Climate Change

6.1 Relative Sea Level Change (RSLC)

In coastal Louisiana, relative sea level rise (RSLR) is the term applied to the difference between the change in eustatic (global) sea level and the change in land elevation. According to Intergovernmental Panel on Climate Change (IPCC 2007), the global mean sea level rose at an average rate of about 1.7 mm/yr during the 20th Century. Recent climate research has documented global warming during the 20th Century, and has predicted either continued or accelerated global warming for the 21st Century and possibly beyond (IPCC 2007).

Land elevation change can be positive (accreting) or negative (subsiding). Land elevations decrease due to natural causes, such as compaction and consolidation of Holocene deposits and faulting, and human influences such as sub-surface fluid extraction and drainage for agriculture, flood protection, and development. Forced drainage of wetlands results in lowering of the water table resulting in accelerated compaction and oxidation of organic material. Areas under forced drainage can be found throughout coastal Louisiana and the study area. Land elevations increase as a result of sediment accretion (riverine and littoral sources) and organic deposition from vegetation. Vertical accretion in most of the area, however, is insufficient to offset subsidence, causing an overall decrease in land elevations. The combination of subsidence and eustatic sea level rise is likely to cause the landward movement of marine conditions into estuaries, coastal wetlands, and fringing uplands (Day and Templet, 1989; Reid and Trexler 1992).

The locations of the RSLC gages are presented in Figure 45 near the southwestern border of the project area. The results in the calculation table were determined with equation 2 from the EC 1165-2-212. The eustatic sea level rise rate of 0.0017 myr^{-1} is combined with 50-year subsidence values of 2.9, 0.9, and 1.8 feet for G88800, G03820, and G76360 respectively. Figure 46 depicts the intermediate RSLC graphically for the three gages in addition to the averaged intermediate rate. The values are tabulated in table 21.

The projections in Figure 46 are based on the parameters defined in EC 1165-2-212, where the rate of eustatic sea level rise is determined with:

Equation Used by this Calculator

EC 1165-2-212, Equation 2 is as follows:

$$E(t) = (0.0017+M)t + bt^2$$

The acceleration constant “b” is adjusted to achieve the medium and high curves, while the low curve is the extrapolated historical rate from gauge data.

The baseline gulf water level is considered to be 1.2 ft. NAVD88. The three gages chosen for estimating future conditions are G88800, G03820, and G76360. These are located near the south end of the lower Atchafalaya guide levee (G03820 & G88800) and south of Morgan City (G76360). The 50-year intermediate rates were averaged resulting in a future sea level condition of 3.0 ft.

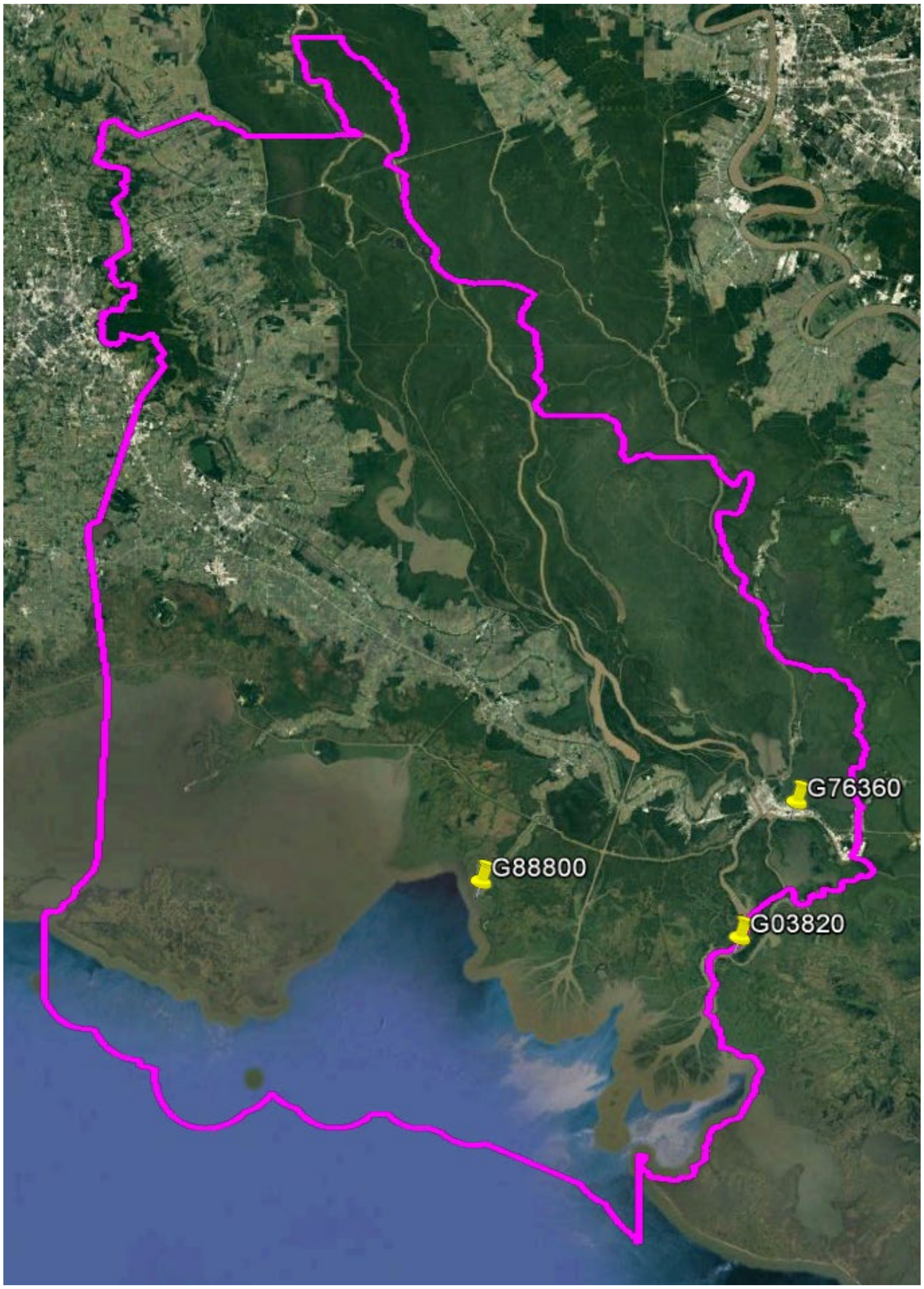

Figure 45. Locations Of The Three RSLC Gages

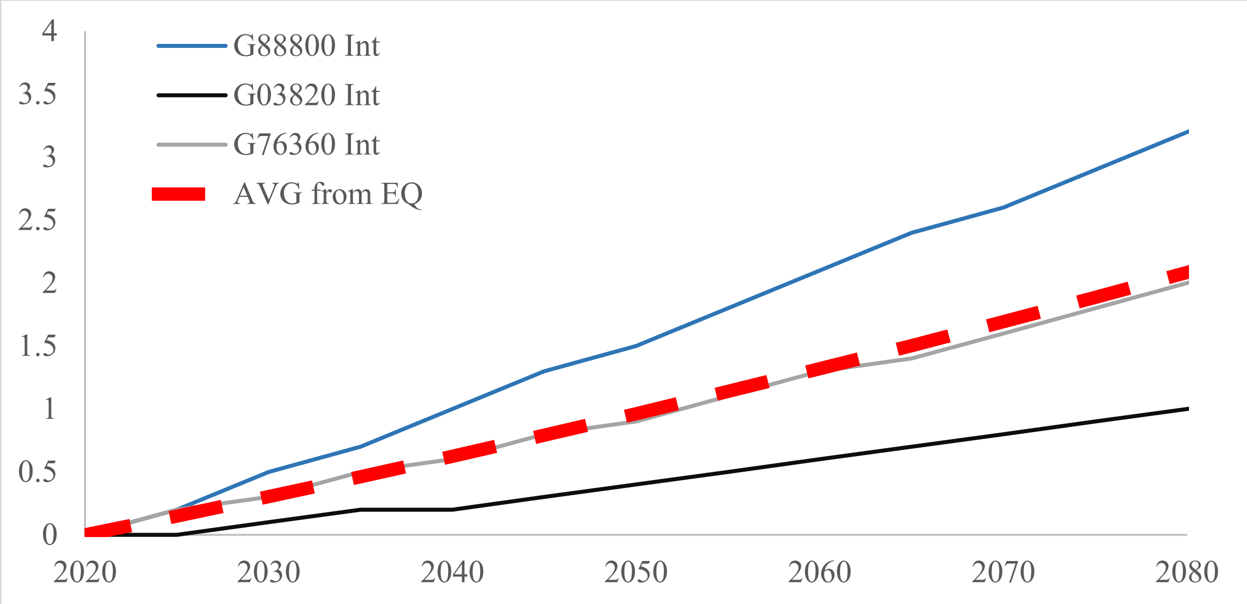

Figure 46. The Relative Intermediate RSLC Average Rate

Table 21. RSLC Rates For The Three Gauges In The Project Area.

Average All values are in feet					
Year	G88800 Int	G03820 Int	G76360 Int	AVG from EQ	AVG from Val
2020	0	0	0	0.0	0.0
2025	0.2	0	0.2	0.1	0.1
2030	0.5	0.1	0.3	0.3	0.3
2035	0.7	0.2	0.5	0.5	0.5
2040	1	0.2	0.6	0.6	0.6
2045	1.3	0.3	0.8	0.8	0.8
2050	1.5	0.4	0.9	1.0	0.9
2055	1.8	0.5	1.1	1.1	1.1
2060	2.1	0.6	1.3	1.3	1.3
2065	2.4	0.7	1.4	1.5	1.5
2070	2.6	0.8	1.6	1.7	1.7
2075	2.9	0.9	1.8	1.9	1.9
2080	3.2	1	2	2.1	2.1
2085	3.5	1.1	2.2	2.3	2.3
2090	3.8	1.2	2.4	2.5	2.5
2095	4.1	1.3	2.6	2.7	2.7
2100	4.4	1.5	2.8	2.9	2.9

6.2 Hydrology and Non-Stationarity

In order to evaluate potential changes in future project performance due to climate-based changes in hydrology, the USACE projected streamflow and nonstationarity detection tools were used. The historical peak instantaneous stream flow for the lower Atchafalaya gage in basin 0808 is shown in Figure 47. The 20-year trend shows no significant change, though the period of record may be insufficient for a longer trend. The projected Annual Monthly Maximum for basin 0808 is shown in Figures 48 and 49. There is no significant positive trend in the mean, however the range of projections around the mean increase. Figures 50 – 53 are results produced by the non-stationarity detection tool. There is no station for the Atchafalaya river for this tool, the most hydraulically relevant nearby gage are two Mississippi river locations: Vicksburg and Baton Rouge. Non-stationarities were not detected at either location.

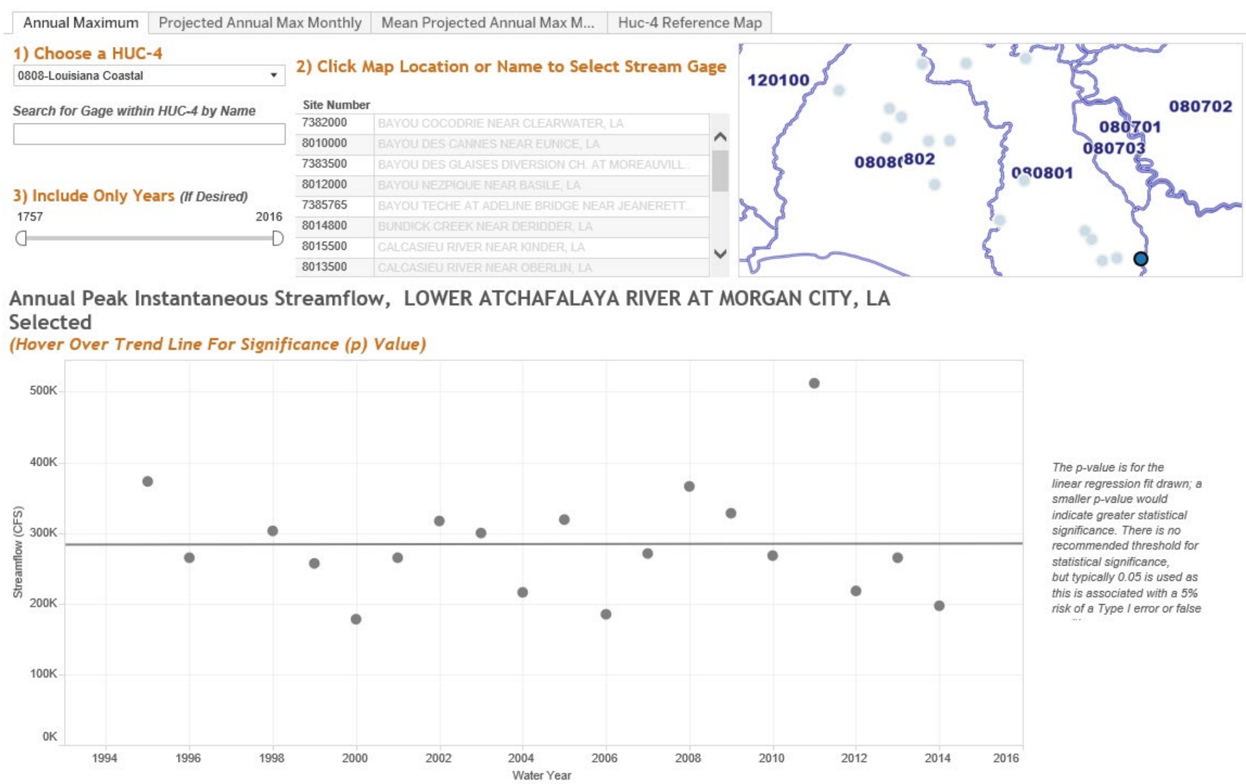

Figure 47. Historical Annual Maximum Streamflow For 0808 South Central Coast LA

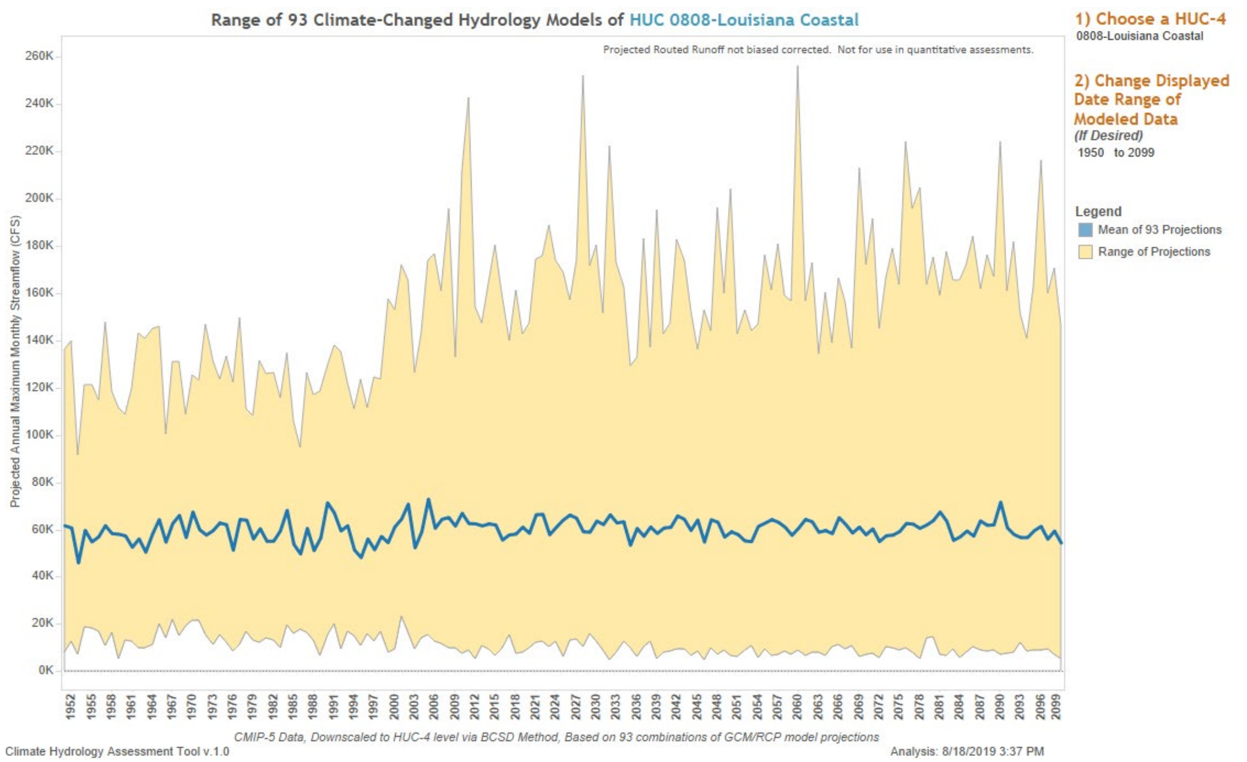

Figure 48. Climate-Changed Hydrology Models For 0808 South Central Coast LA

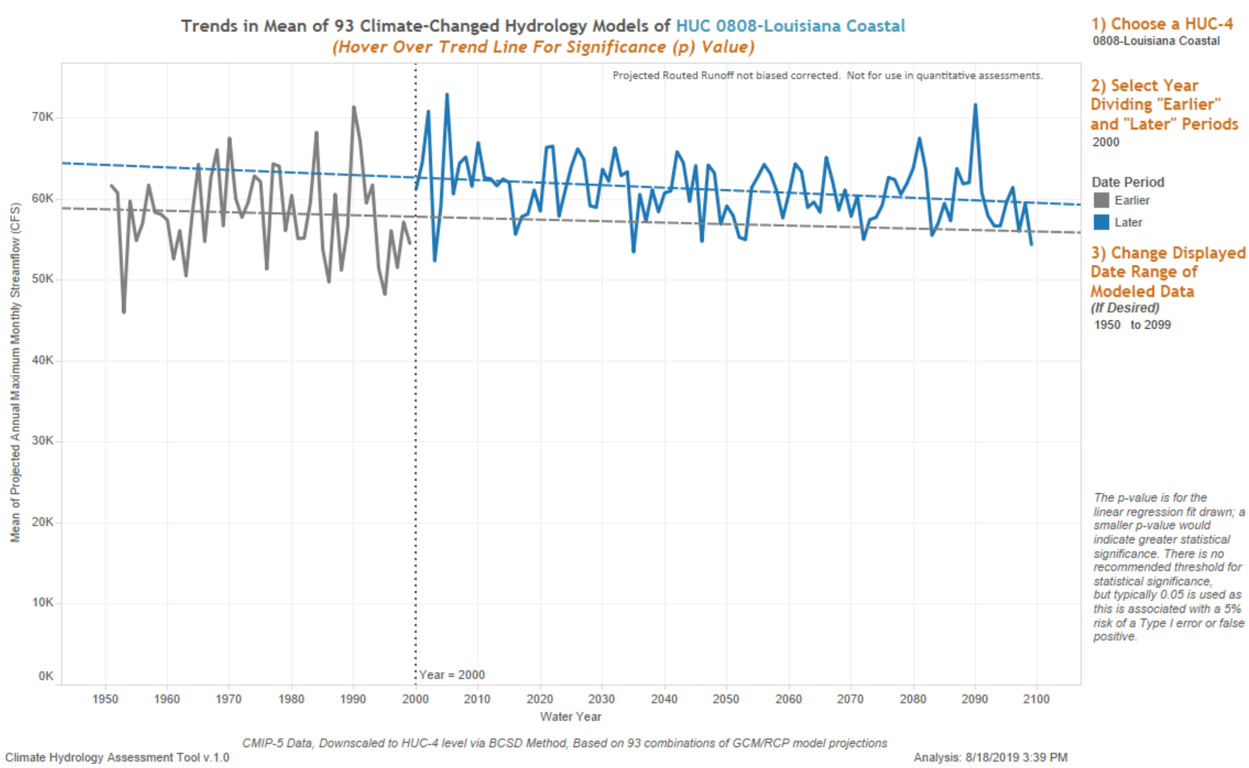

Figure 49. Climate-Changed Hydrology Models For 0808 South Central Coast LA

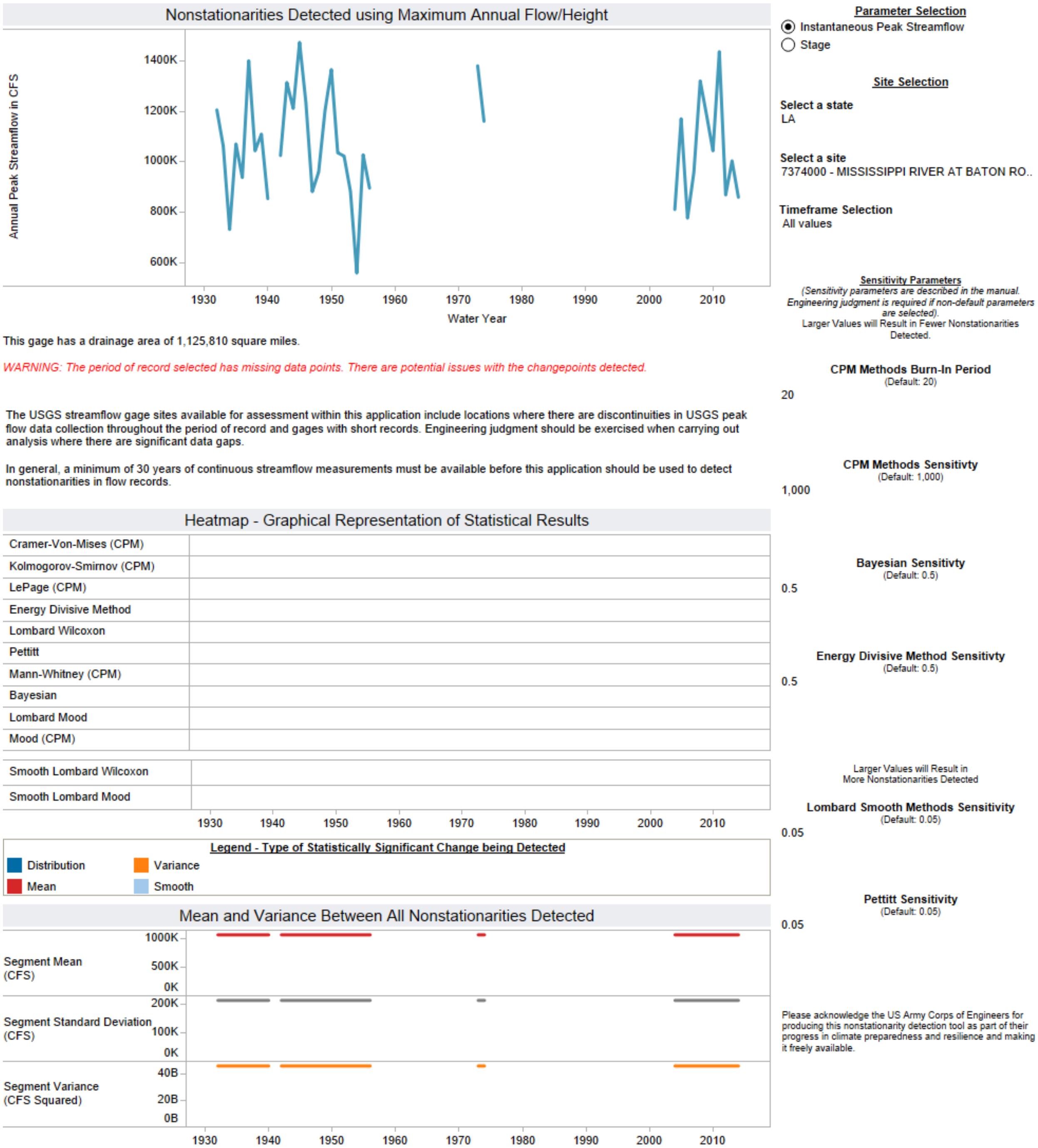

Figure 50. Climate-Changed Hydrology Models For 0808 South Central Coast LA

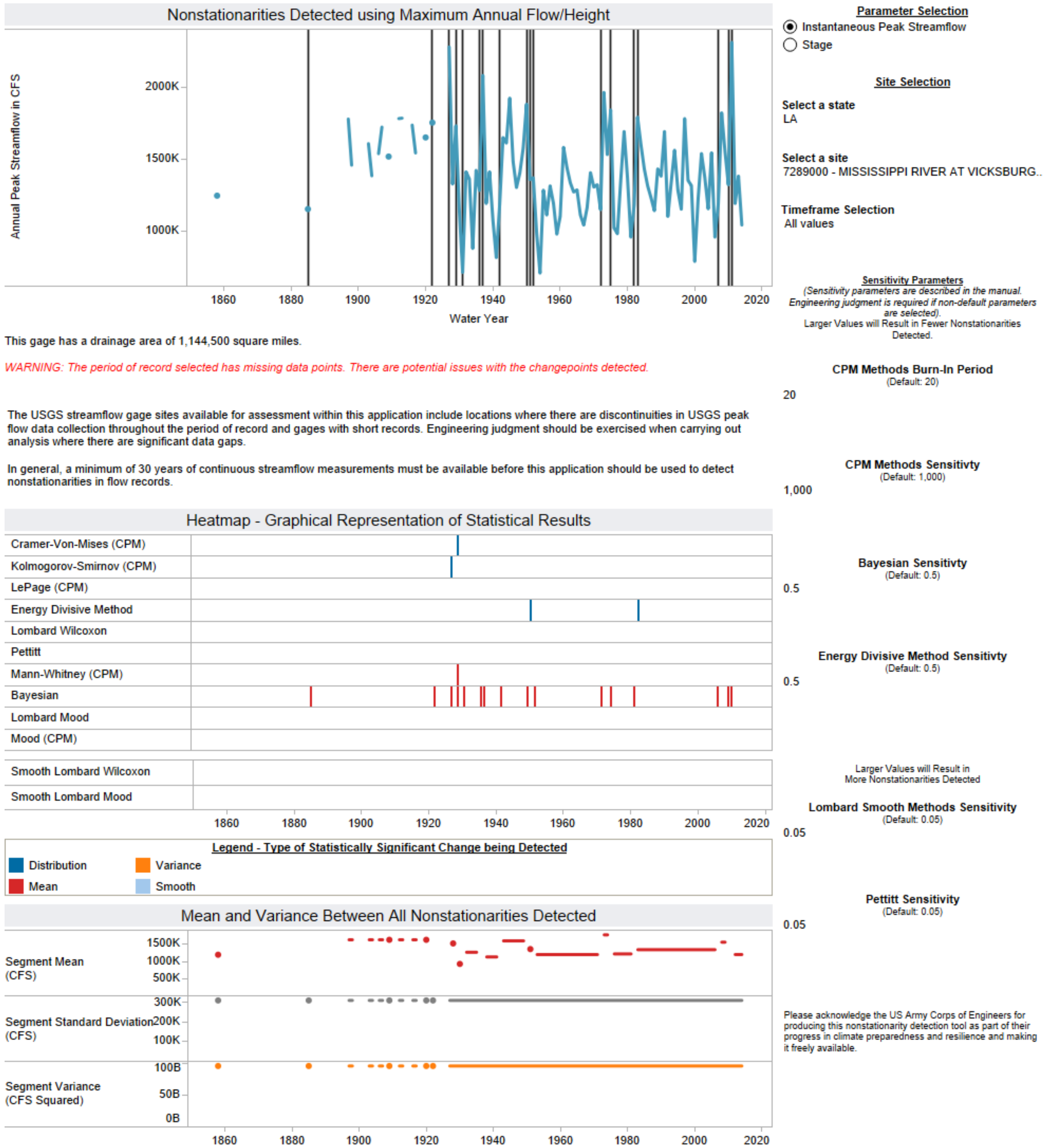

Figure 51. Climate-Changed Hydrology Models For 0808 South Central Coast LA

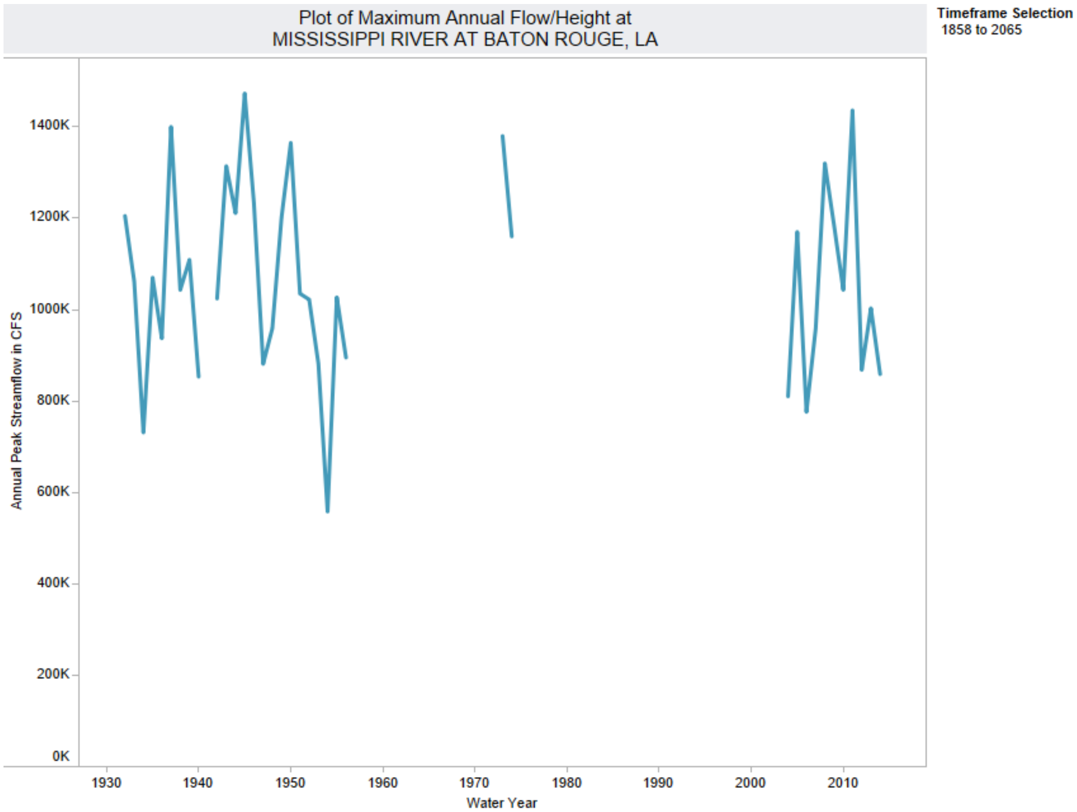

WARNING: The period of record selected has missing data points. There are potential issues with the trends detected.

Monotonic Trend Analysis

Is there a statistically significant trend?
No, using the Mann-Kendall Test at the .05 level of significance. The exact p-value for this test was 0.448.
No, using the Spearman Rank Order Test at the .05 level of significance. The exact p-value for this test was 0.437.

What type of trend was detected?
Using parametric statistical methods, **no trend** was detected.
Using robust parametric statistical methods (Sen's Slope), **no trend** was detected.

Please acknowledge the US Army Corps of Engineers for producing this nonstationarity detection tool as part of their progress in climate preparedness and resilience and making it freely available.

Figure 52. Climate-Changed Hydrology Models For 0808 South Central Coast LA

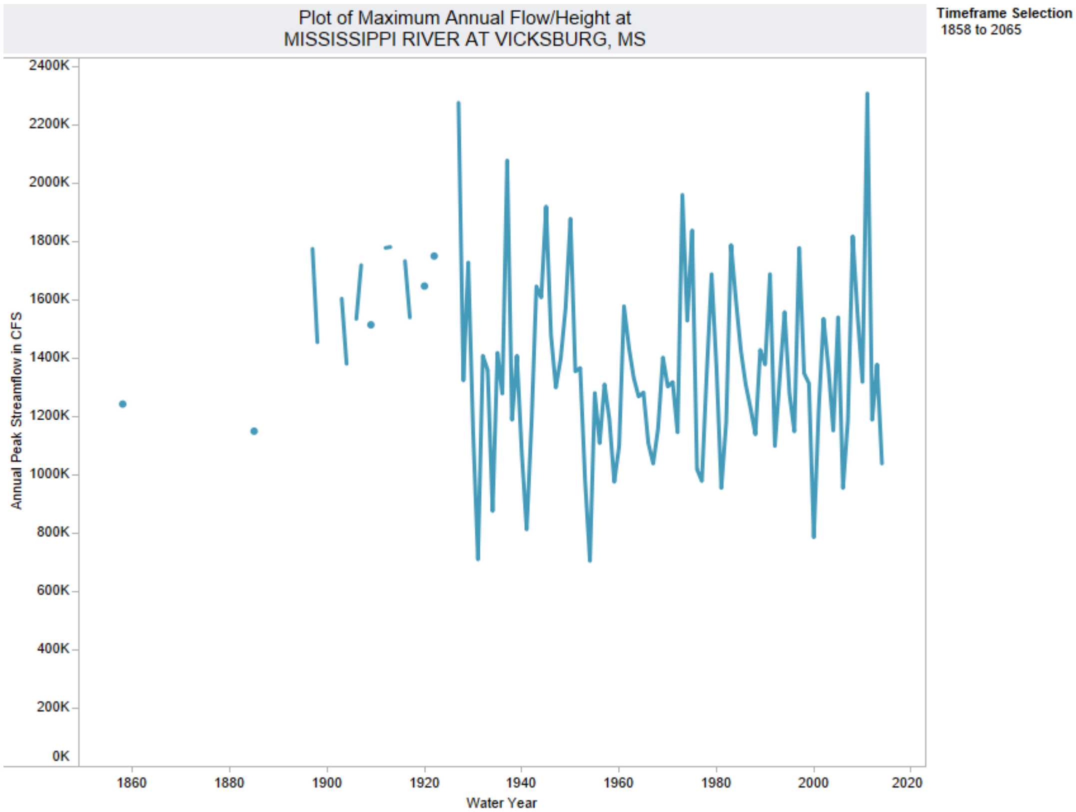

WARNING: The period of record selected has missing data points. There are potential issues with the trends detected.

Monotonic Trend Analysis

Is there a statistically significant trend?
No, using the Mann-Kendall Test at the .05 level of significance. The exact p-value for this test was 0.083.
No, using the Spearman Rank Order Test at the .05 level of significance. The exact p-value for this test was Null.

What type of trend was detected?
Using parametric statistical methods, **no trend** was detected.
Using robust parametric statistical methods (Sen's Slope), **no trend** was detected.

Please acknowledge the US Army Corps of Engineers for producing this nonstationarity detection tool as part of their progress in climate preparedness and resilience and making it freely available.

Figure 53. Climate-Changed Hydrology Models For 0808 South Central Coast LA